

CHAPTER 7

Thermalhydraulic Analysis

prepared by:
 Dr. Wm. J. Garland, Professor Emeritus,
 Department of Engineering Physics,
 McMaster University, Hamilton, Ontario, Canada

Summary:

This chapter is concerned with thermalhydraulic analysis of the process systems that are required to transport heat energy away from the nuclear reactor source and transform this heat energy into useful work (generally electrical energy). Thermal hydraulic system behaviour is largely determined by the simultaneous solution of the equations that govern the four variables (flow, pressure, density and enthalpy). The general mass, energy and momentum conservation equations are presented in general terms and are simplified to the common approximate forms used in systems modelling. The equation of state that is required for closure is explored with particular emphasis on implementation. Process system solution algorithms are investigated.

Table of Contents

1	Introduction	4
1.1	Learning Outcomes	5
1.2	The Chapter Layout	6
2	Basic Equations for Thermalhydraulic Systems Analysis	7
2.1	Introduction	7
2.2	Conservation	7
2.3	Conservation of Mass	10
2.4	Conservation of Momentum	12
2.5	Conservation of Energy	15
2.6	The Equation of State	20
2.7	Empirical Correlations	20
2.8	Solution Overview	21
2.9	Problems	23
3	Nodalization	24
3.1	Introduction	24
3.2	The Node-Link Concept	24
3.3	Nodal Diffusion	28
3.4	Examples	32
3.5	Matrix Notation	34

3.6	Exercises	35
4	Equation of State	36
4.1	Introduction	36
4.2	Thermodynamic Properties	36
4.3	The Iterative Method	38
4.4	The Rate Method	40
4.5	Water Property Fits	46
4.6	Problems	48
5	The Rate Form of the Equation of State	49
5.1	Introduction	49
5.2	The Rate Form	49
5.3	Numerical Investigations: a Simple Case	50
5.4	Numerical Investigations: a Practical Case	61
5.5	Discussion and Conclusion	66
5.6	Problems	67
6	Thermalhydraulic Network Simulation	68
6.1	Introduction	68
6.2	Porsching's Method	68
6.3	Derivation of FIBS	69
6.4	Special Cases	74
6.5	Programming Notes	75
6.6	Conclusion	77
6.7	Problems	77
7	Case Study: Heat Transport System Stability	78
8	References	78
9	Nomenclature	82
10	Acknowledgements	83

List of Figures

Figure 1	The four cornerstone single phase flow equations and the flow of information between them	21
Figure 2	The four cornerstone equations for the two-fluid model.	22
Figure 3	The four cornerstone equations for the full two-fluid model with equal pressure of the two phases	23
Figure 4	A general node and connecting links	24
Figure 5	Two connected nodes	25
Figure 6	Node-link setup for a simple pipe	26
Figure 7	Node-link setup for an area change in a pipe	27
Figure 8	Illustration of convection and diffusion	29
Figure 9	Transmission of a step change using the plug flow model and the mixing tank model (1 to 50 tanks)	30
Figure 10	Transmission of a step change using the plug flow model and a feeder model with	

skewing due to differences in transit times.....	31
Figure 11 Simple Tee junction.....	32
Figure 12 Simple Y junction.	32
Figure 13 Node-link diagram: ¼ circuit CANDU.	33
Figure 14 Sample node-link connection for a header.....	33
Figure 15 4 Node - 5 link diagram.....	35
Figure 16 P-v-T surface for water	37
Figure 17 Numerical search for P given ρ and h for a two-phase mixture.	38
Figure 18 Error correction scheme for pressure in two-phase.....	39
Figure 19 Density vs. pressure at various temperatures in sub-cooled water.....	47
Figure 20 Basis for curve fitting in the subcooled region.	47
Figure 21 Simple 2-node, 1-link system.....	51
Figure 22 Program flow diagram for the normal method.	52
Figure 23 Program flow diagram for the rate method.	54
Figure 24 Number of iterations per pressure routine call for the normal method with a time step of 0.01 seconds and a pressure tolerance of 0.001 of full scale (10 MPa).	56
Figure 25 Integrated flow error for the rate method and the normal method for various fixed time steps, convergence tolerances and adjustment factors.	56
Figure 26 Flow vs. time for the implicit forms of the normal and rate methods.	61
Figure 27 Schematic of control volumes in the pressurizer.....	62
Figure 28 Pressurizer's pressure transient for the rate method.....	65
Figure 29 Pressurizer's pressure transient for the normal method with error tolerance of 0.2%.	65
Figure 30 Average number of iterations per pressure routine call for the normal method in simulating the pressurizer problem.	66

List of Tables

Table 1 Figure of merit comparisons of the normal and rate forms of the equation of state for various convergence criteria (simple case).....	58
---	----

1 Introduction

This chapter is concerned with thermal hydraulic analysis of the process systems that are required to transport heat energy away from the nuclear reactor source and transform this heat energy into useful work (generally electrical energy). Thermal hydraulic design of the process systems is covered in the previous chapter. Design and analysis are, of course, tightly coupled. Nuclear systems design is guided by analysis results. Analysis, in turn, is performed on a specific design to determine its performance. It is a complex, iterative dance. Design and analysis of the reactor process involves a number of interrelated systems:

- reactor core
- heat transport system
- steam generators
- turbines
- pressure control system
- coolant inventory control systems
- power control systems;

a number of system components:

- valves
- pumps
- pipes
- vessels
- heat exchangers;

and a number of engineering and science disciplines:

- reactor physics
- heat transfer
- fluid mechanics
- thermodynamics
- chemistry
- metallurgy
- control
- stress analysis.

The heat transport system (HTS) is of central importance since it is the interface between the heat source and the heat sink. Good HTS performance is essential to reactor integrity, plant performance and safety. Herein, the scope is limited to the modelling tools used in thermal hydraulic analysis of the HTS. This chapter is a systems level chapter, not a components level one. Component modelling is limited to approximate models that are appropriate for systems analysis. Detailed multidimensional modelling of complex components such as steam generators, pumps, calandria vessels, headers, etc., are not attempted.

This chapter is primarily about the interplay the two main actors in hydraulic systems: flow and

pressure. But because we are dealing with systems involving the transfer of heat, local density and enthalpy determine the pressure. Hence, thermal hydraulic system behaviour is largely determined by the simultaneous solution of the equations that govern these four variables (flow, pressure, density and enthalpy).

1.1 Learning Outcomes

The overall objectives for this chapter are as follows:

- The student should be able to explain the roles played by mass, flow, energy and pressure in thermalhydraulic simulation.
- The student should be able to derive appropriate forms of the governing equations, and develop a flow diagram and pseudo-code for a thermalhydraulic system simulator from first principles.
- The student should be able to build a thermalhydraulic system simulator from first principles.
- The student should be able to identify the terms and symbols used in thermalhydraulics.
- The student should be able to distinguish between the differential and integral form and be able to choose, with justification, the correct form to use in various situations.
- The student should be able to recall typical values and units of parameters.
- The student should be able to recognize key physical phenomena.
- The student should be able to recognize the coupling between mass, momentum, energy and pressure in thermalhydraulic systems.
- The student should be able to choose approximations as appropriate (# of dimensions, transient or steady state, averaging, spatial resolution, etc.) with justification.
- The student should be able to develop, with justification, a node-link diagram given a thermalhydraulic system.
- The student should be able to construct the matrix form of the conservation equations for a given node-link structure.
- The student should be able to calculate any dependent thermodynamic property given any two independent state variables using (a) the steam tables, (b) supplied codes, (c) supplied curve fits to the steam tables.
- The student should be able to develop a flow diagram and pseudo-code for the calculation of P and T given density and enthalpy.
- The student should be able to explain the pressure and temperature response of a volume of fluid to perturbations given the F and G functions.
- The student should be able to develop a flow diagram and pseudo-code for the rate method of the equation of state.
- The student should be able to develop a computer code implementing the rate method of the equation of state.
- The student should be able to model a simple thermalhydraulic network using the integral form of the conservation equations and the rate form of the equation of state. The student should be able to check for reasonableness of the answers.

- The student should be able to apply the various numerical methodologies (fully explicit to fully implicit) to special cases of the thermalhydraulic system equations.
- The student should be able to produce a general node-link code based on the cumulative concepts presented in this course.
- The student should be able to evaluate the efficacy of the various numerical algorithms.

1.2 The Chapter Layout

To lay the groundwork for thermal hydraulic systems analysis, Section 2 presents the general mass, energy and momentum conservation equations in very general terms and proceeds to derive the common approximate forms used in systems modelling. Section 3 shows how to model hydraulic piping networks as a system of nodes connected by links and elaborates on the appropriate equation forms for these node-link approximations. The conservation equations requires a relationship between pressure, temperature, density and energy (the equation of state) for closure. In Section 4, the equation of state is explored with particular emphasis on implementation. Sections 5 and 6 cover numerical considerations. Explicit, semi-implicit and implicit techniques are presented. At this point the reader is almost ready to conduct thermal hydraulic simulations. Chapter 6 on Thermalhydraulic design completes the picture by providing heat transfer and hydraulic correlations that are needed for the simulations. A survey of industrial strength tools is outside the scope of this chapter as is a discussion of phenomena identification and evaluation, and code verification and validation.

As with design, there is no one best model for a given analysis task, nor is there even one best solution procedure. Good simulation is evolutionary; we learn from past successes and failures, incorporate the latest experimental, theoretical and numerical results, employ sound engineering principles and a solid understanding of the basics to engineer each and every new simulation tool.

2 Basic Equations for Thermalhydraulic Systems Analysis

2.1 Introduction

This section presents the basic mass, momentum and energy equations used in typical computer codes for thermalhydraulic simulation. The equations are derived from first principles and the necessary approximations lead to the requirements for empirical correlations. Closure is obtained by the equation of state.

The known territory of the basic mass, energy and momentum conservation equations (Bird et al [BIR60]) is explored, herein, from the perspective of thermalhydraulic systems analysis for nuclear reactors. See also [CAR95] for seminal coverage of this topic.

Invariably in the modelling of fluids, the conservation equations are cast in one of two main forms (Currie [CUR74]): integral or distributed approach. The distributed (differential) form sees infrequent use in the analysis of thermalhydraulic systems since the cost and complexity of such a detailed analysis on even a single complex component of a system is enormous, which makes this route to the analysis of systems of such complex components unrealizable. Recourse is generally made to the integral or lumped form so that inter-relationships of various components comprising a system can be simulated. Necessarily, the models used for the individual components are much simpler than that of the detailed models based on the distributed approach. Great care must be taken to ensure that the simpler models of the integral approach are properly formulated and not misused.

It behooves us, then, to develop the models used in thermalhydraulic systems analysis from first principles. This will provide a traceable and verifiable methodology to aid development and validation of system codes, to elucidate the necessary assumptions made, to show pitfalls, to show the common roots and genealogy of specific tools like FLASH [POR69], SOPHT [CHA75a, CHA75b, CHA77a, CHA77b, SKE75, SKE80], RETRAN [AGE82], FIREBIRD [LIN79], CATHENA [HAN95], etc., and to help guide future development.

The exploration proceeds by first establishing and discussing the general principle of conservation. Next, this general principle is applied in turn to mass, momentum and energy to arrive at the specific forms commonly seen in the systems approach. Closure is then given via the equation of state and by supporting empirical correlations. Finally, the ideas developed are codified in a diagrammatical representation to aid in the physical interpretation of these systems of equations and to provide a summary of the main characteristics of fluid systems.

2.2 Conservation

We start, both historically and pedagogically, with a basic experimental observation:

"CONSERVATION".

This was, and is, most easily understood in terms of mass:

"WHAT GOES IN MUST COME OUT UNLESS IT STAYS THERE
OR IS GENERATED OR LOST SOMEHOW".

Although this should be self-evident, it is important to realize that this is an experimental observation.

If we further assume that we have a continuum, we can mathematically recast our basic experimental observation for any field variable, ψ :

$$\frac{D}{Dt} \iiint_V \psi dV = \iiint_V \Gamma dV + \iint_S \mathbf{S} \cdot \mathbf{n} ds \quad (1)$$

where

D/Dt = substantial derivative¹ = change due to time variations plus change due to movement in space at the velocity of the field variable, ψ ,

V = arbitrary fluid volume,

Γ = net sum of local sources and local sinks of the field variable, ψ , within the volume V ,

ψ = field variable such as mass, momentum, energy, etc.,

t = time,

s = surface bounding the volume, V ,

\mathbf{n} = unit vector normal to the surface, and

\mathbf{S} = net sum of local sources and local sinks of the fluid variable, ψ , on the surface s .

We can now use Reynold's Transport Theorem [CUR74]:

$$\frac{D}{Dt} \iiint_V \psi dV = \iiint_V \frac{\partial \psi}{\partial t} dV + \iint_S \psi \mathbf{v} \cdot \mathbf{n} ds \quad (2)$$

where

$\partial/\partial t$ = local time derivative, and

\mathbf{v} = velocity of the field variable,

to give

$$\iiint_V \frac{\partial \psi}{\partial t} dV = - \iint_S \psi \mathbf{v} \cdot \mathbf{n} ds + \iiint_V \Gamma dV + \iint_S \mathbf{S} \cdot \mathbf{n} ds. \quad (3)$$

In words, this states that the change in the conserved field variable ψ in the volume V is due to surface flux plus sources minus sinks. We can use another mathematical identity (Gauss'

¹ For a lucid discussion of the three time derivatives, $\frac{\partial}{\partial t'}$, $\frac{D}{Dt'}$, $\frac{d}{dt'}$, see [BIR60, pp 73-74].

Divergence Theorem):

$$\iint_S \mathbf{A} \cdot \mathbf{n} \, ds = \iiint_V \nabla \cdot \mathbf{A} \, dV, \quad (4)$$

where

\mathbf{A} = any vector, such as velocity, and

∇ = Del operator (eg. $\nabla = \partial/\partial x \mathbf{i} + \partial/\partial y \mathbf{j} + \dots$).

Thus equation 3 can be rewritten:

$$\iiint_V \frac{\partial \Psi}{\partial t} \, dV = - \iiint_S \nabla \cdot \Psi \mathbf{v} \, dV + \iiint_V \Gamma \, dV + \iiint_V \nabla \cdot \mathbf{S} \, dV. \quad (5)$$

If we assume that this statement is universally true, i.e. for any volume within the system under consideration, then the following identity must hold at each point in space:

$$\frac{\partial \Psi}{\partial t} = -\nabla \cdot \Psi \mathbf{v} + \Gamma + \nabla \cdot \mathbf{S}. \quad (6)$$

This is the distributed or microscopic form. Equation 3 is the lumped or macroscopic form. They are equivalent and one can move freely back and forth between the two forms as long as the field variables are continuous.

The above derivation path is not unique. One could start with an incremental volume and derive (1) via (6). It is largely a question of personal choice and the end use. One school of thought, attended by most scientists, applied mathematicians and academics, since they usually deal with the local or microscopic approach, focuses on the conversion of the surface integrals to volume integrals using Gauss' Theorem. The volume integrals are then dropped giving the partial differential or microscopic form. This path works well when a detailed analysis is desired, such as subchannel flow in fuel bundles, moderator circulation in the calandria, etc.

The second school, which sees more favour among engineers, particularly in the chemical industry, evaluates the surface integrals as they stand without converting to volume integrals. This leads to a lumped or macroscopic approach useful for network analysis, distillation towers, etc.

There exists a very large number of possible derivations, each with its own advantages and disadvantages. As more and more detail is picked up in each class of models, numerical means have to be used. In the limit of large numbers of nodes or mesh points, etc., both methods converge to the same solution.

Since the above equations are basic to all subsequent modelling of thermalhydraulic systems, one should keep in mind the basis for these equations:

1) Conservation as an experimental observation.

This is usually taken for granted. However, when the conservation equations for separate phases in a mixture are under consideration, the various sinks and sources of mass, momentum

and energy are not entirely known and the interpretation of experimental data can be difficult because of the complexity. It helps to keep in mind the distinctly different roles that we have historically assigned to the players in the conservation process:

- a) the local time derivative, $\partial\psi/\partial t$,
- b) the advection term (flux), $\nabla\cdot\psi\mathbf{v}$,
- c) the local sinks and sources, Γ , within a volume and
- d) the local sinks and sources, \mathbf{S} , on the surface of a volume.

If a clarity of form is adopted by establishing and maintaining a one-to-one correspondence between the form and the physical processes, then a substantial pedagogical tool will have been achieved. This proves invaluable in experimental design (to zero in on a particular process or parameter), model formulation and interpretation, data analysis and presentation, correlation development, etc. A model could lose its generality because, for instance, fluxes across interfaces are written as a term in Γ , thus making the interfacial flux a local phenomena rather than a boundary phenomena. This may be acceptable for a single geometry but causes the model to break down when applied to diverse geometries.

2) The field variables are continuous within the volume V .

This is also usually taken for granted. But care must be exercised in multiphase flow where discontinuities abound. A common approach, taken to simplify the complexity of multiphase flow, is to average the terms in the conservation equations across the cross-sectional area of the flow path. One could speculate that the error introduced in this manner could separate the model from reality enough to make the solutions be "unreal", i.e. complex numbers, singularities, etc. Further, fluctuating parameters are often smoothed by averaging over an appropriate Δt . These averaged parameters and products of parameters are used in models and compared to experiments. But there is no guarantee that, for instance,

$$\frac{1}{\Delta t} \int_{\Delta t} \psi \mathbf{v} dt = \left(\frac{1}{\Delta t} \int_{\Delta t} \psi dt \right) \left(\frac{1}{\Delta t} \int_{\Delta t} \mathbf{v} dt \right).$$

Thus the use of time averaged parameters can lead to additional errors. Indeed, because of the possibility of error due to space and time discontinuities, several investigators have offered rigorous treatments for the distributed approach (see, for example, Delhay [DEL81]). There is no reason why these treatments could not be applied to the lumped approach, as well. But, at this time, there is little incentive to do so since grid coarseness and experimental data are larger sources of error. As always, the operative rule is - BUYER BEWARE.

We now proceed to treat the mass, momentum and energy equations in turn.

2.3 Conservation of Mass

Historically, mass was the first variable observed to be conserved:

$$\iiint_V \frac{\partial}{\partial t} (\gamma_k \rho_k) dV = - \iint_S \gamma_k \rho_k \mathbf{v}_k \cdot \mathbf{n} ds + \iiint_V \Gamma_k dV + \iint_S \mathbf{S}_k \cdot \mathbf{n} \cdot ds \quad (7)$$

where

- ρ_k = density of phase k (1 = liquid, 2 = vapour),
 γ_k = volume fraction of phase, k, in volume V, and
 Γ_k, \mathbf{S}_k = phase sinks and sources, including chemical and nuclear effects.

The average density is defined as:

$$\rho = \gamma_1 \rho_1 + \gamma_2 \rho_2 = (1 - \alpha) \rho_1 + \alpha \rho_2, \quad (8)$$

where ρ = average density, and

α = void fraction.

Adding both phases together, equation 7 becomes:

$$\begin{aligned} \iiint_V \frac{\partial}{\partial t} [(1 - \alpha) \rho_1 + \alpha \rho_2] dV &= - \iint_S [(1 - \alpha) \rho_1 \mathbf{v}_1 + \alpha \rho_2 \mathbf{v}_2] \cdot \mathbf{n} ds \\ &= + \iiint_V (\Gamma_1 + \Gamma_2) dV + \iint_S (\mathbf{S}_1 + \mathbf{S}_2) \cdot \mathbf{n} ds. \end{aligned} \quad (9)$$

In our case, $\Gamma_1 = -\Gamma_2$ (liquid boils or vapour condenses) and $\mathbf{S}_k = 0$ (no mass sources or sinks at surfaces). Therefore:

$$\iiint_V \frac{\partial \rho}{\partial t} dV = - \iint_S \rho \mathbf{v} \cdot \mathbf{n} ds \quad (10)$$

where

$$\rho \mathbf{v} = (1 - \alpha) \rho_1 \mathbf{v}_1 + \alpha \rho_2 \mathbf{v}_2. \quad (11)$$

If we apply Gauss' Theorem and drop the integrals we have:

$$\frac{\partial \rho}{\partial t} + \nabla \cdot \rho \mathbf{v} = 0 \quad (12)$$

or

$$\frac{\partial}{\partial t} [(1 - \alpha) \rho_1 + \alpha \rho_2] + \nabla \cdot [(1 - \alpha) \rho_1 \mathbf{v}_1 + \alpha \rho_2 \mathbf{v}_2] = 0. \quad (13)$$

This is the distributed form useful for modelling detailed flow patterns such as in the calandria, vessels, steam generators and headers. Component codes such as THIRST [CAR81a] and COBRA [BNW76] use this approach.

In contrast, system codes such as SOPHT [CHA77a], based on Porsching's work [POR71], use the lumped equations. These codes represent a hydraulic network of pipes by nodes joined by links, discussed in detail in section 3. Mass, pressure and energy changes occur at the nodes. Momentum changes occur in the links. Thus the network is treated on a macroscopic scale requiring an integral approach to the fundamental equations. Flow details in pipes are not

considered. That is, diffusion, dispersion, advection, flow regimes, flow profiles, etc. are not fundamentally accounted for but are covered by empirical correlations. Averaging techniques, commonly used in the distributed approach are not used in the lumped approach mainly because there is little incentive to do so. The main sources of error lie elsewhere, mainly in the coarseness of the discretization in the direction of flow (i.e. node size) and in friction factors and heat transfer coefficients.

Now, $\iiint \rho dV$ is the mass, M_i , in the volume, V_i , of the i^{th} node. Also, for our case, the surface integral can be written as surface integrals over the individual flow paths into and out of the volume or node. That is,

$$-\iint_S \rho \mathbf{v} \cdot \mathbf{n} ds = \sum_j \rho_j v_j A_j, \quad (14)$$

where j represents inflow and outflow links with $v_j > 0$ for inflow and < 0 for outflow. Inherent in equation 11 is the assumption that the integral, $\iint_S \rho \mathbf{v} \cdot \mathbf{n} ds$ can be replaced by the simple product $\rho_j v_j A_j$. This implies known or assumed (usually uniform) velocity and density profiles across the face of the link (or pipe).

Thus we now have:

$$\frac{\partial M_i}{\partial t} = \sum_j \rho_j v_j A_j \equiv \sum W_j, \quad (15)$$

where W_j is the mass flow. This is the typical representation in system codes. Thus for the node-link type equations, we must add two more assumptions:

- i) nodalization, and
- ii) assumed velocity and density profile across the cross-section of a pipe.

These assumptions have far reaching ramifications that may not be immediately obvious. This is discussed in more detail in section 3.

To conclude our progressive simplification, we note the steady state form of equation 15:

$$\sum_j \rho_j v_j A_j \equiv \sum W_j = 0. \quad (16)$$

For a simple circular flow loop, the mass flow rate at steady state is a constant at any point in the loop. Local area and density variations thus give rise to velocity variations around the loop.

Local velocity then is:

$$v = \frac{W}{\rho A}. \quad (17)$$

2.4 Conservation of Momentum

Newton observed that momentum is conserved, i.e. a body moves in a straight line unless

forced to do otherwise. This is equivalent to a force balance if the inertial force (a momentum sink of sorts) is recognized. In the integral sense, the rate of change of momentum is equal to the forces acting on the fluid. Thus:

$$\frac{D}{Dt} \iiint_V \gamma_k \rho_k \mathbf{v}_k dV = \iint_S \boldsymbol{\sigma}_k \cdot \mathbf{n} ds + \iiint_V \gamma_k \rho_k \mathbf{f}_k dV + \iiint_V \mathbf{M}_k dV, \quad (18)$$

where

$\boldsymbol{\sigma}$ is the stress tensor (i.e., short range or surface effects including pressure, viscosity, etc.),

\mathbf{f} is the long range or body force (i.e., gravity),

and \mathbf{M} is the momentum interchange function accounting for phase change effects.

Using Reynold's Transport Theorem, we get:

$$\begin{aligned} & \iiint_V \frac{\partial}{\partial t} (\gamma_k \rho_k \mathbf{v}_k) dV + \iint_S (\gamma_k \rho_k \mathbf{v}_k) (\mathbf{v}_k \cdot \mathbf{n}) ds \\ &= \iint_S \boldsymbol{\sigma}_k \cdot \mathbf{n} ds + \iiint_V \gamma_k \rho_k \mathbf{f}_k dV + \iiint_V \mathbf{M}_k dV. \end{aligned} \quad (19)$$

Adding both phases together as per the mass equation, we find:

$$\iiint_V \frac{\partial}{\partial t} \rho \mathbf{v} dV + \iint_S \rho \mathbf{v} (\mathbf{v} \cdot \mathbf{n}) ds = \iint_S \boldsymbol{\sigma} \cdot \mathbf{n} ds + \iiint_V \rho \mathbf{f} dV. \quad (20)$$

To get the microscopic form we use Gauss's theorem and drop the volume integral as before to leave:

$$\frac{\partial}{\partial t} (\rho \mathbf{v}) + \nabla \cdot \rho \mathbf{v} \mathbf{v} = \nabla \cdot \boldsymbol{\sigma} + \rho \mathbf{f}. \quad (21)$$

The stress tensor, $\boldsymbol{\sigma}$, can be split into the normal and shear components:

$$\boldsymbol{\sigma} = -P\mathbf{I} + \boldsymbol{\tau}, \quad (22)$$

where P is the pressure, \mathbf{I} is the unity tensor and $\boldsymbol{\tau}$ is the shear stress tensor. This enables the explicit use of pressure and helps maintain our tenuous link with reality. Of course, it can equally be introduced in the integral form, equation 20, or as a separate pressure for each phase in equation 19. At any rate, equation 21 becomes:

$$\frac{\partial}{\partial t} (\rho \mathbf{v}) + \nabla \cdot \rho \mathbf{v} \mathbf{v} = -\nabla P + \nabla \cdot \boldsymbol{\tau} + \rho \mathbf{f}. \quad (23)$$

This is the form commonly seen in the literature, useful for distributed modelling as per the mass conservation equation. The term, $\nabla \cdot \boldsymbol{\tau}$, is usually replaced by an empirical relation. For the system codes using the node-link structure, we switch back to the macroscopic form, Equation 20.

If the surface integral for the advective term is performed over the inlet and outlet areas of the

pipe (link) in question, then:

$$\iint_S \rho \mathbf{v}(\mathbf{v} \cdot \mathbf{n}) ds = \iint_{A_{in}} \rho \mathbf{v}(\mathbf{v} \cdot \mathbf{n}) ds + \iint_{A_{out}} \rho \mathbf{v}(\mathbf{v} \cdot \mathbf{n}) ds \quad (24)$$

where A_{IN} is the flow inlet area and A_{OUT} is the flow outlet area. If we assume the properties are constant over the areas, then:

$$V \frac{\partial \rho \mathbf{v}}{\partial t} - A_{IN} \rho_{IN} \mathbf{v}_{IN} \mathbf{v}_{IN} + A_{OUT} \rho_{OUT} \mathbf{v}_{OUT} \mathbf{v}_{OUT} = \iint_S \boldsymbol{\sigma}_k \cdot \mathbf{n} \cdot ds + \iiint_V \rho \mathbf{f} dV \quad (25)$$

Alternatively we could perform a cross-sectional average of each term, usually denoted by $\langle \rangle$, where $\langle () \rangle = 1/A \iint_S () ds$. If we assume the properties, V , ρ and A are constant along the length of the pipe, then the second and third terms cancel.

Equation 25 can be rewritten as:

$$\begin{aligned} V \frac{\partial \rho \mathbf{v}}{\partial t} &= - \iint \mathbf{P} \mathbf{I} \cdot \mathbf{n} ds + \iiint (\nabla \cdot \bar{\boldsymbol{\tau}} + \rho \bar{\mathbf{f}}) dV \\ &= -A_{OUT} \mathbf{P}_{OUT} + A_{IN} \mathbf{P}_{IN} - \frac{V\rho}{L} \left(\frac{fL}{D} + k \right) \frac{\mathbf{v}|\mathbf{v}|}{2g_c} - LA\rho \sin(\theta) \left(\frac{\mathbf{g}}{g_c} \right) \end{aligned} \quad (26)$$

where g_c is the gravitational constant, \mathbf{g} is the acceleration due to gravity and where $\nabla \cdot \bar{\boldsymbol{\tau}}$ and $\rho \bar{\mathbf{f}}$ evaluated by empirical correlations (the standard friction factor) plus an elevation change term (θ is the angle w.r.t. the horizontal). Note that if $A_{OUT} \neq A_{IN}$ then, even for constant pressure, there is a net force on the volume causing it to accelerate if it were not restrained. In a restrained system such as HTS piping, the piping supports exert an equal and opposite force on the volume. Thus when the area differences are explicitly modelled, the appropriate body forces must be included. Generally, it is simpler to use an average or representative area for the IN and OUT surfaces and to add entrance and exit frictional losses explicitly in the $(fL/D+k)$ term.

Assuming one dimensional flow and defining the mass flow as $W \equiv \rho VA$, and L as the pipe length, equation 26 becomes:

$$\frac{\partial W}{\partial t} = \frac{A}{L} \left[(P_{IN} - P_{OUT}) - \left(\frac{fL}{D} + k \right) \frac{W^2}{2g_c \rho A^2} \right] - A\rho \frac{g}{g_c} \sin(\theta) \quad (27)$$

which is the form typically used in system codes.

If circumstances require, extra terms can be added. For instance, if a pump is present this can be considered to be an external force acting through head, ΔP_{pump} . Equation 27 would then become:

$$L \frac{\partial W}{\partial t} = -A_{OUT} P_{OUT} + A_{IN} P_{IN} + A \Delta P_{PUMP} \quad (28)$$

The momentum flux terms (ρv^2) in equation 25 could also be added if large area or property changes were present or the effect could be included in the friction term.

In the steady state, for a constant area pipe with no pump and no elevation change:

$$P_{IN} - P_{OUT} = \rho \left(\frac{fL}{D} + k \right) \frac{V^2}{2g_c} = \left(\frac{fL}{D} + k \right) \frac{W^2}{2A^2 \rho g_c} + \Delta P_{PUMP} + \dots \quad (29)$$

As a final note, the assumptions made for the mixture momentum equation are thus similar to those made for the mixture mass equation and the same comments apply. One cannot hope to accurately model such phenomena as void propagation and other two phase transient flow effects using lumped single phase equations unless a large number of nodes and links are used.

2.5 Conservation of Energy

By the early 1800's, philosophical jumps were made in recognizing that heat was not a substance and in the emergence of electromagnetic theory. The concept of energy as we now think of it was formulated and it was found that energy, too, was conserved, as long as we carefully identify all the different forms of energy (kinetic, chemical, potential, nuclear, internal, electromagnetic, ...).

The mathematical statement of the conservation of energy is:

$$\begin{aligned} \frac{D}{Dt} \iiint_V \gamma_k \rho_k \left(e_k + \frac{1}{2} v_k^2 \right) dV = & - \iint_S \mathbf{q}_k \cdot \mathbf{n} ds + \iiint_V E_k dV \\ & + \iiint_V \gamma_k \rho_k \mathbf{f}_k \cdot \mathbf{v}_k dV + \iint_S (\boldsymbol{\sigma}_k \cdot \mathbf{n}) \cdot \mathbf{v}_k ds, \end{aligned} \quad (30)$$

where

- e_k = internal energy of phase k,
- q_k = surface heat flux for phase k, and
- E_k = internal heat sources and sinks of phase k.

The left hand side is the substantial derivative of the internal plus kinetic energy. The right hand side terms are, respectively:

- 1) surface heat flux,
- 2) internal sources and sinks,
- 3) work due to long range body forces (gravity, etc.),
- 4) work due to short range forces (surface tension, pressure, etc.).

Using Reynold's Transport Theorem again:

$$\begin{aligned}
& \iiint_V \frac{\partial}{\partial t} \left[\gamma_k \rho_k \left(e_k + \frac{1}{2} v_k^2 \right) \right] dV + \iint_S \gamma_k \rho_k \left(e_k + \frac{1}{2} v_k^2 \right) \mathbf{v}_k \cdot \mathbf{n} ds \\
& = - \iint_S \mathbf{q}_k \cdot \mathbf{n} ds + \iiint_V E_k dV + \iiint_V \gamma_k \rho_k \mathbf{f}_k \cdot \mathbf{v}_k dV + \iint_S (\boldsymbol{\sigma}_k \cdot \mathbf{n}) \cdot \mathbf{v}_k ds.
\end{aligned} \tag{31}$$

Summing over k , the mixture equation becomes:

$$\begin{aligned}
& \iiint_V \frac{\partial}{\partial t} \left[\rho e + \frac{1}{2} \rho v^2 \right] dV + \iint_S \left[\rho e + \frac{1}{2} \rho v^2 \right] \mathbf{v} \cdot \mathbf{n} ds \\
& = - \iint_S \mathbf{q} \cdot \mathbf{n} ds + \iiint_V E dV + \iiint_V \rho \mathbf{f} \cdot \mathbf{v} dV + \iint_S (\boldsymbol{\sigma} \cdot \mathbf{v}) \cdot \mathbf{v} ds,
\end{aligned} \tag{32}$$

where

$$\rho e = \gamma_1 \rho_1 e_1 + \gamma_2 \rho_2 e_2 \quad E = E_1 + E_2, \text{ etc.}$$

Using Gauss' Theorem to change some of the surface integrals to volume integrals:

$$\begin{aligned}
& \iiint_V \frac{\partial}{\partial t} \left[\rho e + \frac{1}{2} \rho v^2 \right] dV + \iint_S \rho e \mathbf{v} \cdot \mathbf{n} ds + \iiint_V \nabla \cdot \left[\frac{1}{2} \rho v^2 \mathbf{v} \right] dV \\
& = - \iint_S \mathbf{q} \cdot \mathbf{n} ds + \iiint_V E dV + \iiint_V \rho \mathbf{f} \cdot \mathbf{v} dV + \iiint_V \nabla \cdot (\boldsymbol{\sigma} \cdot \mathbf{v}) dV.
\end{aligned} \tag{33}$$

Since

$$\boldsymbol{\sigma} = -P\mathbf{I} + \boldsymbol{\tau},$$

$$\iiint_V \nabla \cdot (\boldsymbol{\sigma} \cdot \mathbf{v}) dV = \iiint_V [\nabla \cdot (\boldsymbol{\tau} \cdot \mathbf{v}) - \nabla \cdot (P\mathbf{v})] dV.$$

This is the total energy equation, composed of thermal terms and mechanical terms. We can separate the two by first generating the mechanical terms from the momentum equation (equation 20). Forming the dot product with velocity we get:

$$\begin{aligned}
& \iiint_V \frac{\partial}{\partial t} (\rho \mathbf{v}) \cdot \mathbf{v} dV + \iiint_V \mathbf{v} \cdot (\nabla \cdot \rho \mathbf{v} \mathbf{v}) dV = \iiint_V \mathbf{v} \cdot (\nabla \cdot \boldsymbol{\tau}) dV \\
& \quad - \iiint_V \mathbf{v} \cdot \nabla P dV + \iiint_V \rho \mathbf{f} \cdot \mathbf{v} dV.
\end{aligned} \tag{34}$$

Now

$$\mathbf{v} \cdot (\nabla \cdot \boldsymbol{\tau}) = \nabla \cdot (\boldsymbol{\tau} \cdot \mathbf{v}) - \boldsymbol{\tau} : \nabla \mathbf{v}, \tag{35}$$

$$\mathbf{v} \cdot \nabla P = \nabla \cdot (P\mathbf{v}) - P \nabla \cdot \mathbf{v}, \tag{36}$$

$$\mathbf{v} \cdot \frac{\partial}{\partial t} (\rho \mathbf{v}) = \frac{\partial}{\partial t} \left(\frac{1}{2} \rho \mathbf{v} \cdot \mathbf{v} \right) = \frac{\partial}{\partial t} \left(\frac{1}{2} \rho v^2 \right) \tag{37}$$

and

$$\mathbf{v} \cdot (\nabla \cdot \rho \mathbf{v} \mathbf{v}) = \nabla \cdot \left(\frac{1}{2} \rho v^2 \mathbf{v} \right). \quad (38)$$

Using these identities and subtracting equation 34 from equation 33, we get:

$$\begin{aligned} \iiint_V \frac{\partial}{\partial t} (\rho e) dV + \iint_S \rho e \mathbf{v} \cdot \mathbf{n} ds = - \iint_S \mathbf{q} \cdot \mathbf{n} ds \\ + \iiint_V E dV + \iiint_V \boldsymbol{\tau} : \nabla \mathbf{v} dV - \iiint_V \rho \nabla \cdot \mathbf{v} dV. \end{aligned} \quad (39)$$

This is the thermal form of the energy equation. This form of the energy equation can be used to generate the thermal conductance equation for solids. By setting fluid velocity to zero and converting surface integrals to volume integrals we get the distributed form:

$$\frac{\partial}{\partial t} (\rho e) = -\nabla \cdot \mathbf{q} + E, \quad (40)$$

where E is the internal energy generation rate term.

From thermodynamics, for solids, we have:

$$\frac{\partial}{\partial t} (\rho e) \geq \rho \frac{\partial e}{\partial t} \geq \rho C_v \frac{\partial T}{\partial t}, \quad (41)$$

and using Fourier's law for heat conduction:

$$\mathbf{q} = -k \nabla T, \quad (42)$$

we have the classical form of the heat conduction equation:

$$\begin{aligned} \rho C_v \frac{\partial T}{\partial t} &= \nabla \cdot k \nabla T + E \\ &= k \nabla^2 T + E \quad \text{space independent } k. \end{aligned} \quad (43)$$

This is useful for determining the temperature distributions in boiler tube walls, piping walls and reactor fuel pencils. To generate the node-link forms we now turn back to the integral form of equation 39. If we assume that the density and enthalpy are uniform over the node (the volume in question), then

$$\iiint_V \frac{\partial}{\partial t} (\rho e) dV = \frac{\partial U}{\partial t}, \quad (44)$$

where

$$U \equiv \int_V \rho e = LA \rho e. \quad (45)$$

The integral of the transport term can be written over the flow surfaces:

$$\iint_S \rho e \mathbf{v} \cdot \mathbf{n} ds = \iint_{A_1} \rho e \mathbf{v} \cdot \mathbf{n} ds + \iint_{A_2} \rho e \mathbf{v} \cdot \mathbf{n} ds + \dots, \quad (46)$$

where A_1 , A_2 , etc., are the pipe flow cross-sectional areas. For inflow, $\mathbf{v} \cdot \mathbf{n}$ is negative. For outflow, $\mathbf{v} \cdot \mathbf{n}$ is positive. Assuming uniform velocity, enthalpy and density across the link (pipe) cross-section gives:

$$\iint_S \rho e \mathbf{v} \cdot \mathbf{n} ds = - \sum_{\text{INFLOW}} \rho e v A_i + \sum_{\text{OUTFLOW}} \rho e v A = - \sum W_{\text{IN}} e_{\text{IN}} + \sum W_{\text{OUT}} e_{\text{OUT}} \quad (47)$$

The heat flux and generation terms of the thermal energy equation can be lumped into a loosely defined heat source for the volume.

$$- \iint_S \mathbf{q} \cdot \mathbf{n} ds + \iiint_V E dV \equiv Q. \quad (48)$$

Therefore, the thermal energy equation becomes:

$$\frac{\partial U}{\partial t} = \sum W_{\text{IN}} e_{\text{IN}} - \sum W_{\text{OUT}} e_{\text{OUT}} + Q + \iiint_V \boldsymbol{\tau} : \nabla \mathbf{v} dV - \iiint_V P \nabla \cdot \mathbf{v} dV \quad (49)$$

The last two terms are the irreversible and reversible internal energy conversion, respectively.

Some system codes track enthalpy rather than internal energy. Defining:

$$h = \text{enthalpy} = e + \frac{P}{\rho} \text{ and } H = Vph. \quad (50)$$

we can rewrite equation 39 as follows:

$$\begin{aligned} \iiint_V \frac{\partial (\rho h - P)}{\partial t} dV + \iint_S (\rho h - P) \mathbf{v} \cdot \mathbf{n} ds = & - \iint_S \mathbf{q} \cdot \mathbf{n} ds \\ & + \iiint_V E dV + \iiint_V \boldsymbol{\tau} : \nabla \mathbf{v} dV - \int_V P \nabla \cdot \mathbf{v} dV. \end{aligned} \quad (51)$$

Collecting the pressure terms and simplifying yields:

$$\begin{aligned} \iiint_V \frac{\partial}{\partial t} (\rho h) dV + \iint_S \rho h \mathbf{v} \cdot \mathbf{n} ds = & - \iint_S \mathbf{q} \cdot \mathbf{n} ds + \iiint_V E dV \\ & + \iiint_V \boldsymbol{\tau} : \nabla \mathbf{v} + \iiint_V \frac{\partial P}{\partial t} dV + \iint_S P \mathbf{v} \cdot \mathbf{n} ds - \iiint_V P \nabla \cdot \mathbf{v} dV. \end{aligned} \quad (52)$$

The surface integral over P can be transformed into a volume integral using Gauss' theorem and combined with the last term to give:

$$\begin{aligned} \iint_S P \mathbf{v} \cdot \mathbf{n} ds - \iiint_V P \nabla \cdot \mathbf{v} dV &= \iiint_V \nabla \cdot (P \mathbf{v}) dV - \iiint_V P \nabla \cdot \mathbf{v} dV \\ &= \iiint_V \mathbf{v} \cdot \nabla P dV. \end{aligned} \quad (53)$$

The enthalpy flux terms can be evaluated in the same manner that the energy flux terms were in equations 46-47. Thus,

$$\iint_S \rho \mathbf{v} \cdot \mathbf{n} ds = -\sum W_{IN} h_{IN} + \sum W_{OUT} h_{OUT}. \quad (54)$$

Finally, using equations 48, 50, 53-54, equation 52 becomes:

$$\frac{\partial H}{\partial t} = +\sum W_{IN} h_{IN} - \sum W_{OUT} h_{OUT} + Q + \iiint_V \boldsymbol{\tau} : \nabla \mathbf{v} dV + \iiint_V \left(\frac{\partial P}{\partial t} + \mathbf{v} \cdot \nabla P \right) dV. \quad (55)$$

The integral term involving pressure is often neglected since it is usually negligible compared to the other terms. For instance, the typical CANDU Heat Transport System operates at a pressure of 10 MPa, a fluid velocity of ~10 m/s, and a pressure gradient of less than 70 kPa/m. This translates into roughly 10 kJ/kg while e is approximately 1000 kJ/kg.

The turbulent heating term is usually approximated by adding pump heat as a specific form of Q .

equation 55 in the steady state, neglecting turbulent heating and the pressure terms, is the familiar:

$$Q = -\sum W_{IN} h_{IN} + \sum W_{OUT} h_{OUT}. \quad (56)$$

For a reactor or a boiler (one flow in, one flow out):

$$Q = W(h_{OUT} - h_{IN}) = WC_p (T_{OUT} - T_{IN}) \text{ in single phase.} \quad (57)$$

Another special case of equation 55 is obtained by expanding the term Q as per equation 48:

$$-\iint_S \mathbf{q} \cdot \mathbf{n} ds + \iiint_V E dV \equiv Q. \quad (48)$$

Using Newton's Law of cooling for convection:

$$\mathbf{q} \cdot \mathbf{n} = h_N (T - T_s), \quad (58)$$

where

$\mathbf{q} \cdot \mathbf{n}$	=	heat flux normal to surface, s ,
T	=	Temperature of fluid
T_s	=	Temperature of surface (wall), and
h_N	=	heat transfer coefficient,

Equation 55, neglecting the pressure terms, becomes:

$$\begin{aligned} \mathbf{v} \frac{\partial \rho h}{\partial t} - \mathbf{v} \frac{\partial P}{\partial t} \left(\equiv \mathbf{v} \frac{\partial \rho e}{\partial t} \approx \mathbf{v} \rho C_v \frac{\partial T}{\partial t} \right) &= \sum W_{IN} h_{IN} - \sum W_{OUT} h_{OUT} \\ -A h_N (T - T_s) + \mathbf{v} E + \iiint_V \boldsymbol{\tau} : \nabla \mathbf{v} dV & \end{aligned} \quad (59)$$

which is useful for accounting for heat transfer between the fluid and the pipe or tube walls (eg: boiler heat transfer).

The heat transfer coefficient, h_N , is supplied through empirical relations. The turbulent heating term $\iiint_V \boldsymbol{\tau} : \nabla \mathbf{v} dV$ generally can be neglected or added as a pump heat term.

2.6 The Equation of State

From the conservation equations, we have three equations for each phase (mass, momentum and energy conservation) and four unknowns:

- 1) density, ρ or mass, $V\rho$,
- 2) velocity, \mathbf{v} , or mass flow, W , or momentum, $\rho\mathbf{v}$,
- 3) energy, e , or enthalpy, $h = e + P/\rho$, or temperature, $T = \text{fn}(e)$ or $\text{fn}(h)$, and
- 4) pressure, P .

The fourth equation required for closure is the equation of state:

$$P = \text{fn}(h, \rho) \quad \rho = \text{fn}(P, T), \text{ etc.} \quad (60)$$

Thermodynamic equilibrium is usually assumed. For water, H_2O or D_2O , tables of properties give the required functional relationship. Often, a curve fit of the tables is used. This data is input to the computer codes and utilized in table lookup schemes or directly via the parametric curve fits.

The equation of state is discussed in detail in Section 4.

2.7 Empirical Correlations

As previously discussed, supporting relations are required to provide the necessary information for the conservation and state equations. The primary areas where support is needed are:

- 1) relationship between quality and void fractions, i.e., slip velocities in two phase flow (to link the mass and enthalpy via the state equation);
- 2) the stress tensor, $\boldsymbol{\tau}$ (effects of wall shear, turbulence, flow regime and fluid properties on momentum or, in a word: friction);
- 3) heat transfer coefficients (to give the heat energy transfer for a given temperature distribution in heat exchangers, including steam generators and reactors);
- 4) thermodynamic properties for the equation of state;
- 5) flow regime maps to guide the selection of empirical correlations appropriate to the flow regime in question;
- 6) special component data for pumps, valves, steam drums, pressurizers, bleed or degasser condensers, etc; and

- 7) critical heat flux information (this is not needed for the solution of the process equations but a measure of engineering limits is needed to guide the use of the solutions of the process equations as applied to process design;

The above list of correlations, large enough in its own right, is but a subset of the full list that would be required were it not for a number of key simplifying assumptions made in the derivation of the basic equations. The three major assumptions made for the primary heat transport system are:

- 1) one dimensional flow;
- 2) thermal equilibrium (except for the pressurizer under insurge); and
- 3) one fluid model (i.e. mixture equations).

These are required because of state of the art limitations (however, two fluid models are being used increasingly in recent years.). Empirical correlations were discussed in more detail in Chapter 6.

2.8 Solution Overview

Because of the complexity of solving the mass, momentum and energy equations plus supporting equations of state and empirical correlations all subject to initial and boundary conditions, it is quite easy to "not see the forest for the trees". A skeleton overview may help in this regard. Figure 1 illustrates the equations and the information links between them. In words, the momentum equation gives the flows or velocities from one node to another, or from one grid point to another, based on a given pressure, flow, mass and energy distribution. The updated flows are used by the mass and energy equations to update the mass and energy contents at each location. The new mass and energy are given to the equation of state to update the pressure distribution. The new pressure, along with the new densities and energies are used by the momentum equation, and so on. In this manner, a time history of the fluid evolution is obtained. Of course, only the main variables are noted. The numerous

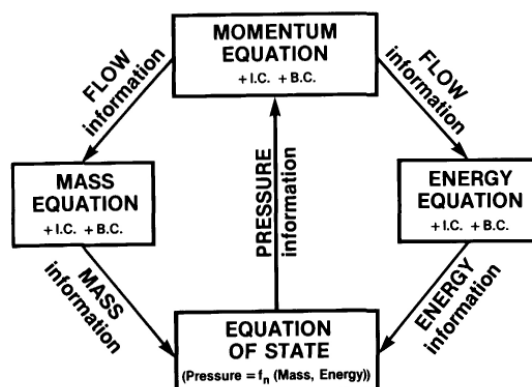


Figure 1 The four cornerstone single phase flow equations and the flow of information between them.

and diverse empirical correlations require updates on the main variables and many secondary variables. This information also "flows" around the calculation.

A further point to note on the solution overview is that each phase in a multiphase flow has a main information flow path as shown in figure 2. In the full UVUEUP (unequal velocity, energy and pressure) model, there are two distinct phases: one for the vapour phase and one for the liquid phase. If a simplified model was imposed, this essentially means that the planes would touch at some point. For instance, if equal pressure in both phases was assumed, then figure 3 would result. Here, the equation of state is common to both planes.

The HEM (homogeneous equilibrium model) is the fully collapsed case where both planes collapse into one (figure 1). You may find these images to be useful in conceptualizing the basic equations and how they fit together.

The precise solution procedure that you might employ is case dependent. At present, no general solution scheme exists because the nuances of specific problems are subtle and because one cannot usually afford to ignore the efficiency and cost savings gained by tuning a method to a particular case. The economics of using a case specific code are changing, however, with developments in the microcomputer field and with the realization that total design and analysis time can often be reduced by using a less efficient but more robust code. Codes such as SOPHT and CATHENA [HAN95] are a direct result of this realization. The near term evolution will likely be affected mostly by microcomputer developments.

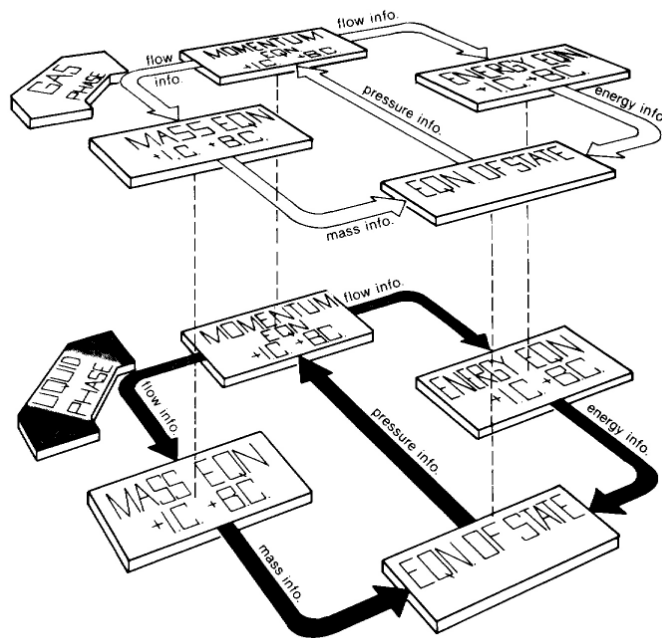


Figure 2 The four cornerstone equations for the two-fluid model.

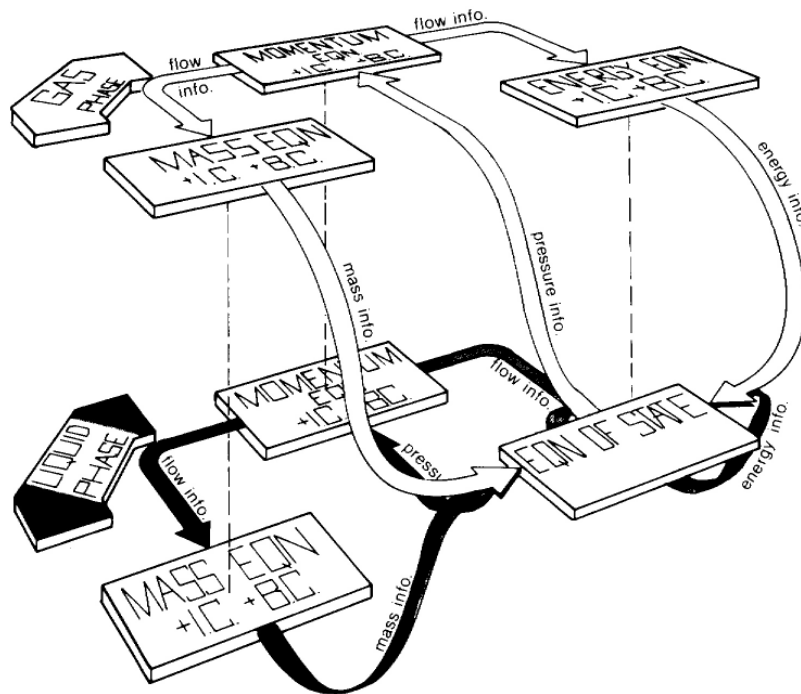


Figure 3 The four cornerstone equations for the full two-fluid model with equal pressure of the two phases.

2.9 Problems

1. Referring to figure 1:
 - a. Explain the inter-relationship between the mass, momentum and energy equations and the equation of state.
 - b. For the integral form, devise a simple solution scheme for the transient equations. Show what equations are being solved and how they are being solved. Flow chart your scheme.

3 Nodalization

3.1 Introduction

This section focuses on establishing a rationale for, and the setting up of, the geometric representation of thermalhydraulic systems. The hydraulic network is represented by a series of interconnected nodes to form a node-link diagram.

The exploration proceeds by first establishing and discussing the governing rationale. Next, limitations of the approximation are presented and examples are given. Finally, the matrix approach is used to capture the system geometry in a succinct form.

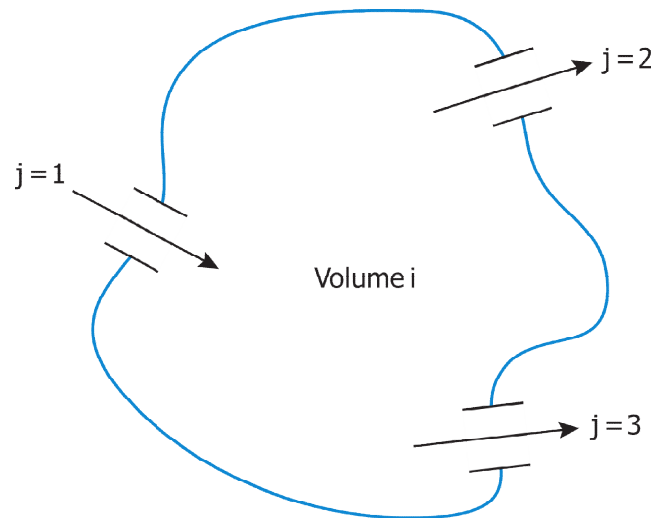
3.2 The Node-Link Concept

From section 2 we have the integral mass, momentum and energy equations for an arbitrary volume, i , with material flow through various surfaces, designated by the subscript j (see figure 4):

$$\frac{\partial M_i}{\partial t} = \sum_j \rho_j v_j A_j \equiv \sum W_j, \quad (61)$$

$$\frac{\partial W}{\partial t} = \frac{A}{L} \left[(P_{IN} - P_{OUT}) - \left(\frac{fL}{D} + k \right) \frac{W^2}{2g_c \rho A^2} \right] - A \rho g / g_c \sin(\theta) \quad (62)$$

$$\frac{\partial H}{\partial t} = \sum W_{IN} h_{IN} - \sum W_{OUT} h_{OUT} + Q \quad (63)$$



Nodes are designated by the subscript i
Links are designated by the subscript j

Figure 4 A general node and connecting links.

These mass and energy equations are averaged over the volume in question, hence they do not capture any detail within the volume. Knowing the mass and energy of a volume, the equation of state gives the pressure. Flow, however, is driven by pressure differences. Hence it naturally follows that the momentum equation should be applied between the points of known pressure, ie, between volumes. In the distributed approach, this is called the staggered grid method. In the lumped approach, it is called the node-link method and is illustrated in figure 5. Volumes are represented by nodes, flow paths are represented by links.

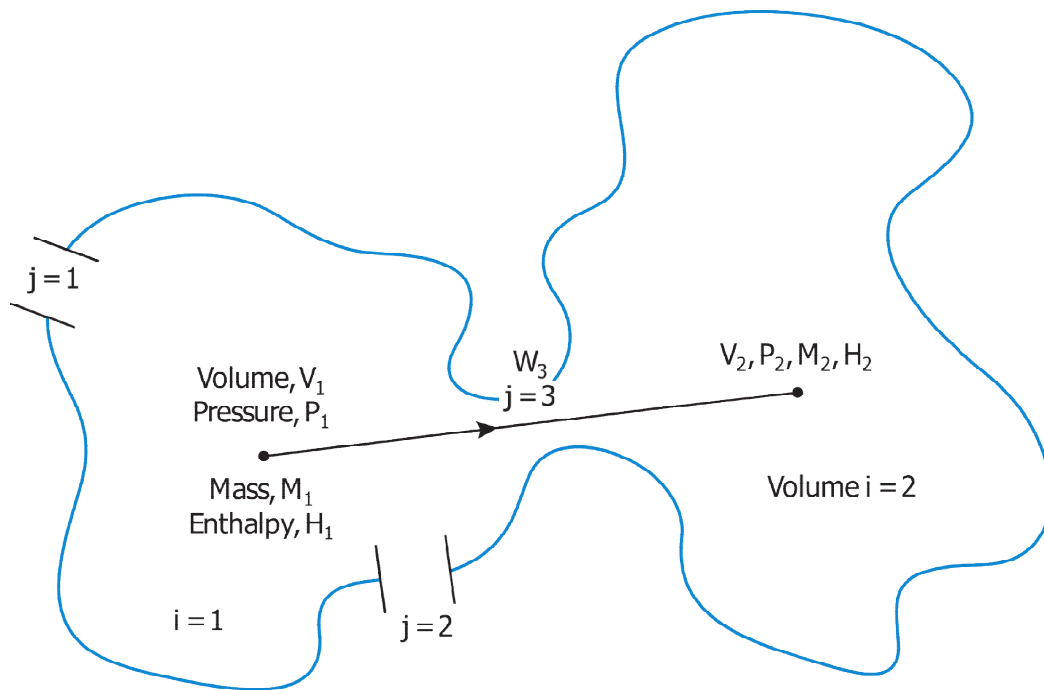


Figure 5 Two connected nodes.

To assign nodes and links to a given piping configuration, say the simple pipe of figure 6, it is best to first focus on the flow modelling. The key question to ask is: Where should the link endpoints (ie the node centres) be placed? The node centre locations define the positions at which the pressure will be evaluated and this is important for correct flow calculations. For constant area pipes, the placement is not critical but at junctions and area changes, modelling is simplified if node centres are placed at junctions and pipe area changes. For the case shown in figure 7 (a), if the flow were going from left to right and the junction resistance were included in link 1, then the pressure at node 2 would be the pressure just downstream of the junction. Carefully plan the node-link configuration to match the problem at hand. If possible, avoid running links across area changes since this inserts ambiguity into the flow area of the link model, as illustrated in figure 7 (b).

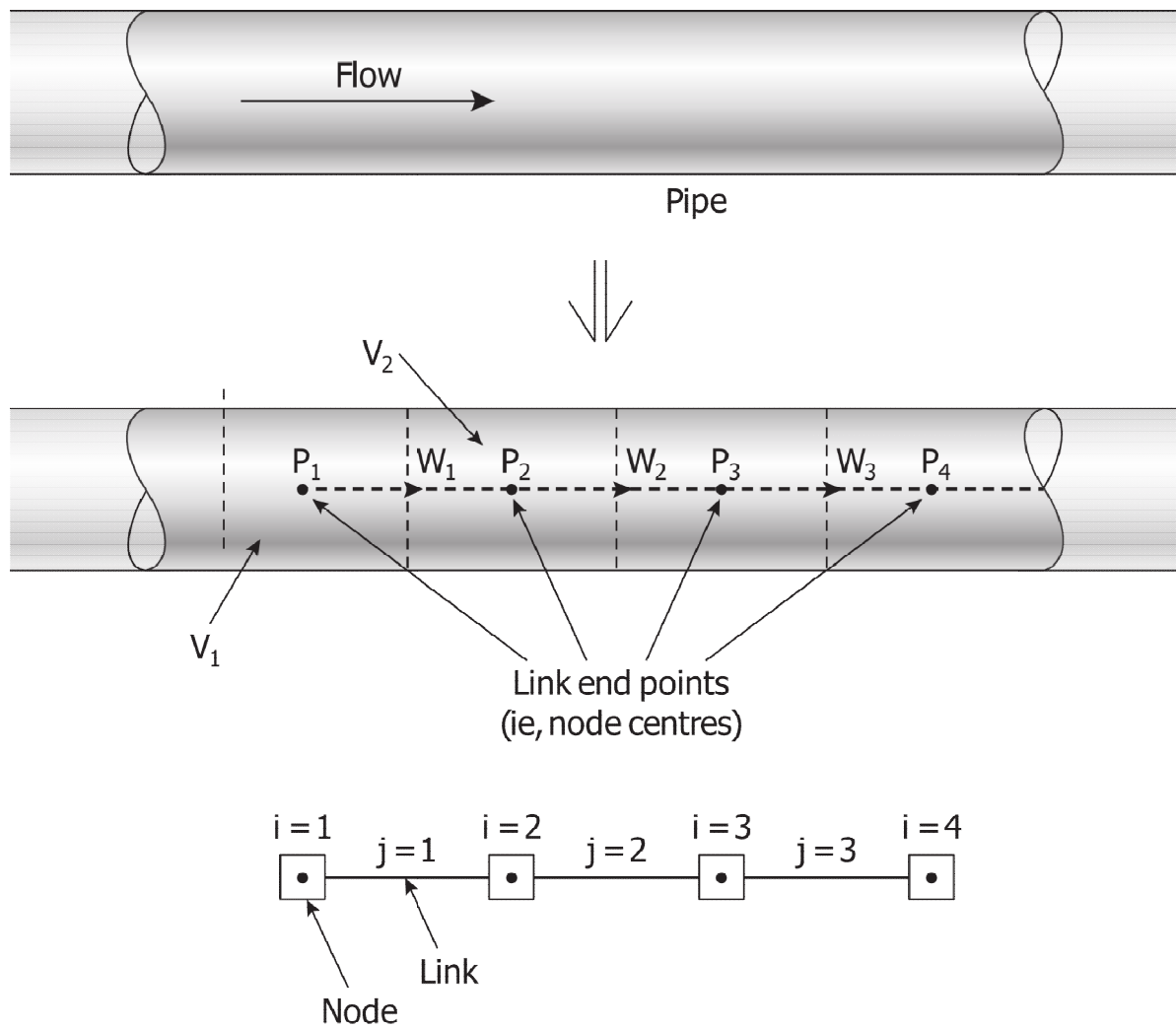
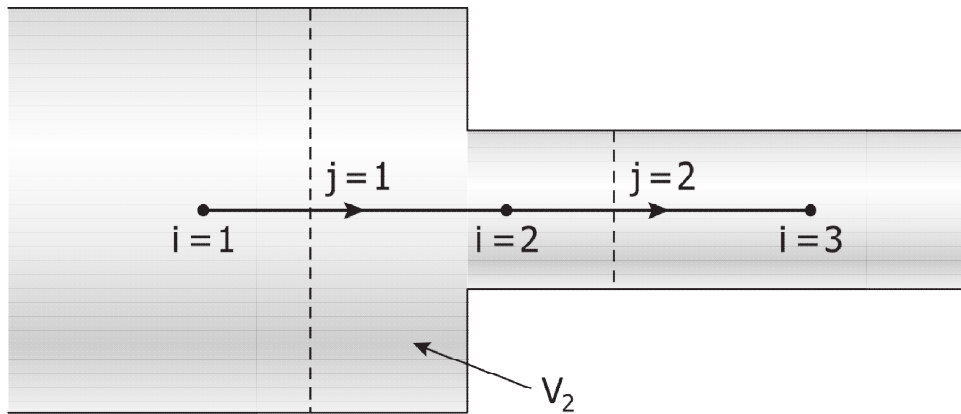
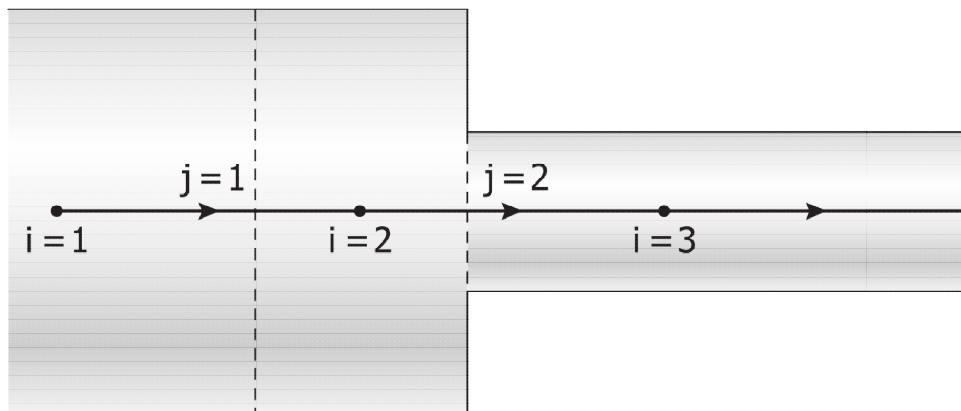


Figure 6 Node-link setup for a simple pipe.



(a) Recommended



(b) Not recommended

Figure 7 Node-link setup for an area change in a pipe.

Hydraulic friction can be affected by flow direction. Figure 7 illustrates a simple pipe flow situation wherein there is a step change in area. Flow from left to right experiences a different junction resistance than flow going from right to left. Direction dependent resistances are usually modelled explicitly in the system codes. The momentum flux terms, $\Delta\rho v^2$, can either be modelled explicitly or through the resistance coefficient, k . Note that a simple force balance around the junction would show that there is a net lateral force on the pipe. This force imbalance would have to be accounted for by a body force if different inlet and outlet pipe areas were used. This is another reason that links are chosen to coincide with constant pipe length sections.

The properties of the fluid within the link are a result of the properties of the upstream node. As the fluid is transported along a flow path (ie along the link), the link properties will change over time. Naturally there will be a transport delay but given that the nodal properties are themselves average values that change relatively slowly over time, system simulation codes typically assume that the link properties are just the same as the upstream nodal properties. For most purposes this is an acceptable assumption that can be lessened by using more nodes and links in the model. One has to be careful, however, of flow reversal situations that involve two-phase flow since this can lead to rapid and large density changes in the link.

The node volume is usually assigned as the fluid surrounding the node centre as shown in figure 7(a). But this is not a critical assignment; the node “centres” can actually be at the edge of the volume if that proves convenient. From a numerical point of view, it is beneficial to divide the hydraulic network up into volumes of roughly equal size since the properties in small volumes can change very rapidly and thus force the use of correspondingly small time steps. This rationalization of the volume assignments may force the user to take some liberties with the notion of a node “centre”.

To recap, the momentum equation is used to solve for W_j in all links, driven by upstream and downstream pressure differences and retarded / accelerated by friction, elevation change, pumps, etc. that appear in the links. This flow transports mass and energy to and from the nodes. Local heat sources and sinks, such as surface heat fluxes, are modelled at the nodes.

3.3 Nodal Diffusion

In the node - link representation of flow in a pipe, no flow detail is considered as the fluid moves along the pipe. Therefore, no diffusion, dispersion, advection, flow profiles or flow regimes are explicitly permitted. This is not too crude an approximation for the calculation of pressure drops and flows but for modelling the propagation of disturbances, this approach is inadequate as it stands unless a large number of nodes and links are used.

To show this, consider a homogeneous or bubbly flow through a pipe, as in the two-phase regions of typical heat transport systems in nuclear reactors, modelled in system codes as nodes connected by links. Perfect mixing at the nodes is assumed. Flow in a pipe, however, has aspects of plug flow. That is, flow is transmitted along the pipe relatively undisturbed. If no diffusion or turbulent dispersion existed, a sharp discontinuity in a property would propagate undisturbed. Figure 8 shows how the discontinuity would move in time and space. The left

to right movement is due to the velocity, v , while the spreading out is due to diffusion. If a single mixing tank (node) represented a section of pipe of volume, $V \text{ m}^3$, and volumetric flow, $f \text{ m}^3/\text{s}$, then a step change to zero in a field property, C , (which could be concentration or density) entering the node would be an exponential by the time it left the node, that is:

$$C_{\text{OUT}} = C_{\text{IN}} \cdot e^{-\frac{t}{\tau}} \quad (64)$$

where $\tau = V/f$; τ is also the transmission time for the plug flow model. If the pipe were modelled by two nodes in series,

$$C_{\text{OUT NODE2}} = C_{\text{IN NODE1}} \left(1 + \frac{2t}{\tau} \right) e^{-\frac{2t}{\tau}} \quad (65)$$

and in general, for n nodes:

$$C_{\text{OUT NODE2}} = C_{\text{IN NODE1}} e^{-\frac{n \cdot t}{\tau}} \sum_{k=1}^N \left(\frac{nt}{\tau} \right)^{k-1} \frac{1}{(n-1)!} \quad (66)$$

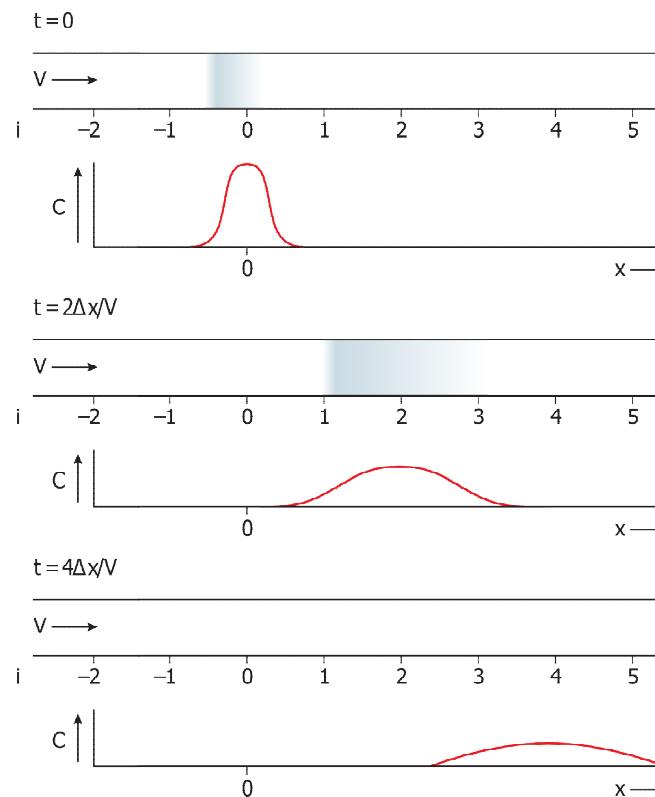


Figure 8 Illustration of convection and diffusion.

Figure 9 compares the transmission of a step change for various numbers of nodes and the plug flow model. It is easy to see why the codes model void propagation poorly. A very large number of nodes are needed to transmit a disturbance without appreciable distortion. The phase relationships or timing, of the propagation is very important in determining the stability of a thermal hydraulic system. A pocket of void reaching a given destination at an earlier or later time may enhance or cancel the phenomenon in question. The smearing of a wave front

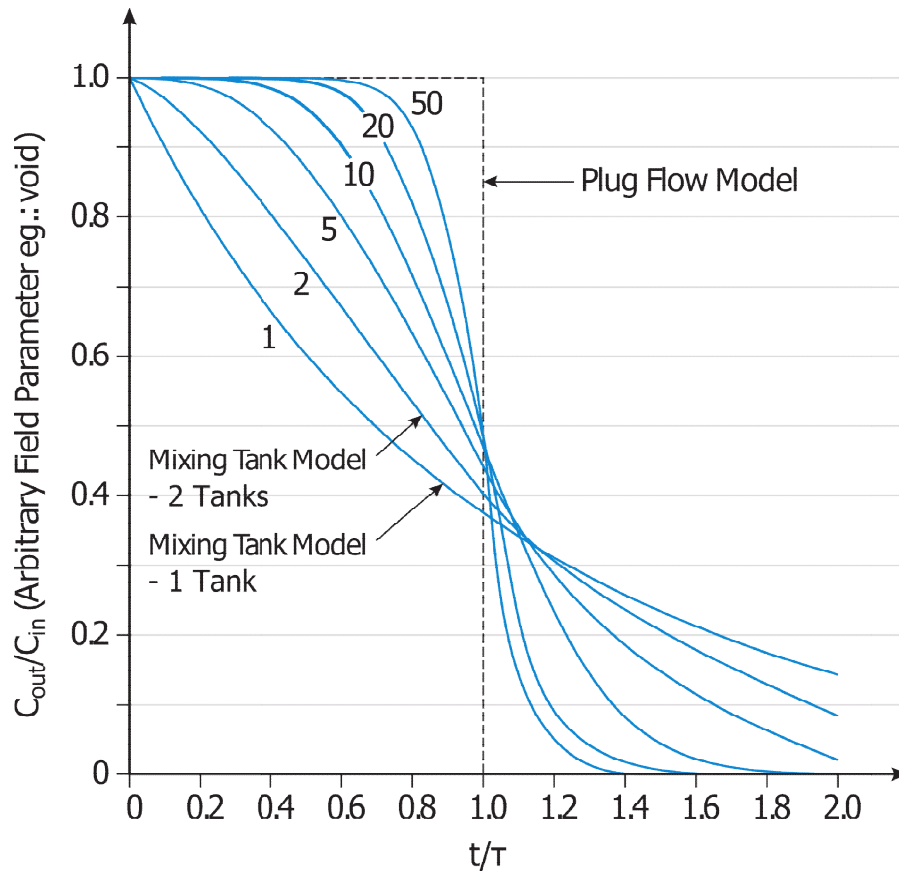


Figure 9 Transmission of a step change using the plug flow model and the mixing tank model (1 to 50 tanks).

alters the timing and gain and hence affects stability. The slow convergence of the mixing model to the plug flow model explains the typically slow convergence of such system codes as more nodes are added to increase accuracy.

Thus, nodalization creates a form of diffusion in much the same manner as finite difference schemes create numerical diffusion (see, for instance, Roache [10]). Attaining convergence in nodalization is, in essence, converging the model to plug flow behaviour. But is the flow in typical heat transport systems plug flow?

Flow in the CANDU feeders (38 to 76 mm) at 15 M/sec may indeed be plug flow. But some turbulent mixing does take place. More importantly, the feeders are of varying length and the flow has a spectrum of qualities. This gives quite a spectrum in transit time. This will skew

the propagation of a disturbance as illustrated in figure 10. Thus, depending on the transit time spectrum, a 5 node approximation (say) may be quite a good representation. The risers and headers may also give more diffusion than plug flow. These pipes are large diameter and the flow is turbulent. Very little is known of flow regimes and propagation properties in these situations.

In short, careful attention should be given to nodalization for meaningful simulation, quite apart from the normal numerical concerns such as the Courant limit, etc.

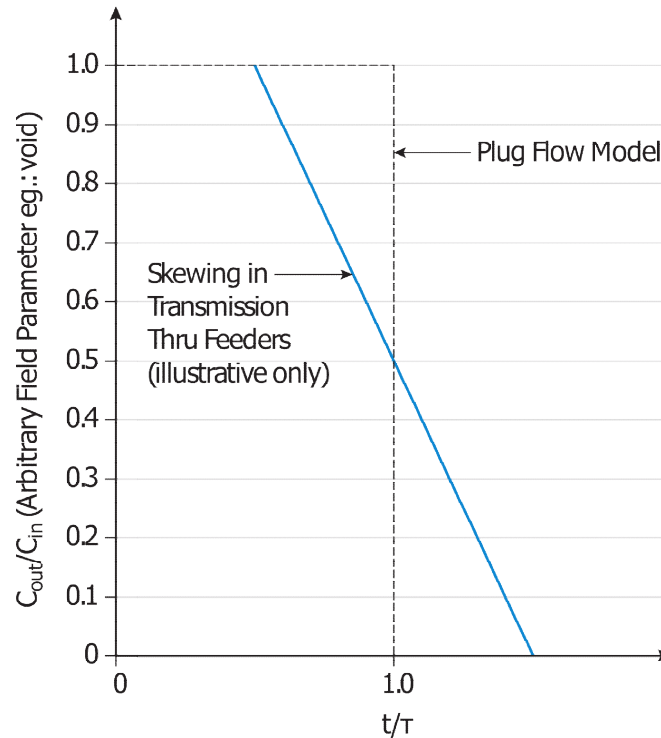


Figure 10 Transmission of a step change using the plug flow model and a feeder model with skewing due to differences in transit times.

3.4 Examples

In figures 11 to 13, some common piping situations are depicted. In figure 11, a simple Tee junction, note that each link has a unique junction resistance associated with the flow path of that link. Note also that a link has a unique upstream node and a unique downstream node. Links are always terminated by nodes at either end; in effect, the nodes provide boundary conditions for the links. There are 2 nodes per link, no more, no less. A node, on the other hand, can have many links connected to it.

The Y junction of figure 12 has a node link structure that is identical to the Tee junction. The differences in the two types of junctions are captured in the details of the correlations for friction, flow regimes, etc.

Figure 13 shows a CANDU HTS header and connecting piping. Note that there is no best or unique node-link representation. The requirements of the problem at hand dictates the number of nodes and links and the layout of the representation. For instance, it is useful to place a node centre at the point of a pressure measuring device so that experimental data can be more readily compared to the simulation results.

Figure 14 shows a typical nod-link diagram for a CANDU Heat Transport System simulation.

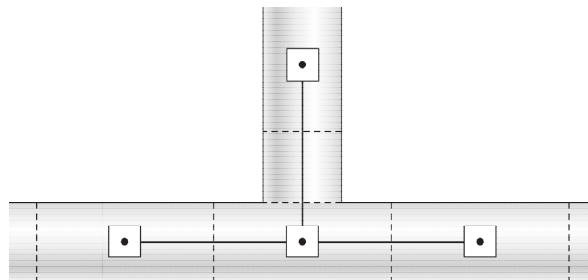


Figure 11 Simple Tee junction.

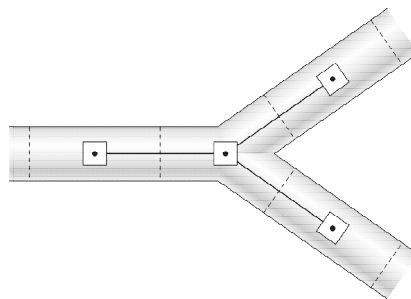


Figure 12 Simple Y junction.

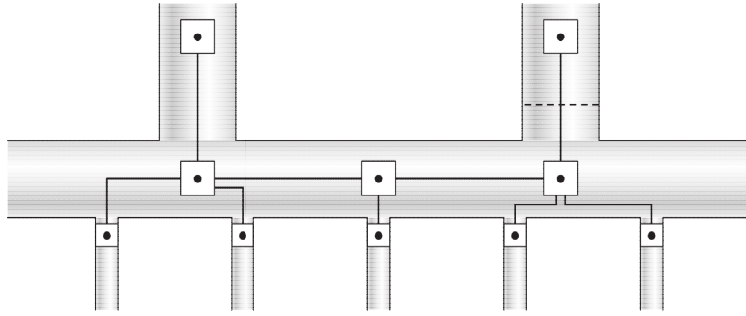


Figure 14 Sample node-link connection for a header.

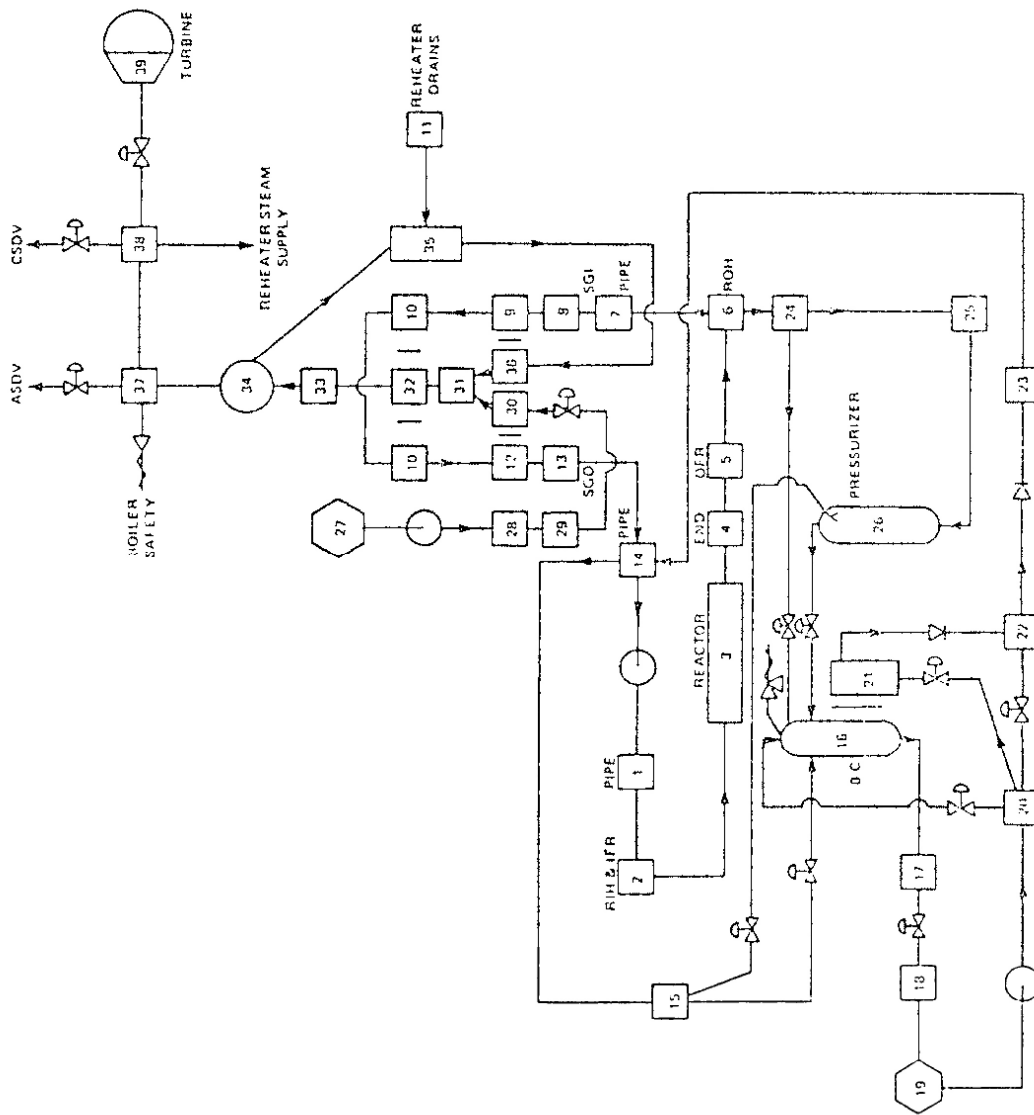


Figure 13 Node-link diagram: 1/4 circuit CANDU.

3.5 Matrix Notation

As we shall see, it is sometimes expedient to cast the governing equations in matrix form. To illustrate, consider the node-link network of figure 15. Nominal flow directions are assigned to be positive in the normal flow direction. The mass balance equations for the 4 nodes are:

$$\begin{aligned}\frac{dM_1}{dt} &= -W_1 + W_4 \\ \frac{dM_2}{dt} &= +W_1 - W_2 + W_5 \\ \frac{dM_3}{dt} &= +W_2 - W_3 \\ \frac{dM_4}{dt} &= +W_3 - W_4 - W_5\end{aligned}\tag{67}$$

If we define $\dot{M}_i \equiv \frac{dM_i}{dt}$ then the mass balance equations can be written

$$\begin{pmatrix} \dot{M}_1 \\ \dot{M}_2 \\ \dot{M}_3 \\ \dot{M}_4 \end{pmatrix} = \begin{pmatrix} -1 & 0 & 0 & 1 & 0 \\ 1 & -1 & 0 & 0 & 1 \\ 0 & 1 & -1 & 0 & 0 \\ 0 & 0 & 1 & -1 & -1 \end{pmatrix} \cdot \begin{pmatrix} W_1 \\ W_2 \\ W_3 \\ W_4 \\ W_5 \end{pmatrix} \equiv \dot{\mathbf{m}} = \mathbf{A}^{MW} \cdot \mathbf{w}\tag{68}$$

where \mathbf{A}^{MW} is a 4x5 matrix (number of rows = number of nodes $N=4$, and number of columns = number of links $L=5$) and \mathbf{w} is the flow vector. Generally, upper case bold will be used to indicate a matrix and lower case bold will be used to indicate a vector. The superscript MW denotes that the matrix relates to the mass equation and to the flow vector. It also indicates the size of the matrix (nodes x links)

There can be up to L entries in a row but only 2 non-zero entries in any column - no more, no less. The \mathbf{A}^{MW} matrix uniquely defines the geometry. The matrix is most easily constructed on a column by column basis, ie on a link by link basis: for each link (column vector) place a -1 in the location of the upstream node and a +1 in the location of the downstream node. As we shall see, all other matrices that arise in the solution to the mass, momentum and energy equations can be derived from the structure of \mathbf{A}^{MW} . This is very handy for computer coding purposes.

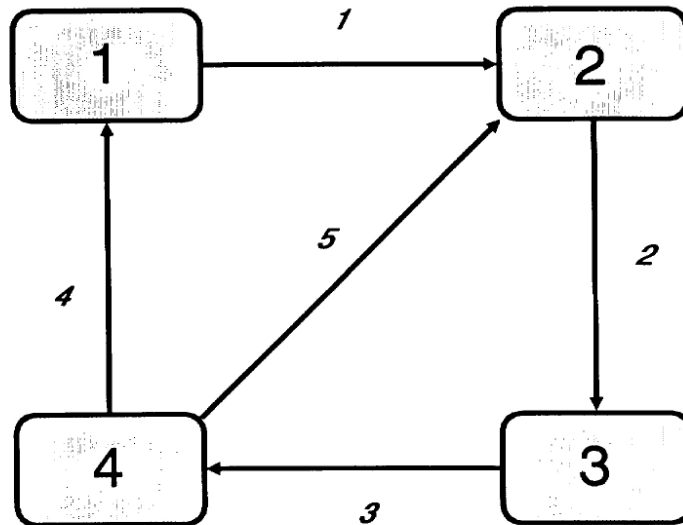


Figure 15 4 Node - 5 link diagram.

3.6 Exercises

1. For the 4 node, 5 link example of section 3.5, write out the flow and enthalpy equations as individual equations and in matrix form. Compare the structure of \mathbf{A}^{WP} and \mathbf{A}^{HW} to \mathbf{A}^{MW} , where the superscript $^{\text{WP}}$ denotes that the matrix relates to the flow equation and the pressure vector, and the superscript $^{\text{HW}}$ denotes that the matrix relates to the enthalpy equation and the flow vector.
2. For the case of 2 connected, open tanks of water with surfaces at different elevations, set up the node-link diagram and the mass, momentum and enthalpy equations.
3. What would be different if the tanks in question 2 were closed?

4 Equation of State

4.1 Introduction

As discussed in the previous sections, the momentum equation gives an update on the flows or velocities from one node to another, or from one grid point to another, based on a given pressure, flow, mass and enthalpy distribution. The updated flows are used by the mass and enthalpy equations to update the mass and enthalpy contents at each location. This information is given to the equation of state to update the pressure distribution which, along with the new densities and enthalpies is used by the momentum equation, and so on. In this manner, a time history of the fluid evolution is obtained. Of course, only the main variables are noted. The numerous and diverse empirical correlations require updates on the main variables and many secondary variables. This information also "flows" around the calculation.

The exploration of the appropriate forms of the equation of state to use for systems analysis begins by reflecting on the thermodynamics and the iterative method of finding pressure. Next a non-iterative method is offered as an improvement. This leads naturally to the water property evaluation. Fast, accurate curve fits are presented.

4.2 Thermodynamic Properties

From a thermodynamics viewpoint (see, for instance Sears [SEA75], the equation of state of a substance is a relationship between any four thermodynamic properties of the substance, three of which are independent. An example of the equation of state involves pressure P , volume V , temperature T and mass of system:

$$\pi (P, V, T, M) = 0 \quad (69)$$

If any three of the four properties are fixed, the fourth is determined.

The equation of state can also be written in a form which depends only on the nature of the system and not on how much of the substance is present, hence all extensive properties are replaced by their corresponding specific values. Thus

$$\pi (P, v, T) = 0 \quad (70)$$

is the specific value form of the above equation of state, where v is the specific volume. If any two of the thermodynamic properties are fixed, the third is determined.

From a thermodynamic point of view, the appropriate way to present water properties is by tables or formula for each property expressed as a function of the independent parameters P and T , as per Meyer [MEY67 or Haar [HAR84] (figure 16). Thus given values of pressure and temperature, the calculation of other thermodynamic properties is usually straightforward. On the other hand, the determination of pressure from known values of other thermodynamic properties is not direct since interpolation and iteration is required. Unfortunately, T and P are rarely the independent parameters in system dynamics since the numerical solution of the conservation equations yield mass and energy as a function of time. Hence, from the point of view of the equation of state, it is mass and energy which are the independent parameters.

Consequently, system codes are hampered by the form of water property data commonly available.

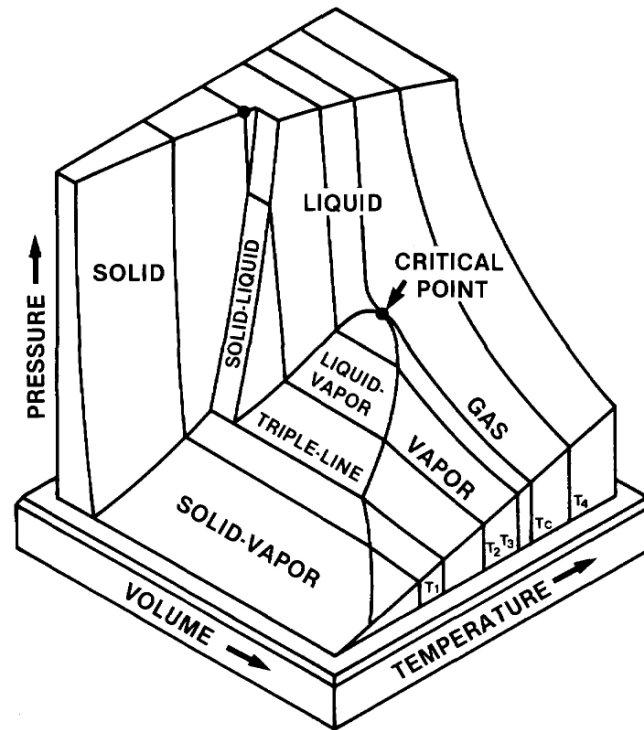


Figure 16 P-v-T surface for water .

A key point to note is that the conservation equations are all cast as rate equations whereas the equation of state is typically written as an algebraic equation. This arises from the basic assumption that, although the properties of mass, momentum and energy must be traced or solved as a function of time and space, the corresponding local pressure is a pure function of the local state of the fluid. Process dynamics are not considered. This is the essence of the equilibrium assumption (in a like manner, of course, we invariably use steady state heat transfer coefficients, etc. in dynamic processes). Historically, this mixture of form arose because thermodynamics endeavours were concerned with equilibrium states and not with system processes. System modellers, on the other hand, emphasized system dynamics and used what was available for constitutive relations. System modellers are more concerned with numerical problems.

But the decisive role of the equation of state in determining system dynamics was recognized early. Paynter [PAY60] identifies the power throughput as being the most important parameter for system dynamics. Power is composed of the product of effort (i.e. force or pressure) and flow. Porsching [POR71] correctly identifies the important role of flow in his work and by keying the formulation of node-link networks to flow, stable, efficient and accurate

solution schemes result. However, the role of pressure has not received the equivalent acknowledgement. Although the system dynamics are captured in Porsching's Jacobian, the essence of the system dynamics is not apparent. Nahavandi [NAH70] comes much closer to recognizing the role of pressure and explicitly casts the equation of state in rate form. Unfortunately, the system essence is again not apparent because Nahavandi's form is very case specific.

Most other popular schemes, for instance, Agee [AGE83], use the algebraic form of the equation of state. This treatment puts the pressure determination on the same level as heat transfer coefficients. Thus, although numerical solution of the resulting equation sets give correct answers (to within the accuracy of the assumption), intuition is not generated and time consuming iterations must be performed to get a pressure consistent with the local state parameters.

We look first at such an iterative scheme and then consider a more efficient alternative (the rate method).

4.3 The Iterative Method

Given the density and enthalpy of a volume of water, the task at hand is to find the associated values of pressure and temperature. Figure 17 shows qualitatively the relation between density, ρ , and enthalpy, h , for a given P . At low enthalpy, the fluid is single phase liquid and the density is high. As heat is added and the fluid reaches saturation temperature, vapour is generated to form a two-phase mixture and the density approaches the vapour density. The curve is well behaved and continuous making it a suitable candidate for numerical search routines.

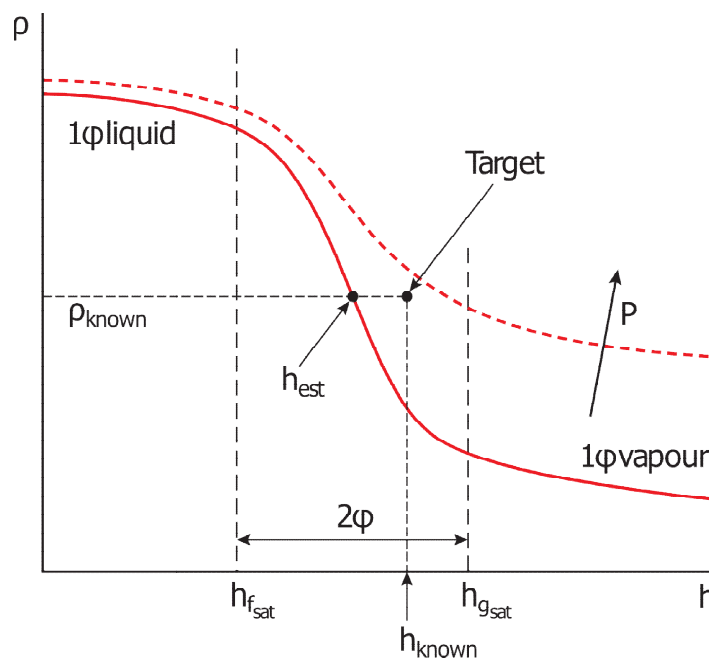


Figure 17 Numerical search for P given ρ and h for a two-phase mixture.

We start the iteration procedure by guessing a pressure. Usually in system transient simulation codes, the value of P at a previous time step is a good choice. Given P we calculate $h_{f_{sat}}$ and $h_{g_{sat}}$, the saturation enthalpies for the liquid and vapour phases, respectively. If $h < h_{f_{sat}}$ then the fluid is single phase liquid. If $h > h_{g_{sat}}$ then the fluid is single phase vapour. Otherwise the fluid is a two-phase mixture with a quality, $x \in [0,1]$.

The case of two-phase equilibrium is considered first. Subsequently, the equations are extended to cover single phase and two-phase non-equilibrium fluid.

4.3.1 Two-Phase Equilibrium Fluid

For two-phase fluid, the density and enthalpy are functions of the pressure and quality. Since we know the density, ρ , we can estimate the quality (x_{est}) for the guessed P (assuming a homogeneous mixture) since:

$$v = \frac{1}{\rho} = v_f(P) + x_{est} v_{fg}(P) \quad (71)$$

and thus calculate the enthalpy based on the guessed P :

$$h_{est} = h_f(P) + x_{est} h_{fg}(P) \quad (72)$$

This estimated value of h will differ from the known value of h . This difference is used to drive the iteration, ie, to update the guessed pressure as illustrated in figure 18:

$$\Delta P = \frac{\Delta h}{\left(\frac{\partial h}{\partial P}\right)_p} \quad (73)$$

The denominator in equation 5 must be evaluated numerically if analytical expressions are not available. The pressure is updated via:

$$P = P + \Delta P \quad (74)$$

and the iteration is repeated until the pressure has converged to some tolerance. The temperature is just the temperature of saturated fluid at that pressure.

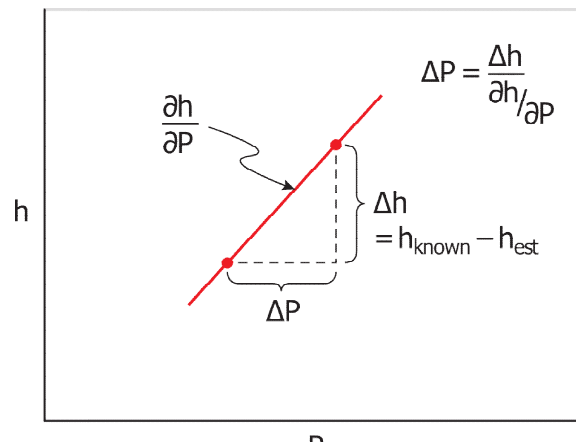


Figure 18 Error correction scheme for pressure in two-phase.

4.3.2 Single-Phase Sub-cooled and Superheated Fluid

For single phase fluid, the density and enthalpy are functions of P and T, ie:

$$\rho = \rho(P, T) \quad h = h(P, T) \quad (75)$$

For a guessed P and T, ρ and h can be found directly from the water property tables. But this is just an estimate since P and T are guessed. The true values of ρ and h lie some distance away and, to a first approximation, the true values and the estimated values are related by a Taylor's series expansion:

$$\rho = \rho_{\text{est}} + \left. \frac{\partial \rho}{\partial T} \right|_P \Delta T + \left. \frac{\partial \rho}{\partial P} \right|_T \Delta P \quad (76)$$

$$h = h_{\text{est}} + \left. \frac{\partial h}{\partial T} \right|_P \Delta T + \left. \frac{\partial h}{\partial P} \right|_T \Delta P \quad (77)$$

Defining $\Delta \rho = \rho - \rho_{\text{est}}$ and $\Delta h = h - h_{\text{est}}$, we solve for ΔP and ΔT :

$$\Delta P = \frac{\left. \frac{\partial h}{\partial T} \right|_P \Delta \rho - \left. \frac{\partial \rho}{\partial T} \right|_P \Delta h}{\left. \frac{\partial \rho}{\partial P} \right|_T \left. \frac{dh}{dT} \right|_P - \left. \frac{\partial \rho}{\partial T} \right|_P \left. \frac{\partial h}{\partial P} \right|_T} \quad (78)$$

$$\Delta T = \frac{\left. \frac{\partial h}{\partial P} \right|_T \Delta \rho - \left. \frac{\partial \rho}{\partial T} \right|_T \Delta h}{\left. \frac{\partial \rho}{\partial T} \right|_P \left. \frac{dh}{dP} \right|_T - \left. \frac{\partial \rho}{\partial P} \right|_T \left. \frac{\partial h}{\partial T} \right|_P} \quad (79)$$

or, more compactly,

$$\Delta P = G_{1P} \Delta \rho + G_{2P} \Delta h \quad (80)$$

$$\Delta T = G_{1T} \Delta \rho + G_{2T} \Delta h \quad (81)$$

The derivatives must be evaluated numerically if analytical expressions are not available.

The pressure and temperature are updated via:

$$P = P + \Delta P \quad T = T + \Delta T \quad (82)$$

and the iteration is repeated until the pressure and temperature have converged to some tolerance.

4.4 The Rate Method

We next consider a scheme (called the Rate Method) that eliminates the need for iteration with no loss in accuracy. The case of two-phase equilibrium is considered first in order to illustrate the method. Subsequently, the equations are extended to cover single phase and two-phase non-equilibrium fluid.

4.4.1 Two-Phase Equilibrium

For a two-phase homogeneous mixture we have:

$$v = v_f + xv_{fg} \quad (83)$$

$$h = h_f + xh_{fg} \quad (84)$$

where $v_{fg} \equiv v_g - v_f$ and $h_{fg} \equiv h_g - h_f$.

We wish to relate rates of change of pressure to rates of change in ρ and h . Specifically, we desire:

$$dP = G_1 d\rho + G_2 dh \quad \frac{dP}{dt} = G_1 \frac{d\rho}{dt} + G_2 \frac{dh}{dt} \quad (85)$$

since $d\rho/dt$ and dh/dt (or equivalently, dM/dt and dH/dt) are available from the mass and enthalpy conservation equations. First concentrating on the case of constant ρ (or v), to obtain G_2 , we differentiate equation (16) to give:

$$\frac{dh}{dt} = \left(\frac{\partial h}{\partial P} \right)_\rho \frac{dP}{dt} = \left[\frac{\partial h_f}{\partial P} + h_{fg} \frac{\partial x}{\partial P} + x \frac{\partial h_{fg}}{\partial P} \right] \frac{dP}{dt}. \quad (86)$$

Using equation (83), holding v constant (i.e., $\rho = \text{constant}$):

$$\frac{dx}{dP} = \frac{\partial \left(\frac{v - v_f}{v_{fg}} \right)}{\partial P} = -\frac{1}{v_{fg}} \left[\frac{\partial v_f}{\partial P} + x \frac{\partial v_{fg}}{\partial P} \right]. \quad (87)$$

Substituting this into equation (86) gives:

$$\frac{dh}{dt} = \left\{ \frac{\partial h_f}{\partial P} + x \frac{\partial h_{fg}}{\partial P} - \frac{h_{fg}}{v_{fg}} \left[\frac{\partial v_f}{\partial P} + x \frac{\partial v_{fg}}{\partial P} \right] \right\} \frac{dP}{dt} \quad (88)$$

or equally:

$$\begin{aligned} \frac{dP}{dt} &= \frac{v_{fg}}{\left\{ v_{fg} \left[\frac{\partial h_f}{\partial P} + x \frac{\partial h_{fg}}{\partial P} \right] - h_{fg} \left[\frac{\partial v_f}{\partial P} + x \frac{\partial v_{fg}}{\partial P} \right] \right\}} \frac{dh}{dt} \\ &= \frac{v_{fg}}{\{\text{DENOMINATOR}\}} \frac{dh}{dt} = G_2 \frac{dh}{dt}. \end{aligned} \quad (89)$$

This gives the pressure rate response due to an enthalpy rate change, holding ρ constant.

If we repeat the above but holding h constant we find:

$$\frac{dP}{dt} = \frac{-h_{fg}}{\{\text{DENOMINATOR}\}} \frac{dv}{dt} = \frac{h_{fg} v^2}{\{\text{DENOMINATOR}\}} \frac{d\rho}{dt} = G_1 \frac{d\rho}{dt}. \quad (90)$$

Note that G_1 and G_2 are functions that depend only on the local saturation fluid properties and their slopes at the local pressure.

Combining equations 89 and 90 to get the total pressure rate response when both h and ρ are varying:

$$\frac{dP}{dt} = G_1(P, x) \frac{d\rho}{dt} + G_2(P, x) \frac{dh}{dt}. \quad (91)$$

This is the rate form of the equation of state for two-phase equilibrium fluid in terms of the intensive rate properties, dp/dt and dh/dt , which are obtained from the continuity equations.

Equation 91 can be cast in the extensive form by noting that, since $\rho = M/V$ and $h = H/M$,

$$\frac{d\rho}{dt} = \frac{1}{V} \frac{dM}{dt} - \frac{M}{V^2} \frac{dV}{dt} \quad (92)$$

and

$$\frac{dh}{dt} = \frac{1}{M} \frac{dH}{dt} - \frac{H}{M^2} \frac{dM}{dt}. \quad (93)$$

Substituting into equation 91 and collecting terms:

$$\frac{dP}{dt} = \left(\frac{G_1}{V} - \frac{G_2 H}{M^2} \right) \frac{dM}{dt} + \frac{G_2}{M} \frac{dH}{dt} - \frac{G_1 M}{V^2} \frac{dV}{dt}. \quad (94)$$

After some simplification and rearrangement we find:

$$\frac{dP}{dt} = \frac{F_1 \frac{dM}{dt} + F_2 \frac{dH}{dt} + F_3 \frac{dV}{dt}}{M_g F_4 + M_f F_5} \quad (95)$$

where:

$$F_1 = h_g v_f - h_f v_g$$

$$F_2 = v_g - v_f$$

$$F_3 = h_f - h_g$$

$$F_4 = \frac{\partial h_g}{\partial P} (v_g - v_f) - \frac{\partial v_g}{\partial P} (h_g - h_f) \quad (96)$$

$$F_5 = \frac{\partial h_f}{\partial P} (v_g - v_f) - \frac{\partial v_f}{\partial P} (h_g - h_f)$$

$$M_g \equiv x M$$

$$M_f \equiv (1 - x) M.$$

The F functions are smooth, slowly varying functions of pressure provided good curve fits are used. The latest steam tables [HAA84] were used to fit saturated properties to less than 1/4% accuracy using low order polynomials and exponentials [GAR88]. Considerable effort was spent on obtaining accuracy and continuous derivatives over the full pressure range. The fact that good fits are available means that the F functions are well behaved which in turn makes the rate form of the equation of state extremely well behaved, as shown later.

The G functions are also well behaved for the same reasons.

The F and G functions have direct physical interpretations which aid in generating intuition. The F functions relate changes in the extensive properties, M, H and V, to changes in pressure. The G functions related changes in the intensive properties, ρ and h , to changes in pressure. Often, a simple numerical evaluation of these functions during a simulation aids in developing an appreciation of the changing roles of the key actors in a dynamic simulation.

For instance, because F_1 is negative, we immediately see that adding mass to a fixed volume of liquid with fixed total enthalpy will cause a depressurization (because the specific enthalpy, $h = H/M$, is decreased). But, since G_1 is positive, an increase in density in a fluid of fixed specific enthalpy causes a pressurization.

4.4.2 Single-Phase Sub-cooled and Superheated Fluid

For the single-phase sub-cooled or superheated case, we do not have to account for the sorting out between phases as we did for the two phase case. thus the derivation is more direct and less complex. We could simply use:

$$P = \pi(\rho, h)(97)$$

to give:

$$\frac{dP}{dt} = \left. \frac{\partial P}{\partial \rho} \right|_h \frac{d\rho}{dt} + \left. \frac{\partial P}{\partial h} \right|_\rho \frac{dh}{dt} \quad (98)$$

but, since the steam tables are given as a function of P and T, the slopes in equation (98) are not easily obtained. To cast the pressure rate equation in terms of the independent variables, P and T, consider:

$$\rho = \rho(P, T) \quad (99)$$

and

$$h = h(P, T) \quad (100)$$

Note that the non-equilibrium case requires the explicit tracking of the temperature in addition to pressure. Taking derivatives of Equations (99) and (100):

$$\frac{d\rho}{dt} = \left. \frac{\partial \rho}{\partial P} \right|_T \frac{dP}{dt} + \left. \frac{\partial \rho}{\partial T} \right|_P \frac{dT}{dt} \quad (101)$$

and

$$\frac{dh}{dt} = \left. \frac{\partial h}{\partial P} \right)_T \frac{dP}{dt} + \left. \frac{\partial h}{\partial T} \right)_P \frac{dT}{dt}. \quad (102)$$

But we desire:

$$\frac{dP}{dt} = G_{1P} \frac{d\rho}{dt} + G_{2P} \frac{dh}{dt} \quad (103)$$

and

$$\frac{dT}{dt} = G_{1T} \frac{d\rho}{dt} + G_{2T} \frac{dh}{dt}. \quad (104)$$

This is easily obtained by solving equations (101) and (102) for dP/dt and dT/dt to yield:

$$\frac{dP}{dt} = \frac{\left. \frac{\partial h}{\partial T} \right)_P \frac{d\rho}{dt} - \left. \frac{\partial \rho}{\partial T} \right)_P \frac{dh}{dt}}{\left. \frac{\partial \rho}{\partial P} \right)_T \frac{dh}{dt} - \left. \frac{\partial \rho}{\partial T} \right)_P \left. \frac{\partial h}{\partial P} \right)_T} \quad (105)$$

and

$$\frac{dT}{dt} = \frac{\left. \frac{\partial h}{\partial P} \right)_T \frac{d\rho}{dt} - \left. \frac{\partial \rho}{\partial T} \right)_T \frac{dh}{dt}}{\left. \frac{\partial \rho}{\partial T} \right)_P \left. \frac{dh}{dP} \right)_T - \left. \frac{\partial \rho}{\partial P} \right)_T \left. \frac{\partial h}{\partial T} \right)_P} \quad (106)$$

which is the intensive form we desire.

The extensive form is obtained as for the two-phase equilibrium case. Equations (92) and (93) are substituted into equations (105) and (106) and after rearrangement we find:

$$\frac{dP}{dt} = \frac{F_{1P} \frac{dM}{dt} + F_{2P} \frac{dH}{dt} + F_{3P} \frac{dV}{dt}}{M_V F_{4P} + M_I F_{5P}} \quad (107)$$

and

$$\frac{dT}{dt} = \frac{F_{1T} \frac{dM}{dt} + F_{2T} \frac{dH}{dt} + F_{3T} \frac{dV}{dt}}{M_V F_{4T} + M_I F_{5T}} \quad (108)$$

where

$$\begin{aligned}
F_{1P} &= \rho \left. \frac{\partial h}{\partial T} \right|_P + h \left. \frac{\partial \rho}{\partial T} \right|_P \\
F_{2P} &= - \left. \frac{\partial \rho}{\partial t} \right|_P \\
F_{3P} &= - \rho^2 \left. \frac{\partial \rho}{\partial T} \right|_P \\
F_{4P} &= 0 \text{ for subcooled, } = \left. \frac{d\rho}{dP} \right|_T \left. \frac{\partial h}{\partial T} \right|_P - \left. \frac{\partial \rho}{\partial T} \right|_P \left. \frac{dh}{dP} \right|_T \text{ for superheated} \\
F_{5P} &= \left. \frac{d\rho}{dP} \right|_T \left. \frac{\partial h}{\partial T} \right|_P - \left. \frac{\partial \rho}{\partial T} \right|_P \left. \frac{dh}{dP} \right|_T \text{ for subcooled } = 0 \text{ for superheated} \\
F_{1T} &= \rho \left. \frac{\partial h}{\partial T} \right|_P + h \left. \frac{\partial \rho}{\partial T} \right|_P \\
F_{2T} &= - \left. \frac{\partial \rho}{\partial t} \right|_T \\
F_{3T} &= - \rho \left. \frac{\partial h}{\partial T} \right|_T \\
F_{4T} &= - F_{4P} \\
F_{5T} &= - F_{5P} \\
M_v &= \text{mass of vapour phase} = 0 \text{ for subcooled, } = M \text{ for superheated} \\
M_l &= \text{mass of liquid phase} = M \text{ for subcooled } = 0 \text{ for superheated}
\end{aligned} \tag{109}$$

4.4.3 Two-Phase Non-Equilibrium

The rate form for the equation of state for the two-phase non-equilibrium case is a simple extension of the single-phase non-equilibrium case. The liquid and vapour phases are treated independently to give:

$$\frac{dP_k}{dt} = G_{1P}^k \frac{d\rho_k}{dt} + G_{2P}^k \frac{dh_k}{dt} \tag{110}$$

$$\frac{dT_k}{dt} = G_{1T}^k \frac{d\rho_k}{dt} + G_{2T}^k \frac{dh_k}{dt} \tag{111}$$

where k represents either l or v for the liquid or vapour phases respectively. In general, the 6 equation model (3 continuity equations for each phase) would be used for the general unequal temperature, unequal velocity, unequal pressure situation. Thus $d\rho_k/dt$ and dh_k/dt are available to the rate form of the equation of state.

4.5 Water Property Fits

To facilitate the calculation of light water properties, the 1984 standard tables were accurately curve fitted as discussed in detail at www.nuceng.ca/water/h2ohome.htm. These fitted functions are supplied in the files H2OPROP.FOR and H2OPROP.C for user convenience. These FORTRAN and C functions cover a wide range of pressures and temperatures and should be sufficient for most nuclear reactor simulations, with the exception of severe accidents that generate extreme conditions. These functions are fast and more than accurate enough given the other errors in system simulation [GAR88, GAR89, GAR92].

The basic overall approach taken in the curve fitting task was that, since the more difficult region to fit was the transition from single to two-phase and since most power plants operate at or near this region, careful attention would be paid the phase transition region at the expense of accuracy away from the saturation line, if necessary. Thus, the first major step was to accurately fit the saturation lines. Then, since density, enthalpy and other properties vary more strongly with T than with P (as shown in figure 19), the property in question, say density, would be calculated based on the deviation from the saturation value at the given T, ie:

Heavy water properties have of course been developed in-house at AECL and Ontario Power Generation for use in their industry computer tool-set. Some tools are available in the public domain; see www.nuceng.ca/d2o/d2ohome.htm.

$$\rho(P,T) = \rho_{\text{sat}}(T) + \left. \frac{\partial \rho}{\partial P} \right|_T (P - P_{\text{sat}}(T)) \quad (112)$$

Figure 20 illustrates the strategy. It should be obvious by now that not only the properties need to be fitted but the slopes are needed as well. Both the properties and the slopes of the properties must be free of discontinuities if numerical searches are to converge.

Having derived the desired rate forms for the equation of state, we proceed to section 5 to illustrate the utility of the approach.

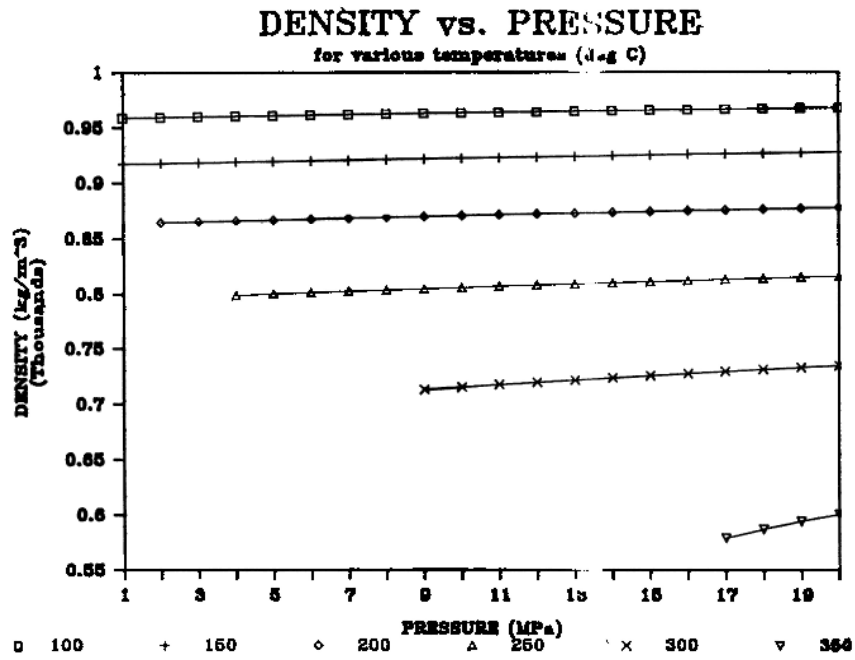


Figure 19 Density vs. pressure at various temperatures in sub-cooled water.

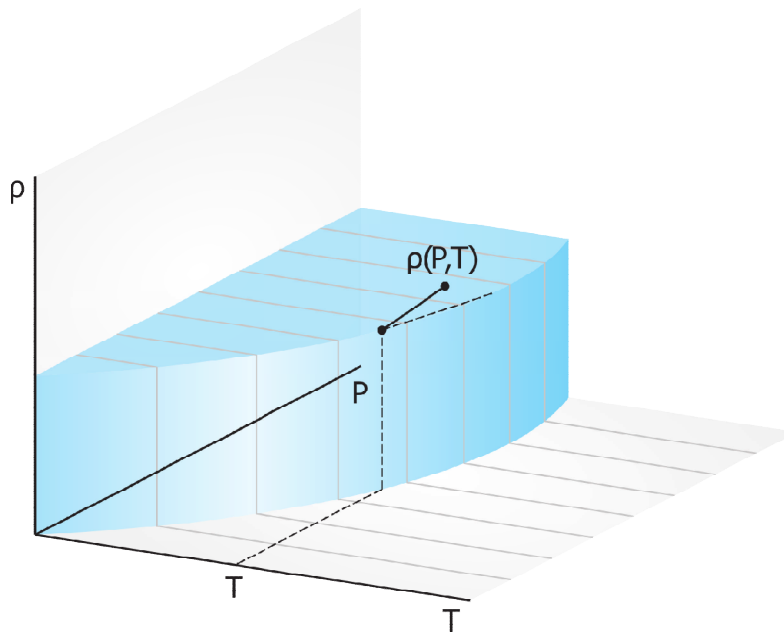


Figure 20 Basis for curve fitting in the subcooled region.

4.6 Problems

4. Using the spread sheet macros for Microsoft Excel supplied by G.R. McGee (as per <http://www.nuceng.ca/water/h2ohome.htm>), calculate and plot the density, enthalpy, quality and void fraction for a range of pressures (1 to 100 atmospheres) and temperatures(50 °C to 350 °C). Make sure you cover the subcooled, saturated and superheated ranges.
5. Using the code, WATERA.EXE (see <http://www.nuceng.ca/water/h2ohome.htm>):
 - a. Calculate ρ and h for $P=10$ MPa and $T=300$ °C. Increase the temperature in steps to see the approach to two-phase.
 - b. Using ρ and h slightly different than that found in (a), calculate P and T .
 - c. Practice calculating ρ given h and P .

5 The Rate Form of the Equation of State

5.1 Introduction

In conjunction with the usual rate forms of the conservation equations, the time derivative form of the Equation of State is investigated from a numerical consideration point of view. By recasting the equation of state in a form that is on equal footing with the system conservation equations, several advantages are found. The rate method is found to be more intuitive for system analysis, more appropriate for eigenvalues extraction, as well as easier to program and to implement. Numerically, the rate method is found [GAR87a] to be more efficient and as accurate than the traditional iterative method.

First, the derivation of the rate form of the Equation of State is presented. Systematic comparison between the new method and the traditional iterative method is made by applying the methods to a simple flow problem. The comparison is then extended to a practical engineering problem requiring accurate prediction of pressure.

5.2 The Rate Form

Presently, the conservation equations are all cast as rate equations whereas the equation of state is typically written as an algebraic equation [AGE83]. This arises from the basic assumption that, although the properties of mass, momentum and energy must be traced or solved as a function of time and space, the corresponding local pressure is a pure function of the local state of the fluid. Hence the equation of state is considered only as a constitutive equation. This treatment puts the pressure determinations on the same level as heat transfer coefficients. Although numerical solution of the resulting equation sets give correct answers (to within the accuracy of the assumption), intuition is not generated and time-consuming iterations must be performed to get a pressure consistent with the local state parameters.

The time derivative form of the Equation of State is investigated, herein, in conjunction with the usual rate forms of the conservation equations. This gives an equation set with two distinct advantages over the use of algebraic form of the Equation of State normally used.

The first advantage is that the equation set used consists of four equations for each node or point in space, characterizing the four main actors: mass, flow, energy and pressure. This consistent formulation permits the straight-forward extraction of the system eigenvalues (or characteristics) without having to solve the equations numerically.

The second advantage is that the rate form of the Equation of State permits the numerical calculation of the pressure without iteration. The calculation time for the pressure was found to be reduced by a factor of more than 20 in some cases (where the flow was rapidly varying) and, at worst, the rate form was no slower than the algebraic form. In addition, because the pressure can be explicitly expressed in terms of slowly varying system parameters and flow, an implicit numeric scheme is easily formulated and coded.

This section will concentrate on this numerical aspect of the equation of state.

The equation of state has been discussed in section 4 where we saw that the determination of pressure from known values of other thermodynamic properties is not direct. Interpolation and iteration is required because the independent (known) parameters are temperature, T , and pressure, P . Unfortunately, T and P are rarely the independent parameters in system dynamics since the numerical solution of the conservation equations yield mass and energy as a function of time. Hence, from the point of view of the equation of state, it is mass and energy which are the independent parameters. Consequently, system codes are hampered by the form of water property data.

Having derived the desired rate forms for the equation of state in section 4, we proceed to illustrate the utility of the approach.

5.3 Numerical Investigations: a Simple Case

The simple two-node, one-link system is (Figure 21) chosen to illustrate the effectiveness of the rate form of the equation of state in eliminating the inner iteration loop in thermalhydraulic simulations. In general, the task is to solve the matrix equation,

$$\frac{\partial \mathbf{u}}{\partial t} = \mathbf{A}\mathbf{u} + \mathbf{b} \quad (113)$$

over the time domain of interest. The key point that we wish to discuss is the difference in the normal method (where $\mathbf{u} = \{M_1, H_1, W, M_2, H_2\}$) and the rate method (where $\mathbf{u} = \{M_1, H_1, P_1, W, M_2, H_2, P_2\}$). For simplicity and clarity, we first summarize work for a fixed time step Euler integration:

$$\mathbf{u}^{t+\Delta t} = \mathbf{u}^t + \Delta t[\mathbf{A}\mathbf{u} + \mathbf{b}] \quad (114)$$

As we shall see, this is sufficient to generate some observations on the utility of the rate method. These observations then guide us in the use of more complicated and efficient algorithms.

5.3.1 Normal Method

The normal method obtains the value of pressure at time, $t+\Delta t$, from an iteration (as discussed previously) on the equation of state using the values of mass and enthalpy at time, $t+\Delta t$, i.e. the new pressure must satisfy:

$$p^{t+\Delta t} = f_n(\rho^{t+\Delta t}, h^{t+\Delta t}) \quad (115)$$

where both p and h are pressure dependent functions. Any iteration requires a starting guess and a feedback mechanism. Here, the starting guess for pressure is the value at time, t : P^t . Feedback in the Newton-Raphson scheme is generated by using an older value of pressure, $P^{t-\Delta t}$, to estimate slopes. Since the slope, $\partial h/\partial P$, was readily available from the rate method, we chose to use this slope to guide feedback. Thus, in the comparison of methods, we have borrowed from the rate method to enhance the normal method. This provides a stronger test of the rate method.

Thus we can now generate our next pressure guess from:

$$P_{new} = P_{guess} + \frac{h-h_{est}}{\partial h/\partial P} * ADJ \tag{116}$$

where h is the known value of h at $t+\Delta t$ and h_{est} is the estimated h based on the guessed pressure as discussed in detail in section 4. ADJ is an adjustment factor $\in [0, 1]$, to allow experimentation with the amount of feedback. This iteration on pressure continues until a convergence criteria, P_{err} , is satisfied. The converged pressure is used in the outer loop in the momentum equation and the time can be advanced one time step. Figure 22 summarizes the logic flow.

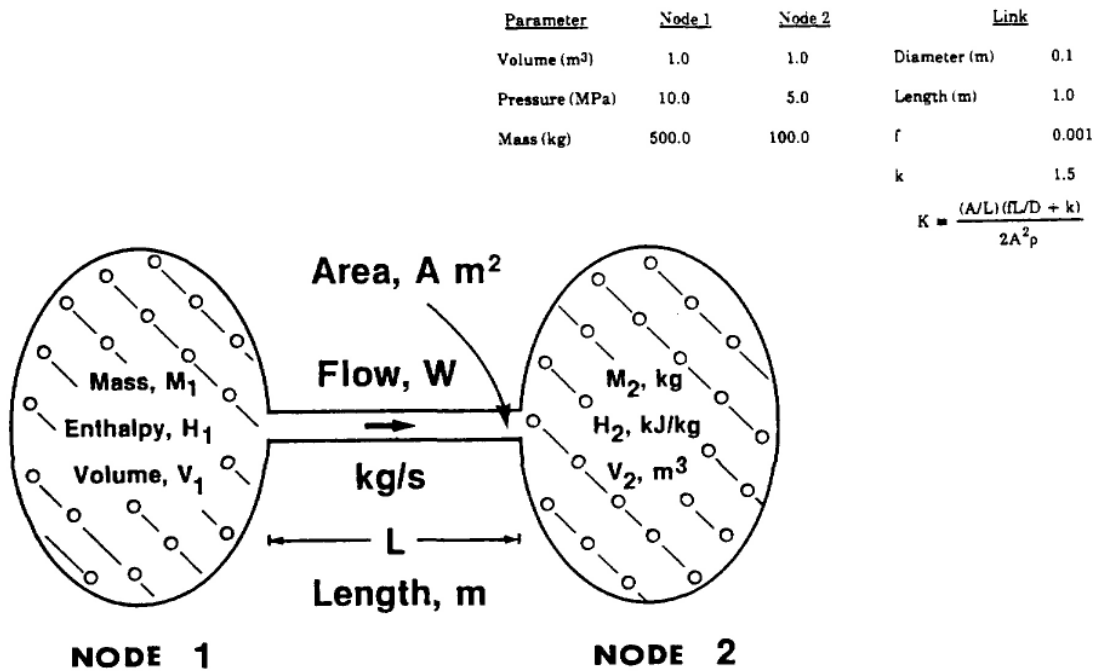


Figure 21 Simple 2-node, 1-link system.

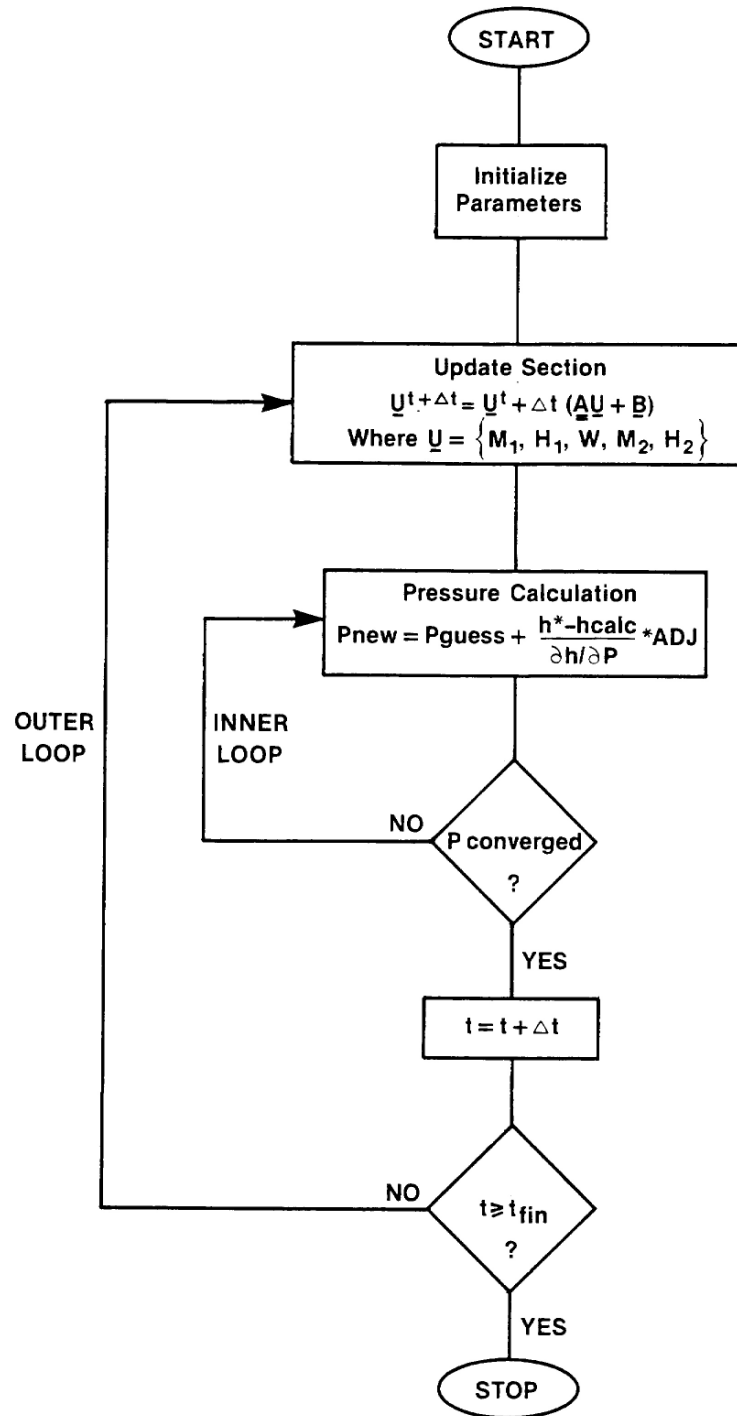


Figure 22 Program flow diagram for the normal method.

5.3.2 Rate Method

The rate method obtains the value of pressure at time, $t+\Delta t$, directly from the rate equation as is done for the conservation equations. Equation 95, gives the rate of change of pressure which can be solved simultaneously with the conservation equations if substitutions for dM/dt and dH/dt are made, leading to:

$$\frac{\partial \mathbf{u}}{\partial t} = \mathbf{A}\mathbf{u} + \mathbf{b} \quad (117)$$

where $\mathbf{u} = \{M_1, H_1, P_1, W, M_2, H_2, P_2\}$.

Thus:

$$\mathbf{P}_i^{t+\Delta t} = \mathbf{P}_i^t + \Delta t[\mathbf{A}\mathbf{u} + \mathbf{b}]_i \quad (118)$$

No inner iteration is required, as shown in Figure 23.

One problem with this approach is that the pressure may drift away from a value consistent with the mass and energy. This problem does not arise with the conservation equations because the equations are conservative in form, by design. It is not possible to cast the rate form of the equation of state in conservative form since pressure is simply not a conserved property. We can surmount the drift problem by using the feedback philosophy of the normal method. Thus the new pressure is given by:

$$\mathbf{P}_i^{t+\Delta t} = \mathbf{P}_i^t + \Delta t[\mathbf{A}\mathbf{u} + \mathbf{b}]_i + \frac{h-h_{est}}{\partial h/\partial P} * ADJ \quad (119)$$

This correction term uses only readily available information in a non-iterative manner.

In essence, the main effective difference between the normal and rate method is that during the time step between t and $t+\Delta t$ the normal method employs parameters such as density, quality etc. derived from the pressure at time, $t+\Delta t$, whereas the rate form employs parameters derived from the pressure and rate of change of pressure at time, t . The normal method is not necessarily more accurate, it is simply forcibly implicit in its treatment of pressure. The rate method can be implicit (as we shall see) but it need not be. Without experimentation it is not evident whether the necessity of iteration in the normal method is outweighed by the possible advantages of the implicit pressure treatment.

The next sections test these issues with numerical experiments.

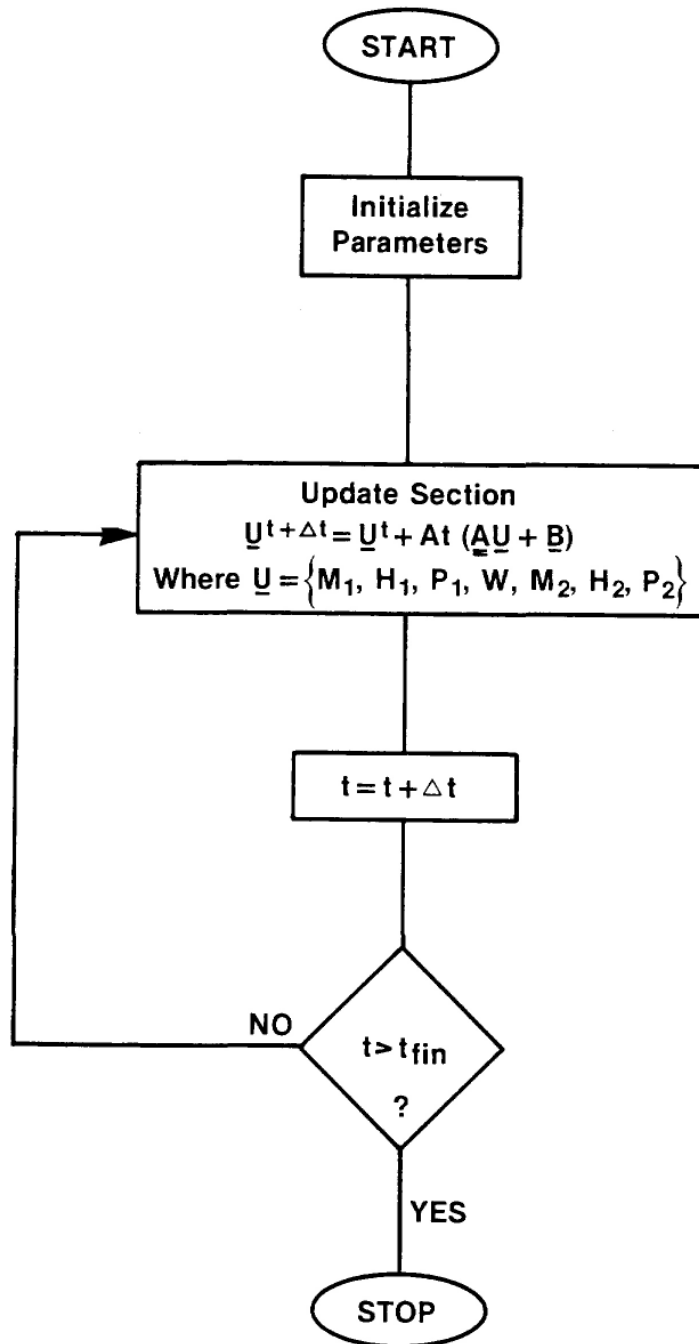


Figure 23 Program flow diagram for the rate method.

5.3.3 Comparison

The two node, one link numerical case under consideration is summarized in figure 21. Perhaps the most startling difference between the normal and rate methods is the difference in programming effort. The rate form was found to be extremely easy to implement since the equation form is the same as the continuity equations. The normal method took roughly twice the time to implement since separate control of the pressure logic is required. This arises directly from the treatment of pressure in the normal method: it is the odd man out.

The second startling difference was ease of execution of the rate form compared to the normal form. The normal form required experimentation with both the pressure convergence tolerance, P_{err} , and the adjustment factor, ADJ, since the solution was sensitive to both parameters. The rate method contains only the adjustment factor ADJ. The first few runs of the rate method showed that since the correction term for drift $(h-h_{est})/(\partial h/\partial p)$ is always several orders of magnitude below the primary update term, $\Delta t\{\mathbf{A} \mathbf{u} + \mathbf{b}\}$, the solution was not at all sensitive to the value of ADJ. Thus the rate method proved easier to program and easier to run than the normal method.

We look at the number of iterations required for pressure convergence as a function of P_{err} and ADJ for the normal method without regard to accuracy. For a Δt of 0.01sec, $P_{ert} = 10^{-3}$ (fraction of the full scale pressure of 10 MPa), the effect of ADJ is seen in figure 24. This result is typical: an adjustment factor of 1 gives rapid convergence (one or two iterations) except where very large pressure changes occur. For the case of very rapid changes, the full feedback (ADJ = 1) causes overshoot. Overall, however, the time spent for pressure calculation is about the same, independent of ADJ.

Allowing a larger pressure error had the expected result of reducing the number of iterations needed per routine call. But choosing a smaller time step (say .001) did not have a drastic effect on the peak iterations required. The rate method, of course, always used 1 iteration per routine call and the adjustment factor ADJ was found to be unimportant since the drift correction factor amounted to no more than 1% of the total pressure update term.

The integrated error for both methods is shown in figure 25. Both methods converge rapidly to the benchmark. The value of P_{err} is not overcritical. A value of P_{err} consistent with tolerances set for other simulation variables is recommended. The time spent per each iteration is roughly comparable for both methods. The main difference is that the rate method requires the evaluation of the F functions over and above the property calls common to both methods. This minor penalty is insignificant in all cases studied since the number of iterations / call dominated the calculation time.

In summary, to this point, the rate method is easier to implement, more robust and is equal to the normal method at worst, more than 20 times faster under certain conditions. We now look at incorporating a variable time step to see how each method compares.

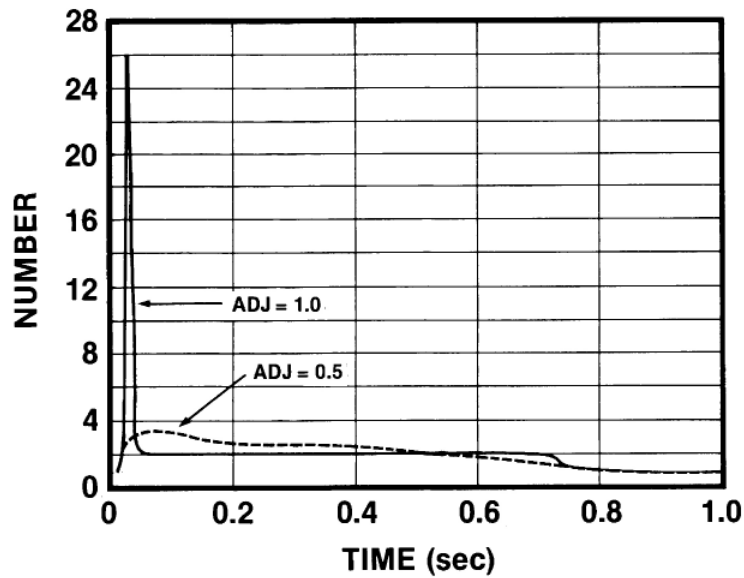


Figure 24 Number of iterations per pressure routine call for the normal method with a time step of 0.01 seconds and a pressure tolerance of 0.001 of full scale (10 MPa).

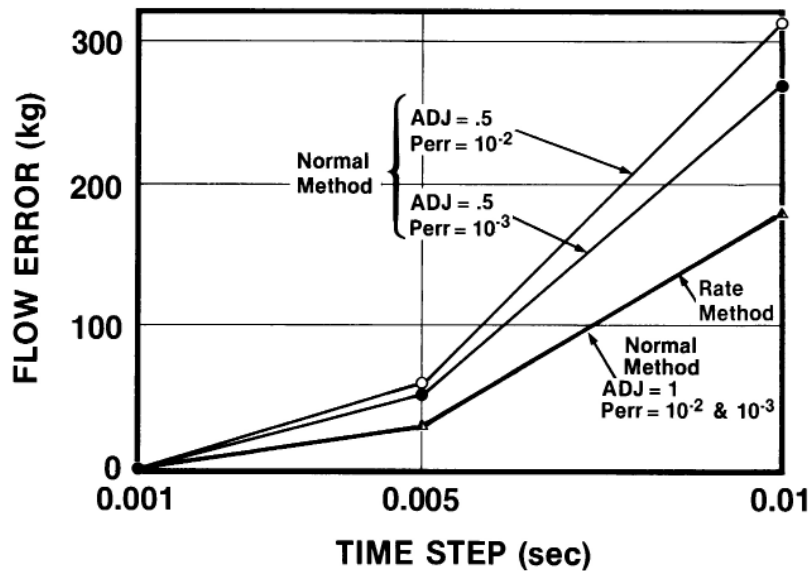


Figure 25 Integrated flow error for the rate method and the normal method for various fixed time steps, convergence tolerances and adjustment factors.

Typical variable time step algorithms require some measure of the rate of change of the main variables to guide the Δt choice. The matrix equation, equation 113, provides the rates that we need. Since the rate method incorporated the pressure into the \mathbf{u} vector, the rate of change of pressure is immediately available. For the normal method, the rate of change of pressure has to be estimated from previous history (which is no good for predicting the onset of rapid changes) or by trial and error. The trial and error method employed here is to calculate the Δt as the minimum of the time steps calculated from:

$$\Delta t_i = \frac{(\text{fractional tolerance}) \times (\text{scale factor for } u_i)}{\partial u_i / \partial t} \quad (120)$$

This restricts Δt so that no parameter changes more than the prescribed fraction for that parameter. This can be implemented in a non-iterative manner for the rate method. However, for the normal method, the above minimum Δt based on \mathbf{u} is used as the test Δt for the pressure routine and the rate of change of pressure is estimated as:

$$\frac{\partial P}{\partial t} = \frac{P^{t+\Delta t} - P^t}{\Delta t} \quad (121)$$

The Δt is then scaled down if the pressure change is too large for that iteration. Then the new Δt is tested to ensure that it indeed satisfies the pressure change limit. This iteration loop has within it the old inner loop.

It is expected then, that the normal method will not perform as well as the rate method primarily because of the "loop within a loop" inherent in the normal method as applied to typical system simulation codes.

A number of cases were studied and the results of the normal method were compared to the rate method. The figure of merit was chosen as

$$\text{F.O.M.} = \frac{10,000}{(\text{integrated error}) \times (\text{total pressure routine time}) \times (\text{No. of adjustable parameters})} \quad (122)$$

Thus, an accurate, fast and robust method achieves a high figure of merit. Some results are listed in table 1. Derating a method with more adjustable parameters is deemed appropriate because of the figure of merit should reflect the effort involved in using that method. On average, about 6 runs of the normal method, with various P_{err} and ADJ were needed to scope out the solution field compared to 1 run for the rate method. Thus a derating of 2 is not an inappropriate measure of robustness or effort required.

The results indicate that the rate method is a consistently better method than the normal method in terms of numerical performance. We see no reason why this improvement would not exist for any thermal hydraulic system in which pressure field determination is required.

Table 1 Figure of merit comparisons of the normal and rate forms of the equation of state for various convergence criteria (simple case).

Case	Method	Convergence (fraction full scale)		ADJ	Integral error	Pressure routine time	AP*	FOM*	Relative* FOM
		Overall	Pressure						
1	P rate	0.01		0.5	180.39	24	1	2.31	
2	P norm	0.01	0.01	0.5	597.61	25	2	0.33	6.90
3	P rate	0.001		0.5	21.13	96	1	4.93	
4	P norm	0.001	0.001	0.5	79.819	119	2	0.53	9.37
5	P norm	0.001	0.00001	1	22.808	246	2	0.89	5.53
6	P norm	0.001	0.0001	1	22.781	229	2	0.96	5.14
7	P norm	0.001	0.001	1	22.761	140	2	1.57	3.14
8	P norm	0.001	0.01	1	22.847	128	2	1.71	2.88
9	P rate	0.0001		0.5	0.534	736	1	25.44	
10	P norm	0.0001	0.0001	0.5	2.2536	852	2	2.60	9.77
11	P norm	0.0001	0.0001	1	0.4907	894	2	11.40	2.23

* AP = # of adjustable parameters

FOM = Figure of merit

Relative FOM = (FOM for rate method)/(FOM for normal method)

Next we briefly discuss implicit numerical schemes.

The nodal equations are:

$$\frac{dM_1}{dt} = -W \quad \frac{dM_2}{dt} = +W \quad (123)$$

$$\frac{dH_1}{dt} = -h_1 W \quad \frac{dH_2}{dt} = +h_1 W \quad (124)$$

$$\frac{dP_i}{dt} = \frac{F_1 \frac{dM_i}{dt} + F_2 \frac{dH_i}{dt}}{M_g F_4 + M_f F_5}, \quad i = 1, 2 \quad (125)$$

Considering just the flow and pressure rate equations, we have (after substituting in for dM/dt and dH/dt):

$$\frac{dW}{dt} = \frac{A}{L}(P_1 - P_2) - \frac{A}{L}K|W|W \quad (126)$$

and

$$\frac{dP_1}{dt} = -\chi_1 W \quad \frac{dP_2}{dt} = +\chi_2 W \quad (127)$$

where χ_1 and χ_2 are > 0 and are given by:

$$\chi = \frac{F_1 + hF_2}{M_g F_4 + M_f F_5} \quad (128)$$

evaluated at the local property values of nodes 1 and 2.

Employing a scheme that is implicit in flow, the difference equations are cast

$$\frac{W^{t+\Delta t} - W^t}{\Delta t} = \frac{A}{L}(P_1^{t+\Delta t} - P_2^{t+\Delta t}) - \frac{A}{L}K|W^t|W^{t+\Delta t} \quad (129)$$

$$\frac{P_i^{t+\Delta t} - P_i^t}{\Delta t} = \pm\chi_i W^{t+\Delta t} \text{ implies } P_i^{t+\Delta t} - P_i^t = \pm\chi_i W^{t+\Delta t} \Delta t \quad (130)$$

Collecting terms and solving for the new flow:

$$W^{t+\Delta t} = \left[1 + \frac{A}{L}K|W^t|\Delta t + \frac{A}{L}(\chi_1 + \chi_2)\Delta t^2 \right]^{-1} \left[W^t + \frac{A}{L}(P_1^t - P_2^t)\Delta t \right] \quad (131)$$

This is the implicit time advancement algorithm employing the rate form of the equation of state. For the normal method, the pressure rate equation in terms of flow (i.e., equation 130) is not available to allow an implicit formulation of the pressure. Consequently, the implicit time advancement algorithm for the normal method is:

$$W^{t+\Delta t} = \left[1 + \frac{A}{L}K|W^t|\Delta t \right]^{-1} \left[W^t + \frac{A}{L}(P_1^{t+\Delta t} - P_2^{t+\Delta t})\Delta t \right] \quad (132)$$

To appreciate the difference between equations 131 and 132, consider the eigenvalues and vectors of

$$\frac{\partial \mathbf{u}(t)}{\partial t} = \mathbf{A}(\mathbf{u}, t)\mathbf{u}(t) \quad (133)$$

If we assume, over the time step under consideration, that $\mathbf{A} = \text{constant}$ and has distinct eigenvalues, then the solution to equation 133 can be written as:

$$\mathbf{u}(t) = \sum_{l=1}^N \mathbf{u}_l e^{\alpha_l t} \quad (134)$$

where \mathbf{u}_l = eigenvectors

α_l = eigenvalues.

It can be shown that for the explicit formalism, the numerical solution is equivalent to:

$$\mathbf{u}^{t+\Delta t} = \sum_{i=1}^N (1+\alpha_i \Delta t) \mathbf{u}_i \quad (135)$$

while the implicit form is:

$$\mathbf{u}^{t+\Delta t} = \sum_{i=1}^N \frac{\mathbf{u}_i}{(1-\alpha_i \Delta t)} \quad (136)$$

The eigenvalues can often be large and negative. Thus, at some Δt , the factor $(1+\alpha_i \Delta t)$ can go negative in the explicit solution causing each subsequent evaluation of \mathbf{u} to oscillate in sign and go unstable. For the implicit method, the contributions due to large negative eigenvalues decays away as $\Delta t \rightarrow \infty$. Thus the implicit formalism tend to be very well behaved at large time steps. Positive eigenvalues, by a similar argument pose a threat to the implicit form. However, this is not a practical problem because $\alpha_i \Delta t$ is kept $\ll 1$ for accuracy reasons. Thus, as long as the solution algorithm contains a check on the rate of growth or decay (effectively the dominant eigenvalues) then the implicit form is well behaved.

With this digression in mind, we see that the implicit rate formalism (equation 131) has more of the system behaviour represented implicitly than the normal method (equation 132). Thus, we might expect the rate form to be more stable than the normal form. Indeed, this was found to be the case as shown in figure 26. For a fixed and large time step (0.1sec.) the normal method showed the classic numerical instability due to the explicit pressure treatment. The rate form is well damped and very stable, showing that this method should permit the user to "calculate through" pressure spikes if they are not of interest.

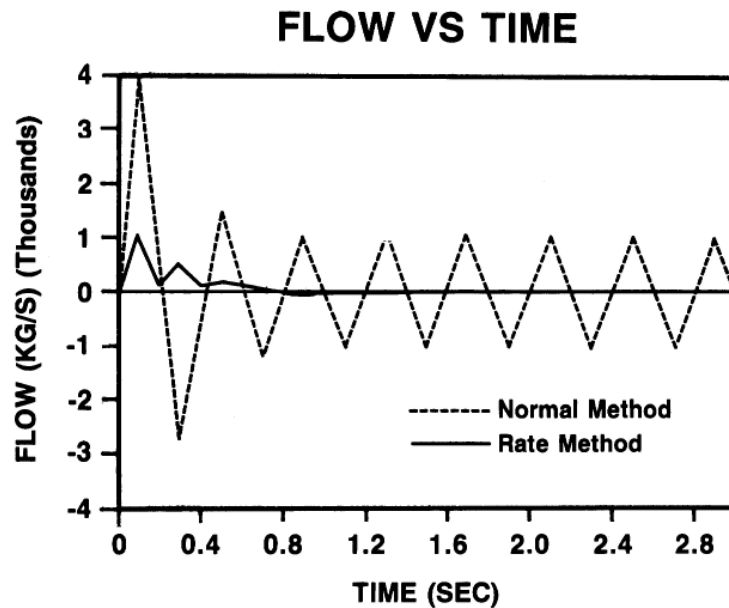


Figure 26 Flow vs. time for the implicit forms of the normal and rate methods.

5.4 Numerical Investigations: a Practical Case

The comparison between the normal and rate methods is extended to a practical application where a two node homogeneous model is used to simulate a transient of a small pressurizer operating at near-atmospheric pressure. The procedure is briefly described in the following [SOL85].

Figure 27 illustrates the problem. Steam and stratified liquid water in the pressurizer are schematically shown as two control volumes (nodes). The nodal fluids are assumed to be at saturated two-phase conditions corresponding to the pressure at their respective control volumes. The overall boundary conditions to the system are the steam bleed flow at the top of the pressurizer, the flow into and out of the pressurizer through the surge line, heat input from heaters at the bottom of the pressurizer and heat loss to pressurizer wall.

The rate of change of mass, M_s in the steam control volume and M_L in the liquid control volume, can be expressed by the following:

$$\frac{dM_s}{dt} = -W_{STB} - W_{CD} - W_{CI} + W_{EI} + W_{BR} \quad (137)$$

$$\frac{dM_L}{dt} = W_{SRL} - W_{EI} - W_{BR} + W_{CD} + W_{CI} \quad (138)$$

where W_{STB} is the steam bleed flow, W_{SRL} is the surge line inflow, W_{CI} is the interface condensation rate at the liquid surface separating the steam control volume from the liquid

control volume, W_{EI} is the interface evaporation rate at the same liquid surface, W_{CD} is the flow of condensate droplets (liquid phase) from the bulk of the steam control volume toward the liquid control volume, and W_{BR} is the rising flow of bubbles (gas phase) from the bulk of liquid volume toward the steam volume.

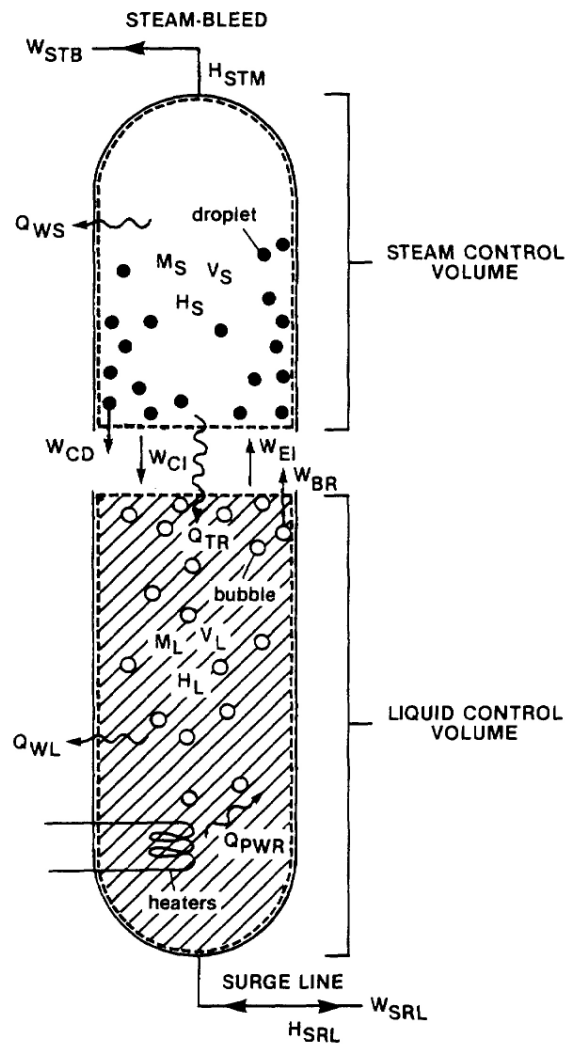


Figure 27 Schematic of control volumes in the pressurizer.

The rate of change of energy in the two control volumes can be expressed by the rate of change in the total enthalpy, H_S and H_L , in the steam and liquid control volumes respectively:

$$\frac{dH_S}{dt} = -W_{STB}h_{gST} - W_{CD}h_{fST} - W_{CI}h_{gST} + W_{EI}h_{sLQ} + W_{BR}h_{gLQ} - Q_{WS} + Q_{TR} - (1-\beta)[(1-\delta)Q_{COND} + Q_{EVPR}] \quad (139)$$

and

$$\frac{dH_L}{dt} = W_{SRL}h_{SRL} - W_{EI}h_{fLQ} - W_{BR}h_{gLQ} + W_{CI}h_{fST} + W_{CD}h_{fST} - Q_{WL} + Q_{PWR} - Q_{TR} - \beta[(1-\delta)Q_{COND} + Q_{EVPR}] \quad (140)$$

where h_{SRL} is the specific enthalpy of the fluid in the surge line, h_{gST} and h_{fST} are respectively the saturated gas phase specific enthalpy and the saturated liquid phase specific enthalpy in the steam control volume, h_{gLQ} and h_{fLQ} are respectively the saturated gas phase specific enthalpy and the saturated liquid phase specific enthalpy in the liquid control volume, Q_{WS} and Q_{WL} are the rate of heat loss to the wall in the steam control volume and in the liquid control volume respectively, Q_{TR} is the heat transfer rate from the liquid control volume to the steam control volume due to any temperature gradient, excluding those due to interface evaporation and condensation; Q_{COND} is the rate of energy released by the condensing steam to both the steam and liquid control volumes during the interface condensation process and Q_{EVPR} is rate of energy absorbed by the evaporating liquid from both the steam and liquid control volumes during the interface evaporation process. The constant, β , represents the fraction of these energies distributed to or contributed by the liquid control volume. The ratio δ represents the portion of energy released during the interface condensation that is lost to the wall.

The calculation of swelling and shrinking of control volumes is only done for the liquid control volume and the volume in the steam control volumes will be related to the volume in the liquid control volume, V_L , as:

$$\frac{dV_S}{dt} = -\frac{dV_L}{dt} \quad (141)$$

The swelling and shrinking of the liquid control volume as well as values of W_{STB} , W_{SRL} , W_{CI} , W_{EI} , W_{CD} , W_{BR} , Q_{WS} , Q_{WL} , Q_{TR} , Q_{PWR} , β and δ are calculated using analytical or empirical constitutive equations. The majority of these parameters depend directly or indirectly on pressure. Any inaccurate prediction of pressure during a numerical simulation will result in severe numerical instability. Hence the above problem is a good testing ground for comparing the performances of the two methods.

During the test simulation, the pressurizer is initially at a quasi-steady state. The steam pressure is at 96.3 kPa. The steam bleed flow, W_{STB} , heater power Q_{PWR} and heat losses Q_{WL} and Q_{WS} are at their quasi-steady values, maintaining the saturation condition of the pressurizer. At time = 11 sec., the steam bleed valve is closed and W_{STB} drops to zero while Q_{PWR} is increased to a fixed value of 300 Watts. At time = 16 sec., the steam bleed valve is reopened and its set

point set at 80 kPa.

Since the thermodynamic properties in the steam control volume and the liquid control volume are functions of P_S and P_L (pressures of the respective control volumes), there are seven unknowns, namely: M_S , M_L , H_S , H_L , V_S (or V_L), P_S and P_L . Adding two equations of state, one for each control volume, will complete the equation set:

$$P_S = \text{fn}(\rho_S, h_S) = \text{fn}\left(\frac{M_S}{V_S}, \frac{H_S}{M_S}\right) \quad (142)$$

$$P_L = \text{fn}(\rho_L, h_L) = \text{fn}\left(\frac{M_L}{V_L}, \frac{H_L}{M_L}\right) \quad (143)$$

Both the normal iterative method and the rate method are tested to solve. The following observations are made:

1. Using the normal method, the choice of adjusting P to converge on h given ρ or converging on ρ given h is found to be very important in providing a stable numerical result. At time step = 10 msec, no complete simulation result can be generated when ρ was the adjusted variable. An explanation of this can be given by referring to $G_1(P, x)$, or $\partial P / \partial \rho$, This factor is proportional to the square of $[x v_g(P) + (1-x)v_f(P)]$. However, the direction of change in the saturated gas phase specific volume with pressure is opposite to that of saturated liquid phase specific volume:
2. $dv_f/dP > 0$
3. $dv_g/dP < 0$
4. Therefore, a fluctuation in the value of pressure during an iteration process will amplify the fluctuation in the value of predicted density when that method is used;
5. Using enthalpy as the adjusted variable to converge on P , simulation results can be generated if an error tolerance E of less than 0.2% is used. The error tolerance is defined as:
6. $E = \frac{\text{ABS}(h-h_{\text{estimate}})}{h} \times 100\%$
7. Figure 28 shows the transient of P_L and P_S for $E = 0.2\%$. Unstable solutions result for E higher than 0.2%. The average number of iteration is found to depend on the error tolerance as shown in figure 30.
8. On the other hand, the performance of the rate method is much more convincing in both accuracy and efficiency. The transient of P_L and P_S predicted using the rate method is shown in Figure 29.

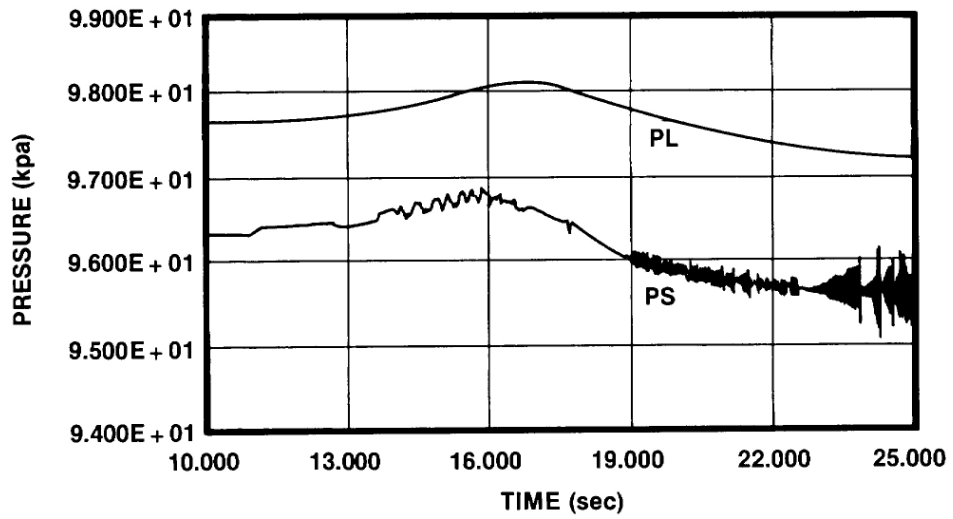


Figure 29 Pressurizer's pressure transient for the normal method with error tolerance of 0.2%.

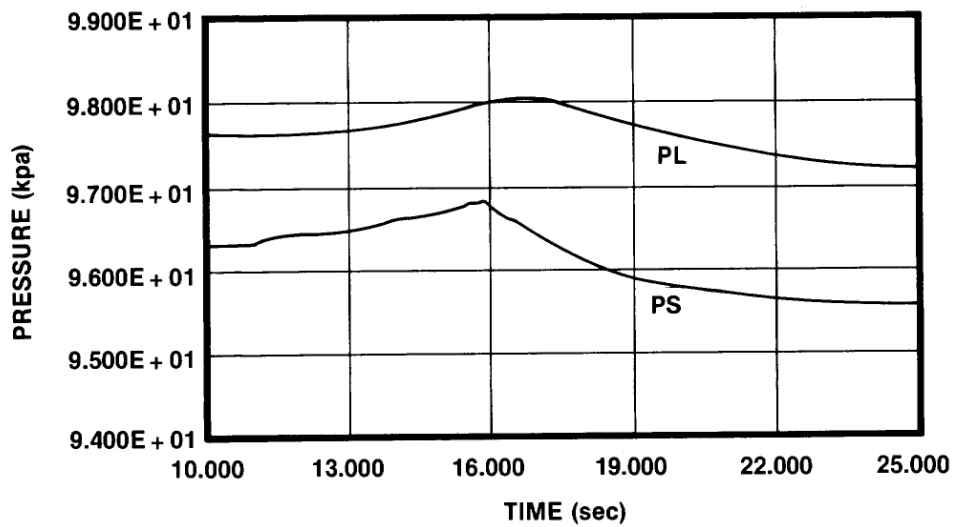


Figure 28 Pressurizer's pressure transient for the rate method.

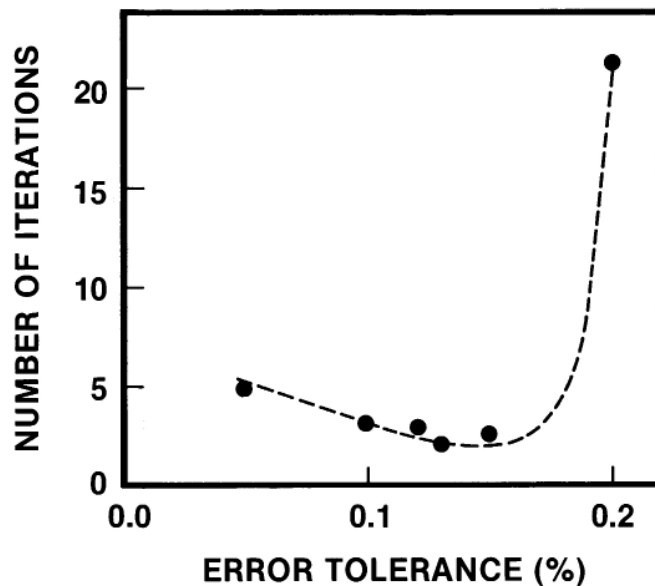


Figure 30 Average number of iterations per pressure routine call for the normal method in simulating the pressurizer problem.

5.5 Discussion and Conclusion

The rate form is a cogent expression of the equation of state that is distinct from the normal algebraic form. The essential difference is that the rate form expresses the relationship between the rates of change of the state variables, while the normal form relates the static values of the state variables. Although this is stating the obvious, the change in viewpoint is revealing.

No barrier is perceived to applying the rate form to the multi-node/link case, to the distributed form of the basic equations, and to eigenvalue extraction (numerical or analytical).

Although we have not made use of it in this work, the non-equilibrium form (equations 110 and 111) is provocative. It entices one to view the non-equilibrium situation as the essentially dynamic situation that it is and helps to focus our attention on the thermal relaxation. Given the temperature rate equations, the non-equilibrium situation should be easy to incorporate without a major code rewrite.

We conclude by restating our major findings. The rate method offers many advantages:

1. It is more intuitive for system work. It permits a proper focus on the two main actors, flow and pressure.
2. The same form is appropriate for eigenvalue extraction as well as numerical simulation. This extends the usefulness of coding.
3. Programs are easier to implement.
4. Programs are more robust and require less hand holding.
5. Time step control and detection of rapid changes (like phase changes) is

improved.

Overall the method is usually faster and more accurate. Time savings peaked at a ratio of 26 for the cases considered.

5.6 Problems

6. Consider 2 connected volumes of water with conditions as shown in figure 21. Model this with 2 nodes and 1 link.
 - a. Solve for the pressure and flow histories using the normal iterative method for the equation of state,
 - b. Solve for the pressure and flow histories using the non-iterative rate method.
 - c. Compare the two solutions and comment.
7. Vary the initial conditions of question 1 so as to cause void collapse in volume 2 during the transient. What problems can you anticipate? Solve this case by both methods.

6 Thermalhydraulic Network Simulation

6.1 Introduction

This section introduces some more advanced numerical algorithms for solving systems of ordinary differential equations such as found in the modelling of thermalhydraulic networks. Explicit algorithms are simple to devise and program but they are restricted in time step so as to ensure stability. The more implicit the formulation, the more stable the solution in most instances. Larger time steps can be used for implicit algorithms but the accompanying matrix manipulation is computationally costly. Herein, we explore the tradeoffs.

Porsching's method is explored to show the methodology and its limitations. Then the rate form of the equation of state is used with the conservation equations to develop a generalized fully implicit (at least in terms of the main variables) formalism. Porsching's method is a special case of the general method. The section concludes with some programming notes.

6.2 Porsching's Method

One of the more successful algorithms for thermalhydraulic simulation is based on the work of Porsching [POR69, POR71]. This algorithm, involving the Jacobian (derivative of the system state matrix), is used originally in the computer program FLASH-4 [POR69] and subsequently in the Ontario Hydro program SOPHT [CHA77] and evolved into forms used in RETRAN [AGE82].

The strength of Porsching's approach lies in its recognition of flow as the most important dependent parameter and, hence, its fully implicit treatment of flow. This leads to excellent numerical stability, consistency and convergence. Further, the Jacobian permits a generalized approach to the linearization of nonlinear systems. This allows the development of a system state matrix which contains all the system dynamics in terms of the dependent parameters of mass, energy and flow. Back substitution finally gives a matrix rate equation in terms of the system flow (the unknown) and the system derivatives. While this approach is certainly a proven and successful one, it has some disadvantages. The matrix rate equation involving the Jacobian is as complicated as it is general. The resulting expressions are somewhat obtuse and it is difficult to obtain an intuitive feel for the system. This complexity also hinders implementation in a simulation code and makes error tracking a tedious process. The pervasiveness and obtuseness of the algorithm begs a revisit so as to distil the salient features, leaving them exposed for pedagogy and further scrutiny.

Section 5 discussed the use of the Rate Form of the equation of state. This work showed that by casting the equation of state in the form of a rate equation rather than the normal algebraic form, the system state matrix can be more logically formed from the normal conservation rate equations for mass, energy and momentum plus the pressure rate equation. These form the four cornerstone equations in thermalhydraulic systems analysis (figure 1). Numerical implementation of the rate form proved to be very successful, leading to roughly a factor of 10 improvement over the algebraic form of the equation of state, largely due to the iterative nature of the algebraic form. Incorporating the implicit pressure dependency in the numerical

method also drastically improved the numerical stability.

Since Porsching's method also carried the pressure dependency implicitly (via the Jacobian), the question arises as to how the Rate form compares the Porsching's method. This section is devoted to an explanatory derivation of the fully-implicit back-substituted form (FIBS), which is a more general than the Rate form. It is shown that the Porsching form is identical to the Rate form and is a subset of the fully-implicit back-substituted form and is easily derived from it [GAR87b]. The FIBS form thus offers an alternative to Porsching, is found to be of some pedagogical usefulness and is far more intuitive and easier to code.

6.3 Derivation of FIBS

Following Porsching [POR71], the general form of system equations can be written

$$\mathbf{u} = \mathbf{f}(\mathbf{t}, \mathbf{u}) \quad (144)$$

where \mathbf{u} is the vector of dependent mass, total enthalpy and flow variables $\{M_i, H_i, W_j\}$ for all nodes $i=1..N$ and all links, $j=1..L$. Equation 1 is linearized, assuming no explicit t dependence to give:

$$\mathbf{u} = \mathbf{f}^t + \Delta t \mathbf{J} \mathbf{u} \quad (145)$$

or

$$\Delta \mathbf{u} = \Delta t \mathbf{f}^t + \Delta t \mathbf{J} \Delta \mathbf{u} \quad (146)$$

to give

$$[\mathbf{I} - \Delta t \mathbf{J}] \Delta \mathbf{u} = \Delta t \mathbf{f}^t \quad (147)$$

where \mathbf{J} is the system Jacobian, composed of elements $\partial f_k / \partial u_l$.

For typical thermalhydraulic systems using the node-link notation²:

$$\begin{aligned} \frac{dW_j}{dt} &= \frac{A_j}{L_j} (P_u + S_{WP} \Delta P_u - P_d - S_{WP} \Delta P_d) + k_j (W_j + S_{WW} \Delta W_j)^2 + b_{wj} \\ &= \frac{\Delta W_j}{\Delta t} \end{aligned} \quad (148)$$

² Porsching actually uses U , total energy rather than H , total enthalpy in a hybrid form:

$$U_i = \sum_{j \in d} (H_j/M_j) W_j - \sum_{j \in u} (H_j/M_j) W_j + Q_i$$

There is no advantage to tracking both H and U in a simulation; thus in this course, H is used throughout.

Typically $b_{wj} = (A_j/L_j) (h_j \rho_j g + \Delta P_{\text{pump}})$ where $h_j = \text{height}$.

$$\frac{dM_i}{dt} = \sum_{j \forall d} (W_j + S_{MW} \Delta W_j) - \sum_{j \forall u} (W_j + S_{MW} \Delta W_j) \geq \frac{\Delta M_i}{\Delta t} \quad (149)$$

$$\begin{aligned} \frac{dH_i}{dt} &= \sum_{j \forall d} (W_j + S_{HW} \Delta W_j) \frac{(H_j + S_{HH} \Delta H_j)}{(M_j + S_{HM} \Delta M_j)} - \sum_{j \forall u} (W_j + S_{HW} \Delta W_j) \frac{(H_j + S_{HH} \Delta H_j)}{(M_j + S_{HM} \Delta M_j)} + Q_i \\ &= \sum_{j \forall d} \left(\frac{W_j H_j}{M_j} + \frac{S_{HW} H_j}{M_j} \Delta W_j + \frac{S_{HH} W_j}{M_j} \Delta H_j - \frac{S_{HM} W_j H_j}{M_j^2} \Delta M_j \right) \\ &\quad - \sum_{j \forall u} \left(\frac{W_j H_j}{M_j} + \frac{S_{HW} H_j}{M_j} \Delta W_j + \frac{S_{HH} W_j}{M_j} \Delta H_j - \frac{S_{HM} W_j H_j}{M_j^2} \Delta M_j \right) + Q_i \\ &\geq \frac{\Delta H_i}{\Delta t} \end{aligned} \quad (150)$$

$$\Delta P_i = \frac{\partial P_i}{\partial M_i} \Delta M_i + \frac{\partial P_i}{\partial H_i} \Delta H_i + \frac{\partial P_i}{\partial V_i} \Delta V_i \quad (151)$$

$$\frac{\Delta P_i}{\Delta t} = C_{1i} \frac{\Delta M_i}{\Delta t} + C_{2i} \frac{\Delta H_i}{\Delta t} \quad \text{for constant volume.}$$

where j indicates a sum over all links for which the node i is a downstream (d) or upstream (u) node.

Switches, S , are used to provide user control over the degree of implicitness:

0 = explicit

1 = implicit.

The system unknowns to be solved for are ΔW , ΔM , ΔH and ΔP using equations 5, 6, 7 and 8. The general strategy is to reduce the number of unknowns so that the size of the matrices to be inverted in the simultaneous solution of these equations is reduced. The mass equation 6 is simple and is used to eliminate ΔM in terms of ΔW . Flow is chosen as the prime variable since it is the main actor in thermalhydraulic systems. The enthalpy equation poses a problem as it is too complex to permit a simple substitution. Porsching surmounts this by setting $S_{HH} = S_{HM} = 0$, ie making the solution explicit in specific enthalpy. **However, we need not make this assumption; by casting the equations in matrix notation, the full implicitness can be retained while still allowing the back substitutions to be made.**

Proceeding then, using matrix notation:

$$\Delta \mathbf{M} = \Delta t \mathbf{A}^{\text{MW}} [\mathbf{W}^t + S_{\text{MW}} \Delta \mathbf{W}] \quad (152)$$

where, for a 4 node - 5 link example (Figure 15):

$$\mathbf{A}^{\text{MW}} = \begin{matrix} & \text{links} \Rightarrow & \\ \begin{pmatrix} -1 & 0 & 0 & 1 & 0 \\ 1 & -1 & 0 & 0 & 1 \\ 0 & 1 & -1 & 0 & 0 \\ 0 & 0 & 1 & -1 & -1 \end{pmatrix} & \Downarrow & \\ & \text{nodes} & \end{matrix} \quad (153)$$

This matrix contains the total system geometry. It is constructed by the following procedure:

For each column (link), insert -1 for the upstream node and +1 for the downstream node for that link since the link supplies (adds) flow to the downstream node and takes it away from the upstream node. Flow reversal is handled automatically since the sign of W will take care of mass accounting properly.

The form of other matrices in the following are derivable from \mathbf{A}^{MW} . This can be used to advantage in coding. The input data for each link need only contain pointers to the upstream node and the downstream node for that link. This allows \mathbf{A}^{MW} to be created. In short, the upstream node and downstream node for each link completely defines the geometry and this can be used to programming advantage.

The flow equation is:

$$\Delta \mathbf{W} = \Delta t \{ \mathbf{A}^{\text{WP}} [\mathbf{P}^t + S_{\text{WP}} \Delta \mathbf{P}] + \mathbf{A}^{\text{WW}} [\mathbf{W}^t + 2S_{\text{WW}} \Delta \mathbf{W}] + \mathbf{B}^{\text{W}} \} \quad (154)$$

Where:

$$\mathbf{A}_m^{\text{WW}} = \begin{pmatrix} -k_1 |W_1| & 0 \\ -k_2 |W_2| & 0 \\ 0 & 0 \\ 0 & 0 \\ 0 & -k_5 |W_5| \end{pmatrix} \quad (155)$$

$$\mathbf{A}_m^{\text{WP}} = \begin{pmatrix} A_1/L_1 & A_1/L_1 & 0 & 0 \\ 0 & -A_2/L_2 & -A_2/L_2 & 0 \\ 0 & 0 & A_3/L_3 & -A_3/L_3 \\ -A_4/L_4 & 0 & 0 & A_4/L_4 \\ 0 & -A_5/L_5 & 0 & A_5/L_5 \end{pmatrix} \quad (156)$$

note that \mathbf{A}^{WP} is formed easily from \mathbf{A}^{MW} by the following procedure:

First multiply \mathbf{A}^{MW} by $\{-A_1/L_1, -A_2/L_2, \dots -A_5/L_5\}^{-1}$

Then transpose the resulting matrix to give \mathbf{A}^{WP} .

$$\mathbf{B}^W = \begin{pmatrix} A_1/L_1(h_1\rho_1g + \Delta P_{\text{pump1}}) \\ A_2/L_2(h_2\rho_1g + \Delta P_{\text{pump2}}) \\ \vdots \\ \vdots \end{pmatrix} \quad (157)$$

Finally:

$$\Delta\mathbf{H} = \Delta t \left(\mathbf{A}^{HW} [\mathbf{W}^t + S_{HW}\Delta\mathbf{W}] + S_{HH}\mathbf{A}^{HH*}\Delta\mathbf{H}^* - S_{HM}\mathbf{A}^{HM*}\Delta\mathbf{M}^* + \mathbf{B}^H \right) \quad (158)$$

where $\Delta\mathbf{H}^*$ and $\Delta\mathbf{M}^*$ refer to the enthalpy and mass associated with upstream properties of the links (ie the transported properties). Thus

$$\Delta\mathbf{H}^* = \begin{pmatrix} \Delta H_1 \\ \Delta H_2 \\ \Delta H_3 \\ \Delta H_4 \\ \Delta H_4 \end{pmatrix}, \quad \Delta\mathbf{M}^* = \begin{pmatrix} \Delta M_1 \\ \Delta M_2 \\ \Delta M_3 \\ \Delta M_4 \\ \Delta M_4 \end{pmatrix} \quad (159)$$

$$\mathbf{A}_m^{HW} = \begin{pmatrix} -H_1/M_1 & 0 & 0 & H_4/M_4 & 0 \\ H_1/M_1 & -H_2/M_2 & 0 & 0 & H_4/M_4 \\ 0 & H_2/M_2 & -H_3/M_3 & 0 & 0 \\ 0 & 0 & H_3/M_3 & -H_4/M_4 & -H_4/M_4 \end{pmatrix} \quad (160)$$

For each link, the elements of the column are formed from the link flow, W_j and the upstream properties (H and M). Each link has a sink and source node.

Similarly

$$\mathbf{A}_m^{HH*} = \begin{pmatrix} -W_1/M_1 & 0 & 0 & W_4/M_4 & 0 \\ W_1/M_1 & -W_2/M_2 & 0 & 0 & W_5/M_4 \\ 0 & W_2/M_2 & -W_3/M_3 & 0 & 0 \\ 0 & 0 & W_3/M_3 & -W_4/M_4 & -W_5/M_4 \end{pmatrix} \quad (161)$$

$$\mathbf{A}_m^{HM*} = \begin{pmatrix} -W_1H_1/M_1^2 & 0 & 0 & W_4H_4/M_4^2 & 0 \\ W_1H_1/M_1^2 & -W_2H_2/M_2^2 & 0 & 0 & W_5H_4/M_4^2 \\ 0 & W_2H_2/M_2^2 & -W_3H_3/M_3^2 & 0 & 0 \\ 0 & 0 & W_3H_3/M_3^2 & -W_4H_4/M_4^2 & -W_5H_4/M_4^2 \end{pmatrix} \quad (162)$$

We wish to write the matrix equations eliminating the * parameters, ie convert $\Delta\mathbf{H}^*$ to $\Delta\mathbf{H}$, $\Delta\mathbf{M}^*$ to $\Delta\mathbf{M}$. To do this we introduce a transfer matrix, \mathbf{I}^{LN} so that

$$\Delta \mathbf{H}^* = \mathbf{I}^{LN} \Delta \mathbf{H} \quad (163)$$

where

$$\begin{array}{c}
 \text{nodes} \quad \Rightarrow \\
 \mathbf{I}_m^{LN} = \begin{pmatrix} 1 & 0 & 0 & 0 \\ 0 & 1 & 0 & 0 \\ 0 & 0 & 1 & 0 \\ 0 & 0 & 0 & 1 \\ 0 & 0 & 0 & 1 \end{pmatrix} \quad \Downarrow \\
 \text{links}
 \end{array} \quad (164)$$

where \mathbf{I}^{LN} is formed by entering 1 for the node that is the upstream or source node for each link. Now, we can define:

$$\begin{aligned}
 \mathbf{A}^{HH*} \Delta \mathbf{H}^* &= \mathbf{A}^{HH*} \mathbf{I}^{LN} \Delta \mathbf{H} \\
 &\equiv \mathbf{A}^{HH} \Delta \mathbf{H}
 \end{aligned} \quad (165)$$

and

$$\begin{aligned}
 \mathbf{A}^{HM*} \Delta \mathbf{M}^* &= \mathbf{A}^{HM*} \mathbf{I}^{LN} \Delta \mathbf{M} \\
 &\equiv \mathbf{A}^{HM} \Delta \mathbf{M}.
 \end{aligned} \quad (166)$$

Thus

$$\Delta \mathbf{H} = \Delta t \{ \mathbf{A}^{HW} (\mathbf{W}^t + S_{HW} \Delta \mathbf{W}) + S_{HH} \mathbf{A}^{HH} \Delta \mathbf{H} - S_{HM} \mathbf{A}^{HM} \Delta \mathbf{M} + \mathbf{B}^H \} \quad (167)$$

Substituting in the mass equation 9:

$$\Delta \mathbf{H} = \Delta t \{ \mathbf{A}^{HW} (\mathbf{W} + S_{HW} \Delta \mathbf{W}) + S_{HH} \mathbf{A}^{HH} \Delta \mathbf{H} - \Delta t S_{HM} \mathbf{A}^{HM} \mathbf{A}^{MW} (\mathbf{W}^t + \mathbf{W}^{MW} \Delta \mathbf{W}) + \mathbf{B}^H \} \quad (168)$$

Solving for $\Delta \mathbf{H}$:

$$\Delta \mathbf{H} = \Delta t [\mathbf{I} - \Delta t S_{HH} \mathbf{A}^{HH}]^{-1} \{ \mathbf{A}^{HW} (\mathbf{W}^t + S_{HW} \Delta \mathbf{W}) - \Delta t S_{HM} \mathbf{A}^{HM} \mathbf{A}^{MW} (\mathbf{W}^t + S_{MW} \Delta \mathbf{W}) + \mathbf{B}^H \} \quad (169)$$

So now we have $\Delta \mathbf{M}$ and $\Delta \mathbf{H}$ in terms of $\Delta \mathbf{W}$. Recalling equation 8, in matrix notation, we have:

$$\Delta \mathbf{P} = \mathbf{C}_1 \Delta \mathbf{M} + \mathbf{C}_2 \Delta \mathbf{H}, \quad (170)$$

where

$$\mathbf{C}_{m1} = \begin{pmatrix} C_{11} & 0 & 0 & 0 \\ 0 & C_{12} & 0 & 0 \\ 0 & 0 & C_{13} & 0 \\ 0 & 0 & 0 & C_{14} \end{pmatrix} \quad (171)$$

Similarly for \mathbf{C}_2 .

We can back-substitute $\Delta \mathbf{M}$ and $\Delta \mathbf{H}$ into equation 8 and the result into the flow equation to

leave a matrix equation in $\Delta \mathbf{W}$ only, which can be solved by traditional numeric means. Hence,

$$\begin{aligned} \Delta \mathbf{P} &= \Delta t \mathbf{C}_1 \mathbf{A}^{\text{MW}} (\mathbf{W}^t + S_{\text{MW}} \Delta \mathbf{W}) + \Delta t \mathbf{C}_2 [\mathbf{I} - \Delta t S_{\text{HH}} \mathbf{A}^{\text{HH}^{-1}}] [\mathbf{A}^{\text{HW}} (\mathbf{W}^t + S_{\text{HW}} \Delta \mathbf{W}) \\ &\quad - \Delta t S_{\text{HM}} \mathbf{A}^{\text{HM}} \mathbf{A}^{\text{MW}} (\mathbf{W}^t + S_{\text{MW}} \Delta \mathbf{W}) + \mathbf{B}^{\text{H}}] \\ &\equiv \Delta t \mathbf{A}^{\text{PW1}} \mathbf{W}^t + \Delta t \mathbf{A}^{\text{PW2}} \Delta \mathbf{W} + \Delta t \mathbf{B}^{\text{P}} \end{aligned} \quad (172)$$

where : $\mathbf{A}^{\text{PW1}} = \mathbf{C}_1 \mathbf{A}^{\text{MW}} + \mathbf{C}_2 [\mathbf{I} - \Delta t S_{\text{HH}} \mathbf{A}^{\text{HH}^{-1}}] [\mathbf{A}^{\text{HW}} - \Delta t S_{\text{HM}} \mathbf{A}^{\text{HM}} \mathbf{A}^{\text{MW}}]$ (173)

$$\mathbf{A}^{\text{PW2}} = S_{\text{MW}} \mathbf{C}_1 \mathbf{A}^{\text{MW}} + \mathbf{C}_2 [\mathbf{I} - \Delta t S_{\text{HH}} \mathbf{A}^{\text{HH}^{-1}}] [S_{\text{HW}} \mathbf{A}^{\text{HW}} - \Delta t S_{\text{HM}} S_{\text{MW}} \mathbf{A}^{\text{HM}} \mathbf{A}^{\text{MW}}] \quad (174)$$

$$\mathbf{B}^{\text{P}} = \mathbf{C}_2 [\mathbf{I} - \Delta t S_{\text{HH}} \mathbf{A}^{\text{HH}^{-1}}] \mathbf{B}^{\text{H}} \quad (175)$$

Thus:

$$\Delta \mathbf{W} = \Delta t \{ \mathbf{A}^{\text{WP}} [\mathbf{P}^t + \Delta t S_{\text{WP}} (\mathbf{A}^{\text{PW1}} \mathbf{W}^t + \mathbf{A}^{\text{PW2}} \Delta \mathbf{W} + \mathbf{B}^{\text{P}})] + \mathbf{A}^{\text{WW}} [\mathbf{W}^t + 2S_{\text{WW}} \mathbf{A}^{\text{WW}} \Delta \mathbf{W}] + \mathbf{B}^{\text{W}} \} \quad (176)$$

Collecting terms in $\Delta \mathbf{W}$:

$$\begin{aligned} &[\mathbf{I} - \Delta t (2 S_{\text{WW}} \mathbf{A}^{\text{WW}} + \Delta t S_{\text{WP}} \mathbf{A}^{\text{WP}} \mathbf{A}^{\text{PW2}})] \Delta \mathbf{W} \\ &= \Delta t \{ [\mathbf{A}^{\text{WW}} + \Delta t S_{\text{WP}} \mathbf{A}^{\text{WP}} \mathbf{A}^{\text{PW1}}] \mathbf{W}^t + \mathbf{B}^{\text{W}} + \mathbf{A}^{\text{WP}} [\mathbf{P}^t + \Delta t S_{\text{WP}} \mathbf{B}^{\text{P}}] \} \end{aligned} \quad (177)$$

which is of the form

$$\mathbf{A} \Delta \mathbf{W} = \mathbf{B}$$

which can be solved by conventional means to yield $\Delta \mathbf{W}$. Then we can directly calculate $\Delta \mathbf{M}$, $\Delta \mathbf{H}$ and $\Delta \mathbf{P}$ using equations 152, 158 (or 167), and 170. Associated changes in temperature can be obtained as for pressure, using the appropriate equation of state coefficients.

6.4 Special Cases

To summarize, the general solution is given by the following equations:

$$\mathbf{A}^{\text{PW1}} = \mathbf{C}_1 \mathbf{A}^{\text{MW}} + \mathbf{C}_2 [\mathbf{I} - \Delta t S_{\text{HH}} \mathbf{A}^{\text{HH}^{-1}}] [\mathbf{A}^{\text{HW}} - \Delta t S_{\text{HM}} \mathbf{A}^{\text{HM}} \mathbf{A}^{\text{MW}}] \quad (178)$$

$$\mathbf{A}^{\text{PW2}} = S_{\text{MW}} \mathbf{C}_1 \mathbf{A}^{\text{MW}} + \mathbf{C}_2 [\mathbf{I} - \Delta t S_{\text{HH}} \mathbf{A}^{\text{HH}^{-1}}] [S_{\text{HW}} \mathbf{A}^{\text{HW}} - \Delta t S_{\text{HM}} S_{\text{MW}} \mathbf{A}^{\text{HM}} \mathbf{A}^{\text{MW}}] \quad (179)$$

$$\mathbf{B}^{\text{P}} = \mathbf{C}_2 [\mathbf{I} - \Delta t S_{\text{HH}} \mathbf{A}^{\text{HH}^{-1}}] \mathbf{B}^{\text{H}} \quad (180)$$

$$\begin{aligned} &[\mathbf{I} - \Delta t (2 S_{\text{WW}} \mathbf{A}^{\text{WW}} + \Delta t S_{\text{WP}} \mathbf{A}^{\text{WP}} \mathbf{A}^{\text{PW2}})] \Delta \mathbf{W} \\ &= \Delta t \{ [\mathbf{A}^{\text{WW}} + \Delta t S_{\text{WP}} \mathbf{A}^{\text{WP}} \mathbf{A}^{\text{PW1}}] \mathbf{W}^t + \mathbf{B}^{\text{W}} + \mathbf{A}^{\text{WP}} [\mathbf{P}^t + \Delta t S_{\text{WP}} \mathbf{B}^{\text{P}}] \} \end{aligned} \quad (181)$$

$$\Delta \mathbf{M} = \Delta t \mathbf{A}^{\text{MW}} [\mathbf{W}^t + S_{\text{MW}} \Delta \mathbf{W}] \quad (182)$$

$$\Delta \mathbf{H} = \Delta t \{ \mathbf{A}^{\text{HW}} (\mathbf{W}^t + S_{\text{HW}} \Delta \mathbf{W}) + S_{\text{HH}} \mathbf{A}^{\text{HH}} \Delta \mathbf{H} - S_{\text{HM}} \mathbf{A}^{\text{HM}} \Delta \mathbf{M} + \mathbf{B}^{\text{H}} \} \quad (183)$$

$$\Delta \mathbf{P} = \mathbf{C}_1 \Delta \mathbf{M} + \mathbf{C}_2 \Delta \mathbf{H} \quad (184)$$

Special cases of this general algorithm are as follows:

Fully explicit: all S's = 0

$$\mathbf{A}^{\text{PW1}} = \mathbf{C}_1 \mathbf{A}^{\text{MW}} + \mathbf{C}_2 \mathbf{A}^{\text{HW}} \quad (185)$$

$$\mathbf{A}^{\text{PW2}} = 0 \quad (186)$$

$$\mathbf{B}^P = \mathbf{C}_2 \mathbf{B}^H \quad (187)$$

$$\therefore \Delta \mathbf{W} = \Delta t \{ \mathbf{A}^{WW} \mathbf{W}^t + \mathbf{B}^W + \mathbf{A}^{WP} \mathbf{P}^t \} \quad (188)$$

$$\Delta \mathbf{M} = \Delta t \mathbf{A}^{MW} \mathbf{W}^t \quad (189)$$

$$\Delta \mathbf{H} = \Delta t \{ \mathbf{A}^{HW} \mathbf{W}^t + \mathbf{B}^H \} \quad (190)$$

$$\Delta \mathbf{P} = \mathbf{C}_1 \Delta \mathbf{M} + \mathbf{C}_2 \Delta \mathbf{H}, \quad (191)$$

as expected.

Porsching's semi-implicit ($S_{HH} = 0$ and $S_{HM} = 0$, all other S 's = 1)

$$\mathbf{A}^{PW1} = \mathbf{C}_1 \mathbf{A}^{MW} + \mathbf{C}_2 \mathbf{A}^{HW} \quad (192)$$

$$\mathbf{A}^{PW2} = \mathbf{C}_1 \mathbf{A}^{MW} + \mathbf{C}_2 \mathbf{A}^{HW} \quad (193)$$

$$\mathbf{B}^P = \mathbf{C}_2 \mathbf{B}^H \quad (194)$$

$$\begin{aligned} & [I - \Delta t(2 \mathbf{A}^{WW} + \Delta t \mathbf{A}^{WP} \mathbf{A}^{PW2})] \Delta \mathbf{W} \\ & = \Delta t \{ [\mathbf{A}^{WW} + \Delta t \mathbf{A}^{WP} \mathbf{A}^{PW1}] \mathbf{W}^t + \mathbf{B}^W + \mathbf{A}^{WP} [\mathbf{P}^t + \Delta t \mathbf{B}^P] \} \end{aligned} \quad (195)$$

$$\Delta \mathbf{M} = \Delta t \mathbf{A}^{MW} [\mathbf{W}^t + \Delta \mathbf{W}] \quad (196)$$

$$\Delta \mathbf{H} = \Delta t \{ \mathbf{A}^{HW} (\mathbf{W}^t + \Delta \mathbf{W}) + \mathbf{B}^H \} \quad (197)$$

$$\Delta \mathbf{P} = \mathbf{C}_1 \Delta \mathbf{M} + \mathbf{C}_2 \Delta \mathbf{H} \quad (198)$$

Fully Implicit: All S 's = 1

$$\mathbf{A}^{PW1} = \mathbf{C}_1 \mathbf{A}^{MW} + \mathbf{C}_2 [I - \Delta t \mathbf{A}^{HH}]^{-1} [\mathbf{A}^{HW} - \Delta t \mathbf{A}^{HM} \mathbf{A}^{MW}] \quad (199)$$

$$\mathbf{A}^{PW2} = \mathbf{C}_1 \mathbf{A}^{MW} + \mathbf{C}_2 [I - \Delta t \mathbf{A}^{HH}]^{-1} [\mathbf{A}^{HW} - \Delta t \mathbf{A}^{HM} \mathbf{A}^{MW}] \quad (200)$$

$$\mathbf{B}^P = \mathbf{C}_2 [I - \Delta t \mathbf{A}^{HH}]^{-1} \mathbf{B}^H \quad (201)$$

$$\begin{aligned} & [I - \Delta t(2 \mathbf{A}^{WW} + \Delta t \mathbf{A}^{WP} \mathbf{A}^{PW2})] \Delta \mathbf{W} \\ & = \Delta t \{ [\mathbf{A}^{WW} + \Delta t \mathbf{A}^{WP} \mathbf{A}^{PW1}] \mathbf{W}^t + \mathbf{B}^W + \mathbf{A}^{WP} [\mathbf{P}^t + \Delta t \mathbf{B}^P] \} \end{aligned} \quad (202)$$

$$\Delta \mathbf{M} = \Delta t \mathbf{A}^{MW} [\mathbf{W}^t + \Delta \mathbf{W}] \quad (203)$$

$$\Delta \mathbf{H} = \Delta t \{ \mathbf{A}^{HW} (\mathbf{W}^t + \Delta \mathbf{W}) + \mathbf{A}^{HH} \Delta \mathbf{H} - \mathbf{A}^{HM} \Delta \mathbf{M} + \mathbf{B}^H \} \quad (204)$$

$$\Delta \mathbf{P} = \mathbf{C}_1 \Delta \mathbf{M} + \mathbf{C}_2 \Delta \mathbf{H} \quad (205)$$

6.5 Programming Notes

It should be noted that the full system geometry is contained in \mathbf{A}^{MW} . All other matrices are derived from this matrix and node/link properties. Programming is thus very straightforward. In addition, the switches, S , can be varied at will to control the degree of implications of the system variables, \mathbf{W} , \mathbf{M} , \mathbf{H} and \mathbf{P} .

The fully-implicit method is more complicated than the semi-implicit method in that it requires the addition and multiplication of more matrices as well as a matrix inversion. The effect of these additional operations is quite costly, especially when a large number of nodes is needed.

In one case study [HOS89], for 9 nodes and links, the cost is a 50% increase in iteration time. But this becomes a 250% increase as one approaches the 36 node/link case. By handling the matrix operations as efficiently as possible, some increase in speed should be attainable for both models. Using efficient assembly routines (rather than FORTRAN) for the matrix operations yielded a 10 to 20% reduction (increasing from 9 nodes to 36 nodes) in the time per iteration for the semi-implicit method and a 15 to 25% reduction in the fully-implicit case.

Usually the matrices contain mostly zeros and, in the case of a circular loop, may be diagonally dominant in nature (i.e. non-zero elements occupy one, two or three stripes through the matrix). By writing routines specific to the nodal layout for handling the matrix operations, significant gains in speed may be possible. However, the simulator will no longer be general in nature and the routines may have to be changed if the nodal layout is altered.

If the multiplication of two large matrices is desired, say $N \times N$ in dimension, the time to carry out the operation (N^3 multiplications and N^3 additions) can be very significant. However, it is possible to reduce the number of individual operations without losing the generality of the method. Take, for example, the multiplication of \mathbf{A}^{WP} and \mathbf{A}^{PW} . The rows in the former term pertain to links and the columns to nodes. Each row will only contain two terms located in the columns corresponding to the upstream and downstream nodes of that particular link. Thus, knowing which are the upstream and downstream nodes for every link, it is only necessary to do two multiplications and one addition to obtain each element of the product matrix ($2N^2$ multiplications and N^2 additions). By taking advantage of having only two elements in each row of the former term or only two elements in each column of the latter term wherever possible, significant savings in time may be observed. With this improvement in the code, a cut in time by a factor of two for 18 nodes and by a factor of three for 36 nodes, regardless of the method (semi- or fully-implicit) was obtained. The cost of the fully-implicit method is reduced slightly to a 32% increase in iteration time over the semi-implicit method when 9 nodes and 9 links are used. This becomes a 214% increase as one approaches the 36 node case.

Since the focus of this section is to provide a less obtuse and more general derivation of thermalhydraulic system equations than Porsching's method, a full comparison of the performance of the fully- and semi-implicit methods will not be made. Suffice it to say that, in general, the semi-implicit method has a Courant limit on the maximum time step that can be taken in order to ensure stability. The fully-implicit method does not have this limitation. As the Courant time step limit is determined by the nodal residence time, the time step limit is dependant on the node sizes and the flows through the nodes. Practical simulations have a further time step constraints such as: the tracking of movement of valves, the maintenance of accuracy, synchronizing of report times, etc. Thus, the choice between the semi- or fully-implicit method depends on the time per iteration multiplied by the number of iterations required to reach the largest time step permitted by the simulation problem. For example, for a 9 node case, the semi-implicit method required 0.10 seconds per iteration and required 2 iterations to meet the report time of 1.0 seconds. The fully-implicit method meet the report time in one iteration which took 0.14 seconds. At 36 nodes however, the semi-implicit method took 2×0.71 seconds while the fully-implicit method took 2.12 seconds. Clearly, one method is not superior to the other in all cases.

Pressure determination involves the use of property derivatives. To avoid the numerical problems associated with discontinuities, smooth functions for properties must be used, such as those derived by [GAR88, GAR89 and GAR92]. These functions and routines permit the quick and fast evaluation of ΔP and ΔT given ΔM and ΔH for all water phases. Automatic adjustment is provided to prevent P and T drift from values consistent with current M and H values. These routines are non-iterative, essential for real-time simulation.

6.6 Conclusion

The FIBS approach for thermalhydraulic system simulation has been compared to the classic work of Porsching. Porsching's algorithm is derived as a subset of the fully implicit approach. Focusing on the system Jacobian, as Porsching did, focuses on the perturbation of the system as a whole. Although general, it tends to obscure the interaction of the main players in typical thermalhydraulic systems: flow and pressure. The FIBS form is shown to be more general than Porsching's method, yet less obtuse. The interplay of flow and pressure is clarified and coding is simplified.

6.7 Problems

1. Rewrite the conservation equations for the 4 node, 5 link case with various explicit / implicit switches set for the following cases:
 - a. fully explicit
 - b. diagonally implicit
 - c. semi-implicit solution scheme (implicit in flow and pressure, explicit in mass and enthalpy)
 - d. fully-implicit solution scheme (implicit in flow and pressure, mass and enthalpy).
2. Build a simulation code that solves the thermalhydraulic equations for a general node-link network for the explicit case using the supplied skeleton code as a starting point. Use the node-link diagrams and equations as developed in section 3, the water property routines as developed in section 4, the rate form of the equation of state as developed in section 5 and the explicit solution as developed in this section.
3. Improve upon your solution to question 2 by implementing a diagonally implicit solution procedure. Is the solution more stable? Is there a cost penalty?
4. Implement a semi-implicit solution scheme (implicit in flow and pressure, explicit in mass and enthalpy). Is the solution more stable? Is there a cost penalty?
5. Implement a fully-implicit solution scheme (implicit in flow and pressure, mass and enthalpy). Is the solution more stable? Is there a cost penalty?

7 Case Study: Heat Transport System Stability

As mentioned in section 6.2, Porsching's Method is one of the more successful algorithms for thermalhydraulic simulation. This algorithm was used in the Ontario Hydro program SOPHT to investigate Heat Transport System stability for the CANDU reactors with a figure-of-eight heat transport loop configuration, such as the CANDU 6 and Darlington, since each loop potentially has two-phase water at the outlet headers at high power. Since there are 2 outlet headers per loop (one at each end of the reactor) separated by 2 single phase regions, we have a coupled spring-mass system that, under the right conditions, could give undesirable flow and pressure oscillations. To enhance heat transport system stability, a reactor outlet interconnect was provided in each loop. This is discussed in detail in [GAR84, GAR86] but, of relevance to this chapter, the code predictions based on the best estimate of the heat transport conditions compared well to the plant tests, confirming both the mathematical methodology and the efficacy of the one dimensional homogeneous thermalhydraulic model for overall system simulation.

8 References

- AGE82 L.J. Agee, "RETRAN Thermalhydraulic Analyses: Theory and Applications", *Progress in Nuclear Energy*, Vol. 10, No. 1, pp. 19-67, 1982.
- AGE83 L.J. Agee, M.P. Paulsen and E.D. Hughes, "Equations of State for Nonequilibrium Two-Phase Flow Models", *Transient Two-Phase Flow Proceedings of the Third CSNI Specialist Meeting*, Hemisphere Publishing Corporation, 1983.
- BAN80 S. Banerjee, "Two-Phase Hydrodynamics: Models and Mechanisms", Keynote Paper, *ANS/ASME Topical Meeting, Nuclear Reactor Thermal-Hydraulics*, Saratoga, New York, October 1980.
- BER81 A.E. Bergles et al., *Two-Phase Flow and Heat Transfer in the Power and Process Industries*, Hemisphere Publishing, 1981.
- BIR60 R.B. Bird, W.E. Stewart and E.N. Lightfoot, *Transport Phenomena*, John Wiley and Sons, Inc., New York, 1960.
- BLO71 Benjamin S. Bloom, J. Thomas Hastings, George F. Madaus, "Handbook on Formative and Summative Evaluation of Student Learning", McGraw-Hill, Library of Congress 75-129488, 1971.
- BNW76 COBRA-IV: An Interim Version of COBRA for Thermalhydraulic Analysis of Rod Bundle Nuclear Fuel Elements and Cores, Battelle Pacific Northwest Laboratories, BNWL-1962, March 1976.
- CAR81a M.B. Carver, L.N. Carlucci and W.W.R. Inch, *Thermalhydraulics in Recirculating Steam Generators*, THIRST Code User's Manual, AECL-7254, April 1981.
- CAR81b M.B. Carver, "Numerical Simulation Involving Large Systems of Equations", Keynote Lecture, *United Kingdom Simulation Council, 1981 Conference on Computer Simulation*,

- Harrogate, May 1981.
- CAR95 M.B. Carver, "Numerical Solution of the Thermalhydraulic Conservation Equations from Fundamental Concepts to Multidimensional Two-Fluid Analysis", Atomic Energy of Canada report AECL-11387, ARD-TD-550, August 1995, amended January 2017, <https://canteach.candu.org>.
- CHA75a Y.F. Chang, "The SOPHT Program and its Applications", *Proceedings of the 1975 Simulation Symposium on Reactor Dynamics and Plant Control*, May 26-27, CRNL, published as CRNL 1369, 1975.
- CHA75b Y.F. Chang, SOPHT-B Bruce GS A Plant Control Simulation Engineers' Manual and Program Specifications, Ontario Hydro CNS-37.3, June 1975.
- CHA77a C.Y.F. Chang and J. Skears, "SOPHT - A Computer Model for CANDU-PHWR Heat Transport Networks and Their Control", *Nucl. Technol.* 35, 591, 1977.
- CHA77b Y.F. Chang, A Thermalhydraulic System Simulation Model for the Reactor, Boiler and Heat Transport System (SOPHT), Ontario Hydro CNS 37-2, Sept. 1977.
- CHE77 Bindi Chexal, NUCIRC - A Computer Code for Nuclear Heat Transport Circuit Thermohydraulic Analysis, User's Instruction Manual, TDAI-116, AECL, Jan. 1977.
- CHO74 W.G. Choe, J. Weisman, Flow Patterns and Pressure Drop in Concurrent Vapour-Liquid Flow, A State-of-the-Art Report, AECL Lib 146648, Sept. 1974.
- COL72 J.C. Collier, *Convective Boiling and Condensation*, McGraw-Hill, 1972.
- CRA57 Crane, *Flow of Fluids Through Valves, Fittings and Pipe*, 410-C (Engineering Units), 410-m (metric), 1957.
- CUR74 I.G. Currie, *Fundamental Mechanics of Fluids*, McGraw-Hill, Inc., 1974.
- DEL81 J.M. Delhay et al., *Thermohydraulics of Two-Phase Systems for Industrial Design and Nuclear Engineering*, Hemisphere Publishing, 1981.
- ELH80 M.A. El-Hawary, Verification of HYDNA-2 and HYDNA-3 Codes against Pertinent Experimental Data, AECL TDAI-231, December 1980.
- FIR84 A.P. Firla, "Approximate Computational Formulas for Fast Calculation of Heavy Water Thermodynamic Properties", *10th Annual Simulation Symposium on Reactor Dynamics and Plant Control*, Saint John, New Brunswick, 1984.
- GAR79 W. Garland, *SOPHT-D User's Guide, Revision 3*, Ontario Hydro, Nuclear Systems Department, 1979-03-01.
- [GAR84] Wm. J. Garland, W.J.G. Brimley, "CANDU 600 Heat Transport System Flow Stability", 10th Simulation Symposium on Reactor Dynamics and Plant Control, Saint John, N.B., 34 pages, April 9-10, 1984. [www.nuceng.ca/papers/conf.htm, paper C8]
- [GAR86] Wm. J. Garland and S. H. Pang, "CANDU 600 Heat Transport Flow Stability", *Nuclear Technology*, Vol. 75, #, pp. 239-260, December 1986.

- [www.nuceng.ca/papers/journal.htm, paper J4]
- GAR87a W.J. Garland and R. Sollychin, "The Rate Form of State for Thermalhydraulic Systems: Numerical Considerations", *Engineering Computations*, Vol. 4, December 1987. [www.nuceng.ca/papers/journal.htm, paper J7]
- GAR87b Wm. J. Garland, "A Comparison of the Rate Form of the Equation of State to the Jacobian Form", *13th Symposium on Simulation of Reactor Dynamics and Plant Control*, Chalk River Nuclear Laboratories, Chalk River, Ont., 28 pages, April 27-28, 1987. [www.nuceng.ca/papers/conf.htm, C21]
- GAR88 W.J. Garland and J.D. Hoskins, "Approximate Functions for the Fast Calculation of Light Water Properties at Saturation", *Int'l J. of Multiphase Flow*, Vol. 14, No. 3, pp 333-348, 1988. [www.nuceng.ca/papers/journal.htm, paper J6]
- GAR89 W.J. Garland and B.J. Hand, "Simple Functions for the Fast Approximation of Light Water Thermodynamic Properties", *Nuclear Engineering & Design*, Vol. 113, pp. 21-34, 1989. [www.nuceng.ca/papers/journal.htm, paper J8]
- GAR92 Wm. J. Garland, R. J. Wilson, J. Bartak, J. Cizek, M. Stasny and I. Zentrich, "Extensions to the Approximation Functions for the Fast Calculation of Saturated Water Properties", *Nuclear Engineering and Design*, # 136, pp. 381-388, 1992. [www.nuceng.ca/papers/journal.htm, paper J13]
- GIN81 Ginoux, *Two-Phase Flows and Heat Transfer with Application to Nuclear Reactor Design Problems*, Hemisphere Publishing, 1981.
- HAA84 L. Haar, J.S. Gallagher, and G.S Knell, *NBS/NRC STEAM TABLES: Thermodynamic and Transport Properties and Computer Programs for Vapor and Liquid States of Water in SI Units*, Hemisphere Publishing Corporation, 1984.
- HAN95 B.N. Hanna and M.E. Laveck, ed., *CATHENA Input Reference*, Atomic Energy of Canada Ltd., RC-982-4 / COG-93-140 (Vol. 4), Rev. 0.4, 1995.
- HOS89 J. D. Hoskins, *A Heat Transport System Operator Companion for a CANDU Nuclear Reactor*, Masters Thesis, McMaster University, Hamilton, Ontario, Canada, July, 1989.
- HSU76 Y. Hsu and R. Graham, *Transport Processes in Boiling and Two-Phase Systems*, Hemisphere Publishing, 1976.
- IDE60 Idel'chik, *Handbook of Hydraulic Resistance - Coefficients of Local Resistance and of Friction*, National Science Foundation, Washington, D.C. (Translation), 1960.
- ITT73 ITT Grinnel Corp., *Piping Design and Engineering*, Providence, Rhode Island, 1973.
- KAY79 R.A. Kay, *AESOP, Atomic Energy Station Optimization Program*, TDAI-114/Revision 1, AECL-EC, December 1976, revised by M. Gold March 1979.
- KIN73 F.K. King, *Steam Generators for CANDU Nuclear Power Stations, Sizing and Cost Analysis Program, User's Instruction Manual*, no file: see N. Subash, Process Systems Development Department, AECL-EC, May 1973, revision 1 by N. Subash, July 1976.

- LAH77 R.T. Lahey, Jr., and F.J. Moody, *The Thermal Hydraulics of a Boiling Water Nuclear Reactor*, ANS/AEC Monograph Series on Nuclear Science and Technology, ANS, 1977.
- LIN79 M.R. Lin et al., *FIREBIRD-III Program Description*, AECL-7533, September 1979.
- MER80 E.E. Merlo, et al, *HYDNA-3 Program Description*, AECL TDAI-205, April 1980.
- MEY67 Meyer, C.A. et al., *Thermodynamic and Transport Properties of Steam*, ASME, New York, 1967.
- MIL71 D.S. Millar, *Internal Flow, A Guide to Losses in Pipe and Duct Systems*, British Hydromechanics Research Association, 1971.
- MUR68 J.H. Murphy and J.A. Redfield, *WASP - A Program to Generate Water and Steam Thermodynamic Properties*, WAPD-TM-839, 1968.
- NAH70 A.N. Nahavandi, and S. Makkenchery, "An Improved Pressurizer Model with Bubble Rise and Condensate Drop Dynamics", *Nuclear Engineering and Design* 12, p135-147, 1970.
- PAY60 H.M. Paynter, *Analysis and Design of Engineering Systems*, MIT Press, 1960.
- POR69 T.A. Porsching, J.H. Murphy, J.A. Redfield, and V.C. Davis, *FLASH-4: A Fully Implicit FORTRAN IV Program for the Digital Simulation of Transients in a Reactor Plant*, WAPD-TM-840, Mar. 1969.
- POR71 T.A. Porsching, J.H. Murphy, J.A. Redfield, "Stable Numerical Integration of Conservation Equations for Hydraulic Networks", *Nuc. Sci. and Eng.* 43, p 218-225, 1971.
- REL76 RELAP4/MOD5 - A Computer Program for Transient Thermalhydraulic Analysis of Nuclear Reactors and Related Systems, User's Manual, Vol. I: RELAP4/MOD5 Description, Vol II: Program Implementation, Vol. III: Checkout Applications, ANCR-NUREG-1335, Sept. 1976.
- ROA76 Patrick J. Roache, *Computational Fluid Dynamics*, Hermosa Publishers, P.O. Box 8172, Albuquerque, NM, 87108, 1976.
- SEA75 F.W. Sears and G.L. Salinger, *Thermodynamics, Kinetic Theory, and Statistical Thermodynamics*, Addison-Wesley Publishing Company, 1975.
- SKE75 J. Skears and T. Toong, *SOPHT Programmers Manual*, Revision 0.0, Ontario Hydro, Engineering Systems Department, May 1975.
- SKE80 J. Skears and T. Toong, *SOPHT User's Manual*, Version 2.0, Ontario Hydro, Engineering Systems Department, January 1980.
- SOL85 R. Sollychin,, S.A. Adebisi, and W.J. Garland, "The Development of a Non-Iterative Equation of State for Two-phase Flow Systems", *11th Annual Symposium on Simulation of Reactor Dynamics and Plant Control*, Kingston, Ontario, 1985.
- STE48 A.J. Stepanoff, *Centrifugal and Axial Flow Pumps*, John Wiley & Sons, Inc. 1948.
- TON65 L.S. Tong, *Boiling Heat Transfer and Two-Phase Flow*, John Wiley and Sons, Inc., 1965.

10 Acknowledgements

This chapter is based on a graduate level course given by the author at McMaster University and on research funded by McMaster University and the Natural Sciences and Engineering Research Council of Canada. The author is indebted to Atomic Energy of Canada Ltd. and to Ontario Power Generation since this work is inextricably linked to past involvements with these companies. Special thanks go to students, John Hoskins and Brian Hand, for water property development, and to Raymond Sollychin for his central role in the development of the rate method for the equation of state. A general thanks to all students over the years; their freshness is a constant delight. Their sharp eyes caught many a mistake; of course the responsibility for any errors or omissions lies entirely with the author.

